

The Magnetic Field of Planet Earth

G. Hulot · C.C. Finlay · C.G. Constable · N. Olsen ·
M. Mandea

Received: 22 October 2009 / Accepted: 26 February 2010
© The Author(s) 2010. This article is published with open access at Springerlink.com

Abstract The magnetic field of the Earth is by far the best documented magnetic field of all known planets. Considerable progress has been made in our understanding of its characteristics and properties, thanks to the convergence of many different approaches and to the remarkable fact that surface rocks have quietly recorded much of its history. The usefulness of magnetic field charts for navigation and the dedication of a few individuals have also led to the patient construction of some of the longest series of quantitative observations in the history of science. More recently even more systematic observations have been made possible from space, leading to the possibility of observing the Earth's magnetic field in much more details than was previously possible. The progressive increase in computer power was also crucial, leading to advanced ways of handling and analyzing this considerable corpus

G. Hulot (✉)

Equipe de Géomagnétisme, Institut de Physique du Globe de Paris (Institut de recherche associé au CNRS et à l'Université Paris 7), 4, Place Jussieu, 75252, Paris, cedex 05, France
e-mail: gh@ipgp.jussieu.fr

C.C. Finlay

ETH Zürich, Institut für Geophysik, Sonneggstrasse 5, 8092 Zürich, Switzerland

C.G. Constable

Cecil H. and Ida M. Green Institute of Geophysics and Planetary Physics, Scripps Institution of Oceanography, University of California at San Diego, 9500 Gilman Drive, La Jolla, CA 92093-0225, USA

N. Olsen

DTU Space and Niels Bohr Institute of Copenhagen University, Juliane Maries Vej 30, 2100 Copenhagen Ø, Denmark

M. Mandea

Helmholtz-Zentrum Potsdam Deutsches GeoForschungsZentrum, 14473 Potsdam, Germany

Present address:

M. Mandea

Equipe de Géophysique Spatiale et Planétaire, Institut de Physique du Globe de Paris (Institut de recherche associé au CNRS et à l'Université Paris 7), Bâtiment Lamarck, 5 rue Thomas Mann, 75013 Paris, France

of data. This possibility, together with the recent development of numerical simulations, has led to the development of a very active field in Earth science. In this paper, we make an attempt to provide an overview of where the scientific community currently stands in terms of observing, interpreting and understanding the past and present behavior of the so-called main magnetic field produced within the Earth's core. The various types of data are introduced and their specific properties explained. The way those data can be used to derive the time evolution of the core field, when this is possible, or statistical information, when no other option is available, is next described. Special care is taken to explain how information derived from each type of data can be patched together into a consistent description of how the core field has been behaving in the past. Interpretations of this behavior, from the shortest (1 yr) to the longest (virtually the age of the Earth) time scales are finally reviewed, underlining the respective roles of the magnetohydrodynamics at work in the core, and of the slow dynamic evolution of the planet as a whole.

Keywords Earth · Geomagnetism · Archeomagnetism · Paleomagnetism · Magnetic observations · Archeomagnetic records · Paleomagnetic records · Spherical harmonic magnetic field models · Statistical magnetic field models · Geomagnetic secular variation · Geomagnetic reversals · Core magnetohydrodynamics · Numerical dynamo simulation · Geodynamo · Earth's planetary evolution

1 Introduction

Earth's magnetism has been known to man for a very long time. The successive discoveries of the needle's rough orientation towards the geographic North, of the concepts of declination, inclination, and intensity, and of the fact that the Earth's magnetic field changed through time (in a process known as secular variation) progressively led to a growing body of magnetic observations. The usefulness of a precise knowledge of the declination for navigation purposes and the need to monitor the secular variation of the field to regularly update maps, also quickly led to systematic observations all over the globe, both at sea and on land, and to the establishment of permanent magnetic observatories. Nowadays, these observatories and satellite observations make it possible to closely monitor and investigate the various fields that add up to produce the observed field, with sources in the core (which produces by far the largest component of the field), the crust, the ionosphere, the magnetosphere and, to a lesser extent, the mantle and oceans.

Such direct observations only extend back approximately four centuries. This is long enough for significant changes to be observed in "movies" of the reconstructed core field evolution, but far too short to infer anything about the long-term field behaviour. Fortunately considerable additional information is also available from indirect observations provided by the magnetization of both human artefacts (such as bricks, tiles, potteries), and various types of rocks (mainly basalts and sediments) that can be sampled and measured. Each such magnetized sample carries some quantitative information about the field it experienced at the time it acquired its magnetization. These indirect observations can be used to extend our knowledge of Earth's ancient field very far back in time.

The accuracy with which those samples can be measured is however limited and only information about the dominant core field can reasonably be recovered (other contributions being at best of comparable magnitude to measurement errors). Dating accuracy is also an important limiting factor for spatio-temporal analysis of the ancient field behavior, which

requires temporal synchronization of the information provided by distant samples. This important constraint is the main reason our knowledge of the historical patterns of field evolution cannot yet be expanded very far back in time. Nonetheless, the time evolution of the largest scales of the core field can, and has been, reconstructed over the past few millennia, using techniques akin to those used for historical data analysis.

Information concerning the more ancient geomagnetic field can also be recovered, but this requires other types of analysis. In fact, and as we shall see, quite a few different types of analysis can be used, depending on the sample studied, the time span considered and the geomagnetic information to be recovered. Perhaps the single most important information revealed by the paleomagnetic record in general, is that the core field has always remained predominantly an axial dipole of comparable magnitude to the present field (which varies within the range 25.000–65.000 nT at the Earth's surface), except during relatively short periods of time (on order 10 ky) when the field dropped significantly and became dominated by non-dipole components. Those short periods of time always led the field to grow back to its usual axial dipole dominated structure either with the same polarity (in which case one usually refers to these events as “excursions”), or with the opposite polarity (events known as “reversals”). Between two such events, the field is then said to have been of “stable polarity”.

Because of their continuous nature, sediment records are particularly well suited for the investigation of the long-term temporal behaviour of the field at a particular location. But only relatively recent sediments (up to a few million years old) with fast sedimentation rates can provide high-resolution temporal information. This is enough to provide very useful information with respect to recent excursions and reversals. Unfortunately, acquiring high accumulation rate sediment records with good global coverage on much longer time scales (several hundreds of millions of years) is much more difficult. The available records heavily smooth the magnetic signal, and mainly provide information about the rate at which the dipole component of the field evolved and reversed in the past.

Very useful complementary information is also provided by rocks that acquired so-called thermo-remanent magnetization (TRM), some of which testify for a very ancient field (over 3 Gy old). The bulk of this data comes from lava flows. Their main advantage is that they provide instantaneous spot readings of the ancient core field. Their main disadvantage is that they do not sample time in a regular way. Such data can nevertheless catch the field at times of excursions or reversals. More often however, they provide information about the field at times of stable polarity. All those data can be used to characterize long-term statistical properties of the core field, including the rate of reversals in the past.

Another efficient way of recovering information about past reversal rates is the analysis of the extensive record provided by the magnetized ocean crust, at least over the time period covered by the seafloor age range (back to a couple hundred million years). As new sea floor is created at ridge crests because of sea floor spreading, it cools, acquires a TRM and therefore captures a record of past field variation. The beauty of this specific record is that it is directly available in the form of the worldwide distribution of ocean crust magnetization with alternating polarities, the signal of which produces characteristic linear magnetic anomalies (parallel to the ridges) in marine magnetic surveys. Although the detailed analysis of such signals is far from being trivial, appropriate procedures can be used to recover the polarity, and to some extent the intensity, of the field that produced the magnetization.

All those different types of data complement each other. They have led to a fairly comprehensive view of the various sources that contribute to the Earth's magnetic field and of the way this field evolved in time. Here, however, we will only focus on the field produced within the core. We first provide an overview of the various types of data routinely used to investigate this field (Sect. 2), next describe the way these data can be used to recover the

behavior of the present and past core field (Sect. 3), and finally review the way this behavior is currently understood in terms of planetary core dynamics (Sect. 4). External sources will be briefly mentioned only to the extent those need to be taken into account in the analysis of modern data. Likewise, crustal sources will be mentioned only to the extent they provide a record of the ancient core field. For more details about those and other non-core sources in a planetary context, the reader is referred to the companion papers of Baumjohann et al. (2010), Olsen et al. (2009b), Langlais et al. (2009) and Saur et al. (2009).

2 Observations

2.1 Satellite Observations

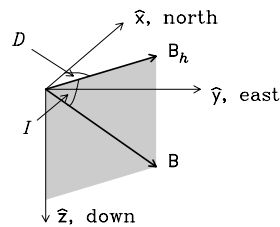
The biggest advantage of measuring Earth's magnetic field from space with low Earth-orbiting satellites is that it yields an excellent spatial data coverage, an important prerequisite for obtaining good global models of the geomagnetic field. It also ensures that different regions of Earth are sampled with the same instrumentation. However, because satellites are moving fast (at typically 8 km/s for low-Earth orbiting satellites), the field changes they sense are a combination of both changes due to the movement of the satellite within the field, and actual temporal changes of the field. As we will later see, this makes the identification of the contributions of the various sources of the magnetic field quite challenging.

The first global satellite observations of the Earth's magnetic field were taken by the POGO satellites that operated between 1965 and 1971. POGO measured only the scalar field (magnetic intensity) but not the vector components (Fig. 1). This, we now know, unfortunately only provides partial information about the field, and leads to a fundamental ambiguity in its determination (Backus 1970; Lowes 1975). Although such ambiguity can be overcome with the help of additional information (Khokhlov et al., 1997, 1999; Ultr -Gu erard et al. 1998; Holme et al. 2005), the need for measurements of the full vector magnetic field quickly became obvious.

The first such vector satellite mission was Magsat, which flew for 8 months in 1979–80 at an altitude of 300 to 550 km. After this very successful (see e.g. Langel and Hinze 1998) but short-lived mission, quite a few satellite missions were proposed. But it was not until 20 years later that these efforts paid off, with the successful launch of the  rsted satellite in February 1999, which marked the beginning of a new era of continuous space magnetometry. Being the first satellite of the *International Decade of Geopotential Research*,  rsted and its instrumentation (in particular, its combined set of an absolute scalar magnetometer, vector magnetometer and star tracker to achieve high precision oriented vector magnetic field measurements at 1 Hz and 50 Hz sampling rates, see e.g. Neubert et al. 2001) has since become a model for other missions such as CHAMP (launched in July 2000, Reigber et al. 2002) and SAC-C (November 2000–December 2004). More than 10 years of continuous measurements of the Earth's magnetic field from space are now available, with a typical accuracy of 0.5 nT for intensity measurements, and somewhat less good (2nT for the best CHAMP data) for individual field component measurements.

The low altitude (350–450 km) of CHAMP has proved extremely useful for the investigation of the ionospheric and crustal fields, while the combination of simultaneous observations taken by  rsted (650–850 km altitude), CHAMP and SAC-C (\approx 700 km altitude) led to considerable progress in the investigation of the temporal behavior of the core field. Building on this past experience, ESA's *Swarm* satellite constellation is to be launched

Fig. 1 Geomagnetic elements in a local coordinate system:
 D declination, I inclination;
 B magnetic field strength;
 B_h horizontal component of magnetic field



in 2011, will consist of a pair of side-by-side satellites at an initial altitude of 450 km, and a third satellite orbiting at higher altitude (530 km) with a different orbital drift rate. This configuration will allow for an even better separation of internal and external fields, and an enhanced sensitivity to small-scale structures of the crustal field (Olsen et al. 2006; Sabaka and Olsen 2006). Such an improved continuation of magnetic field observation from space is thus expected to lead to even more progress in our understanding of all sources of the Earth's magnetic field (Friis-Christensen et al. 2006, 2009).

2.2 Magnetic Observatories

Before the advent of satellites, all magnetic measurements were carried out on ground and at sea. Because it was recognized that the magnetic field displayed significant changes on historical time scales, regular measurements of field elements (at first only Declination and Inclination, see Fig. 1) at fixed known locations were soon carried out for instance in London (Malin and Bullard 1981), Paris (Alexandrescu et al. 1996a), Rome (Cafarella et al. 1992) and Edinburgh (Barraclough 1995). But it was not until the 1840's, under the impulse of Gauss and Weber, that a global network of fully dedicated Magnetic Observatories (by then measuring all magnetic field elements, including its intensity) started to develop to monitor temporal changes of the Earth's magnetic field (see Fig. 2, which shows the current distribution observatories, and Fig. 3, which shows records of the magnetic field as measured in the Niemeck observatory since 1890). Measurements carried out in such magnetic observatories have generally involved regular *absolute measurements* to monitor instrumental drift of variometers, which otherwise provided continuous *variation measurements* of the three components of the magnetic field.

Nowadays, variations are continuously measured and digitally recorded, either by three-component fluxgate magnetometers or by magnetometers based on sensors which measure field components by a scalar sensor equipped with coil systems. The elements of the geomagnetic field vector are then recorded in instrument-related coordinate systems. Such variometers are unfortunately subject to drifts arising both within the instrument (e.g., temperature effects) and because of the limited stability of the instrument mounting. To monitor and correct for those drifts, and also to convert such measurements into absolute units in the geographical reference frame, additional absolute measurements are carried out. For the field direction, this is usually done with the help of a flux-gate theodolite, searching for the plane perpendicular to the field (which is detected when the highly sensitive single-component flux-gate sensor sees no more field). Absolute measurements of the field intensity are otherwise directly measured with the help of an absolute scalar magnetometer. Several measurements are usually carried out using appropriate procedures to remove all systematic instrument errors (for more details see e.g. Jankowski and Sucksdorff 1996; Turner et al. 2007). This requires well-trained personnel and one complete measurement takes about 30 min. Such absolute measurements are typically performed on a weekly basis.

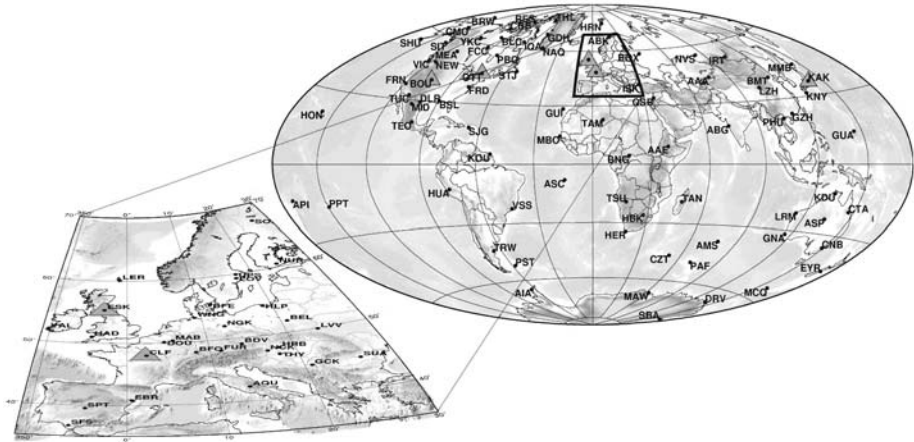


Fig. 2 Distribution of currently operating geomagnetic observatories from the INTERMAGNET worldwide network

Current quality standards for geomagnetic observatory data ask for an accuracy better than ± 5 nT, including a long-term stability of variation recordings better than 5 nT/yr. An accuracy of 1 nT can be achieved for absolute measurements by well-trained observatory staff. Recently, however, the wish to record one-second data has been expressed by the community, especially in view of the upcoming *Swarm* mission, and indeed some observatories are already able to provide such high-resolution data. Many of the better magnetic observatories, which maintain a higher-level standard for data measurement and provide near real-time distribution, collectively form the INTERMAGNET worldwide network of observatories.¹

As is clear from Fig. 2, one important drawback of the current network of magnetic observatories is that it is unevenly distributed, with high concentration in Europe and North America, and a dearth in the Southern Hemisphere and over the oceans. Efforts to correct for this drawback is currently oriented towards developing fully automated observatories that could be installed in remote areas (e.g., Gravrand et al. 2001; Van Loo and Rasson 2006; Auster et al. 2006, 2007).

2.3 Historical Records

Going further back in time the importance of Earth's magnetic field as a navigational tool, together with the intrigue it generated amongst prominent early scientists, result in large numbers of well documented direct field observations spanning the past four centuries. This period is commonly referred to as the 'historical era' in the geomagnetic literature. Here only a brief summary of the most important historical sources are given; for further details readers should consult the landmark paper of Bloxham et al. (1989) and the review article of Jonkers et al. (2003) where a comprehensive database comprising 151,560 declination, 19,525 inclination and 16,219 intensity observations made between 1510 and 1930 (available from the World Data Centre for Geomagnetism at the British Geological Survey,

¹ www.intermagnet.org.

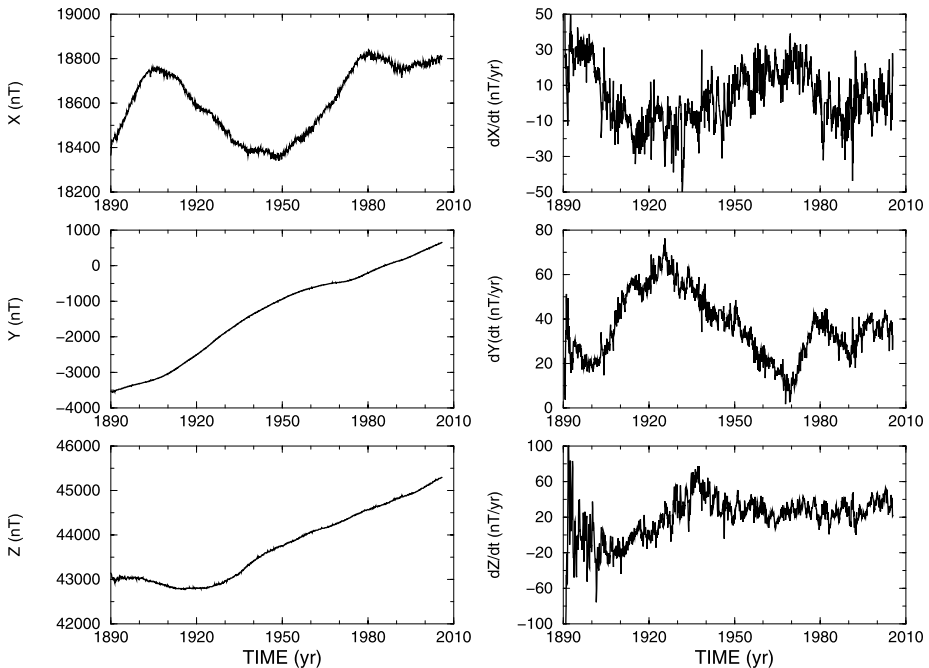


Fig. 3 Monthly means for the magnetic field and its corresponding first time derivative, recorded at the Niemegek Observatory (Early observations were actually carried out in Potsdam between 1890 and 1907, and Seddin between 1907 and 1930, and are here reported after correcting for the current location of the Niemegek observatory). Note the sudden changes of trends in the secular variation, best seen in the East component dY/dt , for instance in 1970. Those events are known as geomagnetic jerks (Courtilot et al. 1978, see Sect. 4.1.2)

Edinburgh) is described. Interesting accounts of the history of geomagnetism are otherwise given by Schröder (2000), Stern (2002) and Courtilot and Le Mouél (2007).

Historical observations of the geomagnetic field are dominated by directional measurements. By the second half of the 16th century compasses were widely employed to measure declination. Inclination, which required measuring the dip of the magnetic vector below the horizontal plane (Fig. 1), was determined on a number of vessels in the late 16th and early 17th centuries. However since it never attained a place in standard navigational practice, inclination measurements are much more scarce. Useful relative intensity measurements were made only after 1790 while absolute intensity measurements were first carried out by Gauss in 1832.

The majority of the useful historical geomagnetic observations were made by mariners involved in merchant and naval shipping during their travels across the globe (Records from more than 2000 such voyages are included in Jonkers et al. 2003). There are only a small number of observations available prior to AD1590. Between AD1590 and AD1700 many more of observations exist, thanks particularly to records made by mariners working for the Dutch and English East Indian companies. From AD1700 to AD1800 the number of observations again increased due to a dramatic expansion of naval traffic especially along Atlantic and Arctic trade routes. 18th century declination observations are plotted geographically in Fig. 4. Between 1800 and 1930, in addition to observations made on the oceans by mariners, extensive land surveys were also carried out in continental interiors. All those observations

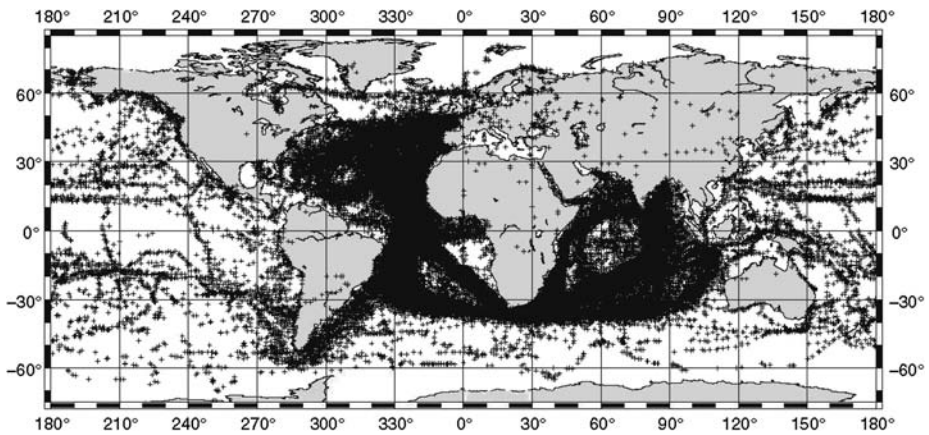


Fig. 4 Geographical distribution of the 68,076 declination observations made from AD1700–1799; some points may overlap; cylindrical equidistant projection (after Jonkers et al. 2003)

nically complement the long time series provided by magnetic observatories at fixed locations.

It remains possible that major new archives of historical records could be unearthed. However the majority of recently discovered historical data are comparatively modest, for example in newly discovered records made by explorers crossing continental interiors (Vaquero and Trigo 2006). Another possibility is that accurate indirect archeomagnetic data (see next section) could be used to supplement the historical observations especially during the 16th and 17th centuries when direct observations are scarce.

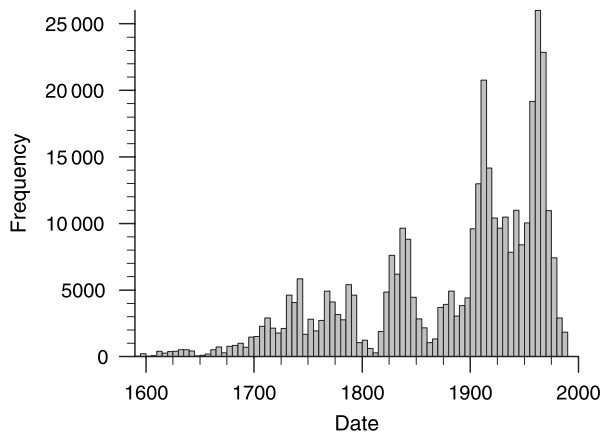
The heterogeneous origin of historical observations dictates that there are significant variations in the number of observations as a function of time. In Fig. 5 the number of historical data per 5 years is plotted together with a selection of modern data used by Jackson et al. (2000) to construct the *gufml* field model (see Sect. 3.2). Note there are rather few data available pre-AD1650. In the mid-19th century there is a sharp increase in the number of available data, thanks in part to the magnetic endeavours of Gauss and Sabine. Clearly the number of observations available in the 20th century dwarfs the number of direct observations available at earlier times. Note that it is not just the number of available data but also the type of measurement (from declination and inclination to three component vector measurements) that changes with time.

Also noteworthy are the major variations in the density of measurements with geographical location (recall Fig. 4). A bias towards commercially and militarily important shipping routes is obvious, with trans-Atlantic paths very well covered. In contrast Pacific and Polar regions are sparsely covered. There also are few observations in continental interiors, especially outside Europe. In addition, the vast majority of the maritime observations are of declination with inclination and intensity measurements much rarer due to the greater difficulties involved in their measurement.

Such a heterogeneous distribution of historical data must clearly be borne in mind when carrying out historical field modeling. Somewhat fortunately however, potential field theory shows this not to be so severe an issue, if the goal is to recover the large scales of the field produced at the core surface (Gubbins and Roberts 1983).

In order to extract the maximum amount of information from historical observations an understanding of their inherent errors is also of great importance. Jackson et al. (2000)

Fig. 5 Overall number historical data (as described by Jonkers et al. 2003), together with observatory annual means, twentieth century survey data, repeat station data and satellite data used in the construction of *gufm1* (Jackson et al. 2000). Note that this depicts a subset of data available, as some data selection has taken place, based on criteria designed to avoid the effect of the correlation in errors due to the crust



studied this issue in depth, developing error budgets accounting for observational errors, errors due to the influence of unknown crustal magnetic fields, and errors in positions due to positional uncertainty. Jackson et al. (2000) also showed that historical declination measurements were surprisingly accurate, with a typical error of only 0.5 degrees; the total error budget for such data is consequently dominated by the unknown crustal field in a manner similar to modern survey measurements. This surprising accuracy of the historical measurements, together with their worldwide extent, are the crucial factors allowing detailed reconstruction of the evolution of Earth's magnetic field over the past 400 years.

2.4 Archeomagnetic Records

The indirect observations of the magnetic field characterized as archeomagnetic records comprise the recovery of at least one of the magnetic elements, namely declination, inclination, or field strength (D , I , or B , recall Fig. 1) with accompanying age information either from a man-made structure or archeological artifact or from a relatively young volcanic flow. The term archeomagnetic usually carries with it an implicit restriction on the age of the record under consideration. Most of the archeological artifact and accurately dated lava flows are younger than 10 ka (see e.g. Korte et al. 2005; Genevey et al. 2008). But it is reasonable to suggest a temporal range of 0–50 ka, corresponding to the upper age limit on all records included in GEOMAGIA50, currently the most comprehensive database of such records (<http://geomagia.ucsd.edu/>, Donadini et al. 2006, 2009; Korhonen et al. 2008). In archeological samples or lava flows the recording mechanism for the magnetic field is typically a thermal remanent magnetization (TRM), acquired as the material cools through its magnetic blocking temperature spectrum in an ambient magnetic field (e.g. Dunlop and Özdemir 2007). Standard sampling techniques that preserve the orientation in geographic coordinates, followed by laboratory cleaning procedures (described in e.g. Constable 2007; Turner et al. 2007) allow the recovery of the ancient field directions and often the field strength too (e.g. Tauxe and Yamazaki 2007). The usual assumption is that the resulting magnetization will be aligned with the ambient field and its intensity will be linearly dependent on its strength. In some cases one or both of these assumptions will be violated and some care is required to detect this: correction for an anisotropic response to the ancient field can be accomplished for both directions and field strength; non-linearity is harder to detect, and complications in recovering the ancient field strength using the most widely

used Thellier-Thellier (and related) methods (see e.g. Tauxe and Yamazaki 2007 and Genevey et al. 2008 for details) are common since the technique requires reheating the sample in the laboratory and may produce undesired alterations to the magnetic mineralogy (not to mention that the material under study may have also suffered chemical alteration affecting the magnetic mineralogy prior to sample collection). The strength of the thermal remanence also depends on the cooling rate when it was acquired. Although corrections are possible to account for the more rapid cooling rate in the laboratory (see e.g. Genevey et al. 2003), the original rate is often difficult to estimate accurately. Considerable effort has been invested in developing new and improved laboratory procedures over the past decade, so that well-documented experimental data are easier to evaluate than they used to be. It is generally expected that declinations and inclinations can in principle be recovered to within a few degrees, and intensities to within 10%.

As with the historical geomagnetic data set there are large variations in the number of archeomagnetic data available as a function of time and place. These reflect the development of human settlements and associated artifacts and geophysical constraints on temporal and spatial distributions of lava flows. Europe for instance has a very rich archeological record that makes it possible to reconstruct the field directional behavior fairly continuously since 1000 BC (Fig. 6, Gallet et al. 2002). Considerable efforts are also put into reconstructing similar continuous regional records of the field intensity, which are generally more difficult to recover (see Fig. 7, and e.g. Genevey et al. 2009). It is worth also noting that the past decade has led to new projects targeting the construction of regional records outside the European region. In particular the use of more novel materials such as lime plasters (e.g., in Mexico, Hueda-Tanabe et al. 2004), non-welded pyroclastic deposits (e.g., in West Indies, Genevey et al. 2002) and slag deposits from copper mining (e.g., in the middle east, Ben-Yosef et al. 2008a, 2008b, 2009), offer promise of extending the archeomagnetic record in both time and space. Figure 7 demonstrates that large changes in field strength (10–15 μT) commonly occur on time-scales of just a few hundred years. Initial paleointensity results from the slag deposits even suggest that on occasion the local field strength may have been twice its current strength, and subject to rapid change (Ben-Yosef et al. 2009). Unfortunately, the number of archeomagnetic data falls off sharply prior to about 3 ka and even since that time the spatial coverage is very inhomogeneous, with almost no southern hemisphere data (e.g. Korte et al. 2005; Genevey et al. 2008). Figure 8(b) and (c) illustrate the spatial distribution for the CALS7K.2 data set of Korte et al. (2005) covering the past 7 kyr.

These archeomagnetic data can be supplemented with sedimentary records from more homogeneously distributed locations (Fig. 8(a)). Such records are fortunately available thanks to the fact that the magnetic mineral grains contained in the sediments settle under the influence of the geomagnetic field, thus producing a weak but measurable continuous magnetization (and therefore geomagnetic record) in the sedimentary section (see e.g. Dunlop and Özdemir 2007).

Archeological artifacts are the main contribution to the rise in total number of data since 1000 BC seen in Fig. 9 while the time series of variations acquired from sediments are generally much more uniform in temporal coverage. Ongoing efforts with data gathering and compilations are generating significantly larger global data sets (Donadini et al. 2009), but with similar intrinsic limitations.

Fig. 6 Directional variations of the Earth’s magnetic field in France since 1000 BC, as recovered from French archeological artifacts (all data were reduced to Paris), adapted from Gallet et al. (2002). Note the occurrence of sharp changes, or cusps, at roughly 800 BC, AD 200, AD 800 and AD 1400, known as “archeomagnetic jerks” (Gallet et al. 2003) (see Sect. 4.1.3)

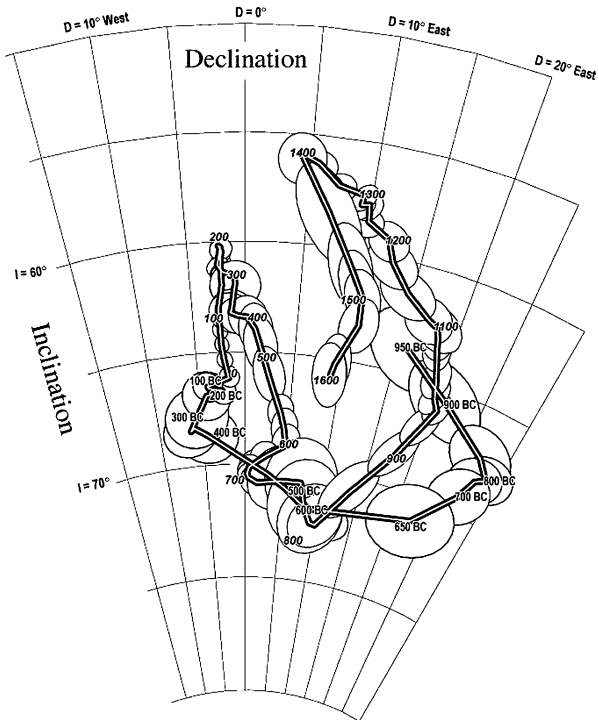
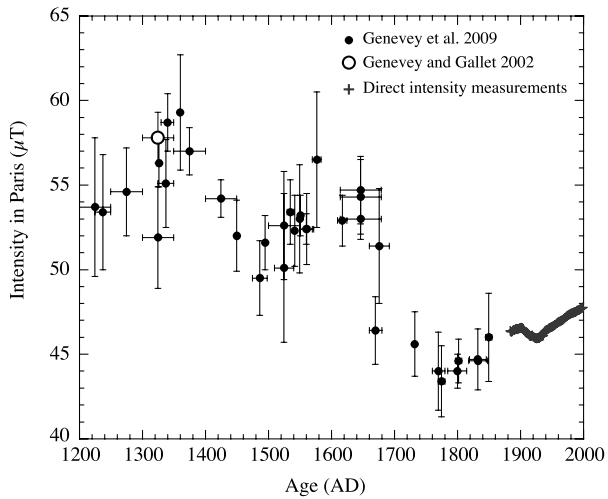


Fig. 7 Intensity of the Earth’s magnetic field in France since AD 1200, as recovered from French archeological artifacts (all data were reduced to Paris), after Genevey et al. (2009). The single open circle is from a previous study by Genevey and Gallet (2002). Direct observatory measurements for recent epochs are also shown for reference



2.5 Paleomagnetic and Seafloor Records

For longer term variations of the geomagnetic field we distinguish three major sources of data, igneous rocks, sediment records, and marine magnetic anomalies, each with their own advantages and limitations.

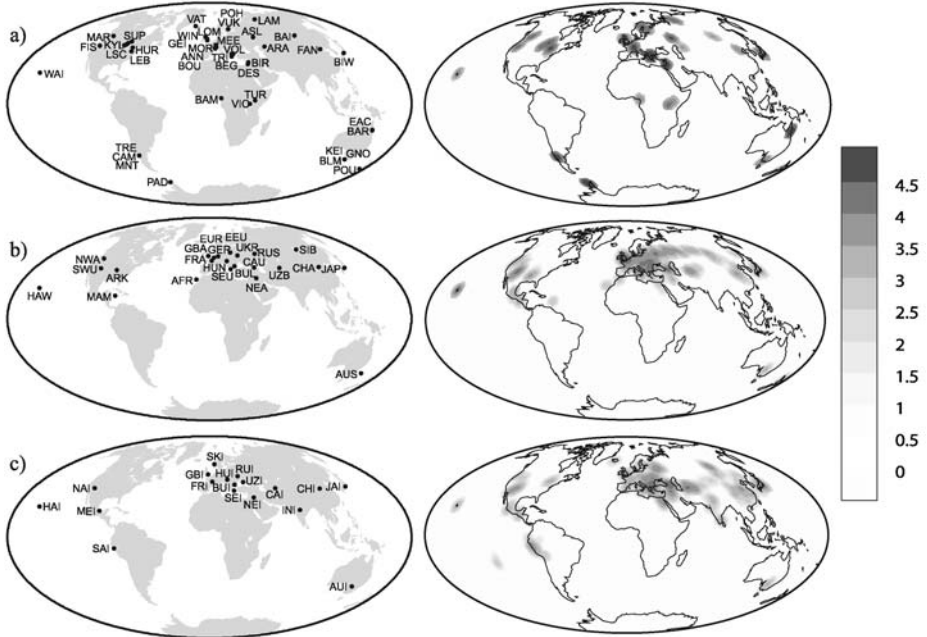


Fig. 8 Locations represented in the Korte et al. (2005) global data compilation for the 0–7 ka time interval. Sites of (a) lakes, (b) archeomagnetic directional data, and (c) archeomagnetic intensity data. *Left side* gives locations for individual sediment records, and average locations for archeomagnetic regions, *right side* contours of data concentration

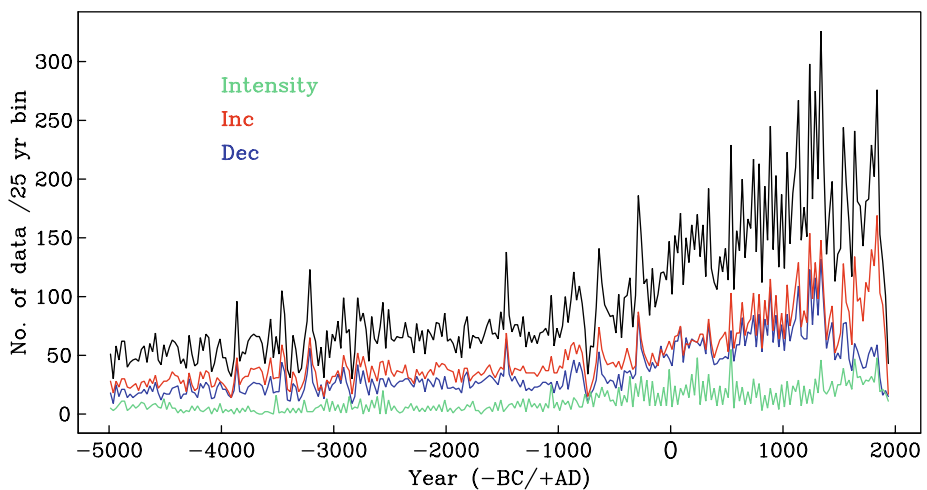
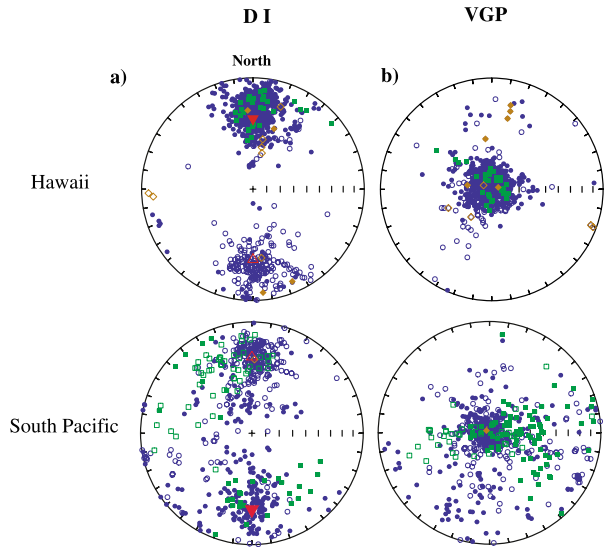


Fig. 9 Numbers of each element type available in the Korte et al. (2005) global data compilation for the 0–7 ka time interval (*blue*, declination; *red*, inclination; *green*, intensity; *black*, total number of data)

Fig. 10 Equal area projections of directional data compilations from 0–5 Ma from Hawaii and South Pacific region near 20° latitude to show (D, I) projection (left). Also shown (red triangles), the direction a pure geocentric axial dipole field would predict. Green symbols reflect sites affected by post-emplacement tectonic rotation, and brown symbols are directions derived from less than 3 samples per flow. Solid (open) circles represent normal (reverse) directions. The right panels show the same data plotted in terms of VGP positions (see Sect. 3.3). After Lawrence et al. (2006)



Igneous rock data, and in particular lava flow data which make the bulk of such data, comprise spot records (from a geological perspective) in time and space of the direction and/or intensity of the geomagnetic field. Figure 10 illustrates the nature of typical directional lava flow data and several concerns using regional compilations for two general locations, the Hawaiian islands and volcanic islands in the South Pacific region near 20° latitude. Those data sets cover the 0–5 Ma time period and are discussed in some detail by Lawrence et al. (2006), where it is noted that some flows may have undergone post-emplacement rotations that render the recovered directions unsuitable for geomagnetic field studies. Much care must be taken to avoid such lava flows. Other limitations worth noting are that the accuracy of the directions recovered depends on acquiring average results from multiple independently oriented samples distributed across each flow (< 5 samples is now generally considered marginal), and that, contrary to the much younger lava flows that qualify as archeomagnetic records, the age control usually provided by radioisotopic dating is most often not adequate to construct a time series of variations. As we shall later see (Sect. 3.3), this major limitation is one that will force a different (i.e. statistical) analysis of the paleomagnetic data compared to the one (deterministic) used when considering historical and archeomagnetic data (Sect. 3.2).

Also of some concern is the fact that as a result of plate tectonics, sites of old lava flows will usually have moved and rotated since the magnetization was acquired. Obviously, the initial location and orientation of such flows must also be recovered for their optimal use in paleomagnetic field modeling. Recent plate tectonic motions are fortunately well enough known (e.g. DeMets et al. 1994) that the bulk of the data (most of which is less than 5 Ma) can be assigned to their correct locations for when the magnetization was acquired. But such corrections grow more problematic as one goes further back in time, not least because as we shall later see (Sect. 3.3) directional information provided by such lava flows are used in ancient plate tectonic reconstructions. This will again force a different approach to the oldest of the available lava flow data. Note that this issue will also affect any other type of very ancient paleomagnetic data.

As already pointed out in the previous section, lava flows can also be used to recover intensity of the ancient field. But alteration issues (even more critical for old sam-

ples) make paleointensities difficult to recover and lava flows that provide paleodirections often fail to provide reliable paleointensities. The same issue affects other igneous rocks, such as plutonic rocks, which are also subject to additional uncertainties with respect to evaluating their cooling rates. This unfortunate state of affairs has led to intense search for improved measurement strategies less prone to alteration issues and better suited to the recovery of paleointensities. One interesting strategy has been proposed by Cottrell and Tarduno (1999) (see also Tarduno et al. 2006 for a recent review), which consists in using plagioclase crystals, extracted from igneous rocks that otherwise provide poor paleointensity, but good paleodirection records. When the plagioclase contains single domain magnetic inclusions, these are less susceptible to *in situ* chemical alteration than magnetic minerals that form part of the rock ground mass. Single crystal intensity estimates of this kind have been benchmarked using historical lava flows from Hawaii. They are especially useful for very old materials, including studies of the field during Proterozoic and Archean times. Submarine basaltic glasses have also been confirmed as good candidates for paleointensity work (Pick and Tauxe 1993; Carlot and Kent 2000; Tauxe and Staudigel 2004) despite some criticism (e.g. Heller et al. 2002). But such deep-sea submarine samples are difficult to orient with respect to geographical coordinates (Cogne et al. 1995) and therefore often fail to provide associated paleodirections. Discussions of these and other recent methods can be found in Valet (2003), Tauxe and Yamazaki (2007).

Figure 11 shows locations with igneous data ranging from 0–2 Ma in age that have been used in various recent studies of geomagnetic field structure and variability (see Johnson and McFadden 2007). As in the case of archeomagnetic data, one can see that such data are once again affected by uneven geographic sampling, with large areas of the globe lacking information. This problematic issue has recently prompted a major multi-institutional effort, the Time-Averaged Field Investigations (TAFI) project, to improve on this situation, at least as far as data younger than 5 Ma are concerned (Johnson et al. 2008). Efforts to improve the collection of igneous data of older ages (up to 3.2 Ga so far; Tarduno et al. 2007) are also ongoing (e.g. Smirnov and Tarduno 2004; Biggin et al. 2008a, 2008b), particularly in view of improving the existing paleointensity IAGA (International Association of Geomagnetism and Aeronomy) data basis (Perrin and Schnepf 2004; Biggin et al. 2009). Both the newer direction and intensity data and legacy collections are now the subject of a systematic archival project under the Magnetics Information Consortium (MagIC) at <http://earthref.org/MAGIC/>.

Marine sediment records extending to million year time scales can also be used with the advantage that they provide nominally continuous records, with well-defined stratigraphy and (barring anomalous variations in sedimentation rate) a reasonably uniform temporal sampling. However, individual sediment cores are generally less accurately oriented than the average of multiple samples from a single lava flow, there is no independence in the orientation errors among successive directions in the stratigraphic column, and in many cases only relative declination is acquired. Since there is no adequate general theory or laboratory mechanism for replicating the acquisition of remanence in sediments, only relative variations in geomagnetic field strength can be recovered, and even these rely on assumptions of uniformity in magnetic mineralogy and appropriate normalization for concentration variations (see e.g. Levi and Banerjee 1976; Valet 2003; Tauxe and Yamazaki 2007). It is likely that these assumption are violated at some level, leading to systematic bias in individual relative paleointensity estimates. An assessment of regional and global consistency among records thus plays an important role in evaluating the validity of sedimentary paleomagnetic records. The calibration of relative paleointensity variations is usually accomplished by a scaling inferred from comparison with globally

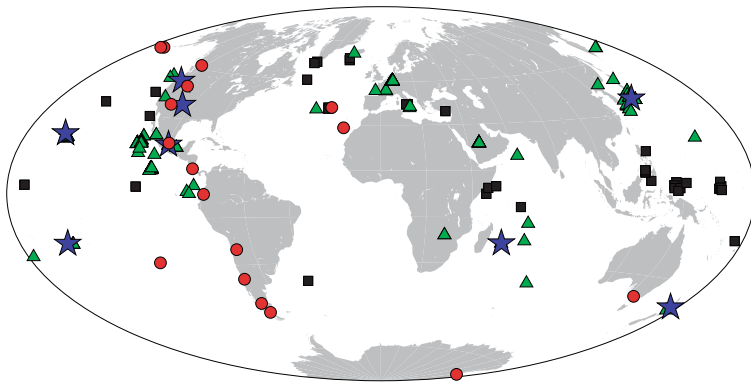
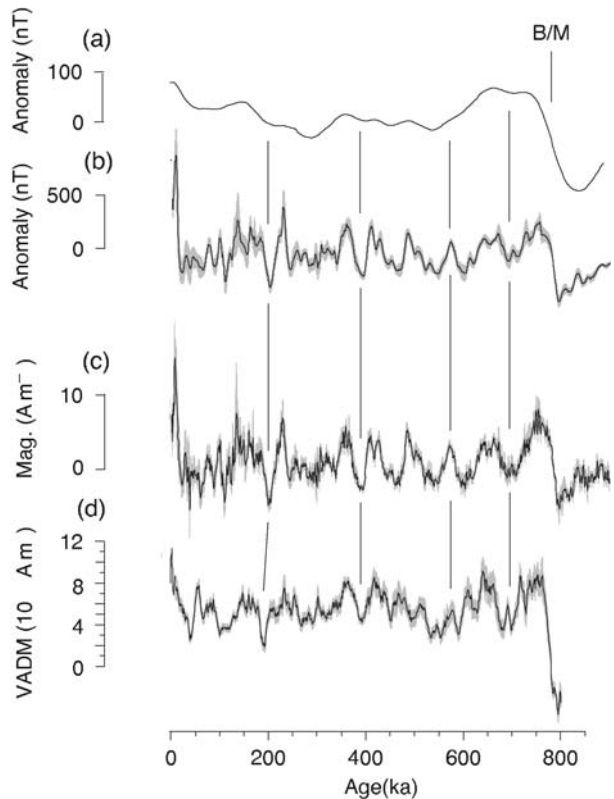


Fig. 11 Current status of global paleomagnetic data sets for 0–2 Ma paleomagnetic field modeling. The figure includes studies of lava flows (mainly directional data), that were part of the recent TAFI project (*red circles*), but lacks data from some published individual flows. *Blue stars* indicate published regional compilations of directional information from lava flows. The *green triangles* are absolute paleointensity data sites, where Thellier-Thellier measurements with specific alteration checks have been performed. Also shown as *black squares* are sediment cores included in either the Sint800 stack (Guyodo and Valet 1999) or the Sint2000 stack (Valet et al. 2005) (see Johnson and McFadden 2007 for details)

distributed absolute intensities derived from igneous rocks. The absolute values are usually converted to virtual axial dipole moments (VADM, see Sect. 3.3.1) an instantaneous measure of global axial dipole moment variation, albeit contaminated with non-axial-dipole field contributions. The resultant scaling for sedimentary records can produce intensity values that are uncertain by 10–25%. Stacking and averaging of globally distributed records (see Fig. 11) over time intervals ranging from some tens of thousands of years up to 2 My improves the reliability of the intensity record. But it also smoothes the signal which is then expected to mainly reflect variations in the axial dipole moment (Guyodo and Valet 1996, 1999; Laj et al. 2000, 2004; Valet et al. 2005). The temporal resolution in these stacks is determined by the sedimentation rate, the quality of the age control, and ability to match coeval events in different cores. Mismatches in age contribute to smoothing and bias in the results. The sint800 stacked sediment record of paleointensity variations (Guyodo and Valet 1999) for the time interval 10–800 ka is shown as the lowermost trace in Fig. 12.

Figure 12 also draws on work by Gee et al. (2000) that shows sea-surface and near-bottom marine magnetic anomaly profiles from the East Pacific Rise, along with an estimate of the sea-floor magnetization that accounts for those. Such profiles are obtained by towing a scalar magnetometer behind a ship (or a submarine), and processing the measurements to remove contributions from the external and core fields (by relying on nearby magnetic observatory or temporary fixed based station synchronous measurements, and using a contemporary IGRF field model, see Sect. 3.2). The resulting magnetic anomaly profiles are thus indeed expected to reflect contributions from the magnetized ocean crust below the ship (see e.g. Tivey 2007a). This magnetization is known to result from the oceanic crust acquiring an essentially TRM type of magnetization when it forms from rising magma at ridge axis, before moving away from those ridges (with its frozen-in magnetization) in the general context of sea floor spreading, as had originally been proposed by Vine and Matthews (1963), Morley and Larochelle (1964) (see e.g. Tivey 2007b). Provided the local ocean spreading rate can be recovered, and the process of oceanic crust production has been regular enough over the time period of interest, magnetic anomaly profiles can thus directly be interpreted in terms of records of the ancient magnetic field variations as a function of time (see e.g. Gee

Fig. 12 Comparison of geomagnetic intensity variations over the past 800 ky from sedimentary records and in seafloor and near-bottom magnetic anomalies from the East Pacific Rise at 19° S. (a) Stack of sea-surface anomaly profiles coincident with the near-bottom magnetic anomaly in (b) and inversion solution stacks in (c) (see Gee et al. 2000 for details of inversion). Ages calculated assuming constant spreading rate and an age of 780 ka for Brunhes/Matuyama (B/M) boundary. Lower panel (d), shows Sint800 sedimentary relative paleointensity stack for 10–800 ka (Guyodo and Valet 1999) combined with global archeomagnetic data for past 10 ky (Merrill et al. 1996), all scaled as virtual axial dipole moment (VADM). Modified from Gee et al. (2000)



and Kent 2007). In particular, it is clear from Fig. 12 that detailed magnetic anomaly profiles have the ability to provide a measure of relative geomagnetic paleointensity variations with broad similarities to the SINT800 record. Note that just like SINT800, such measures however mainly capture low frequency intensity variations, essentially dominated by variations in the axial dipole field. Substantial efforts are currently under way to try and recover similar detailed information about earlier field intensity variations from both sea-surface and near-bottom marine magnetic anomaly profiles (e.g. Pouliquen et al. 2001; Bowers et al. 2001; Bouligand et al. 2006; Tivey et al. 2006; Tominaga et al. 2008).

The strongest of the marine magnetic anomalies however, and those that are therefore best known and understood, are those reflecting the occurrence of magnetic field reversals, the times at which the geomagnetic field has changed polarity in the past (see Sect. 4.2). The signature of the most recent reversal (the Brunhes/Matuyama reversal, which occurred some 780 kyr ago) can also be seen in Fig. 12. Such reversals produce very strong marine magnetic anomaly signatures because of the opposite signs of the magnetization recorded in the ocean crust before and after the reversal. Extensive marine magnetic anomaly records extending back as far as the oldest sea-floor (roughly 180 Ma) have been used in successively more refined constructions of the geomagnetic polarity times scale (GPTS). Considerable work has also been devoted to providing independent checks of the GPTS with the help of magnetostratigraphy, i.e. piecewise continuous sedimentary records, and radiometrically dated igneous rocks, both of which obviously also have the ability to provide direct evidence of geomagnetic reversals. Combining all this information, the calibration of sea-floor spreading to absolute age makes it possible to provide a reliable record

of reversals for the past 160 My (see Fig. 13 and Gee and Kent 2007 for a recent detailed review). Most sea-floor magnetic anomalies from earlier times have unfortunately been subducted along with the oceanic crust so that longer term data only comes to us in a piecemeal fashion from the available geological record. Nevertheless, there are records of the reversal history quite far back, thanks in particular to the availability of very ancient sediment records (up to almost 2 Ga, see e.g. Gallet et al. 2000; Elston et al. 2002; Dunlop and Yu 2004; Pavlov and Gallet 2005, 2010).

3 Core Field Models

3.1 Satellite Era

The challenge of geomagnetic field modeling is that of converting a (sometimes very large) database of magnetic observations into a set of mathematical descriptions of the various magnetic fields that add up to produce the observed geomagnetic field. In the case of very precise satellite observations, many different sources contribute significantly. Those sources can be above the satellite (in the magnetosphere), well below the satellite (in the core, the magnetized crust or the slightly conducting mantle), but also in the immediate environment of the satellite which orbits in the upper layers of the ionosphere. The most serious issues in producing geomagnetic field models from satellite data are related to local small-scale irregularly fast-changing sources, mainly currents the satellite is bound to cross at high latitudes (where magnetospheric currents connect to the ionosphere). Several strategies can be used to avoid the signal produced by such sources, ranging from data-selection to avoid contaminated data (relying on e.g. night-side quiet-time data, see e.g. Thomson and Lesur 2007), to only using the least-affected intensity data at high-latitude. Simplified mathematical modeling of the local sources encountered by the satellite can also be used. Details of the way this can be achieved can be found in Hulot et al. (2007) and Olsen et al. (2009b). For the sake of simplicity, and since most published models actually rely on selection procedures that avoid local ionospheric sources, we will now briefly describe how models of the core field can be recovered from satellite data, assuming the data are acquired in a shell devoid of local sources.

In that case the magnetic field $\mathbf{B} = -\nabla V$ can be expressed as the negative gradient of a scalar potential V . Expanding V into series of spherical harmonics yields

$$V = V^{\text{int}} + V^{\text{ext}}$$

$$= a \sum_{l=1}^{L_{\text{int}}} \sum_{m=0}^l (g_l^m \cos m\phi + h_l^m \sin m\phi) \left(\frac{a}{r}\right)^{l+1} P_l^m(\cos\theta) \quad (1a)$$

$$+ a \sum_{l=1}^{L_{\text{ext}}} \sum_{m=0}^l (q_l^m \cos m\phi + s_l^m \sin m\phi) \left(\frac{r}{a}\right)^l P_l^m(\cos\theta) \quad (1b)$$

(Chapman and Bartels 1940; Langel 1987), where $a = 6371.2$ km is a reference radius, (r, θ, ϕ) are geographic coordinates, P_l^m are the associated Schmidt semi-normalized Legendre functions, L_{int} is the maximum degree and order of the internal potential coefficients g_l^m, h_l^m , and L_{ext} is that of the external potential coefficients q_l^m, s_l^m .

The corresponding internal potential recovered from satellite data may also include some signal from the ionospheric sources below the satellite (which the satellite indeed sees as internal sources). This issue is well-recognized. But most of this signal can be avoided through

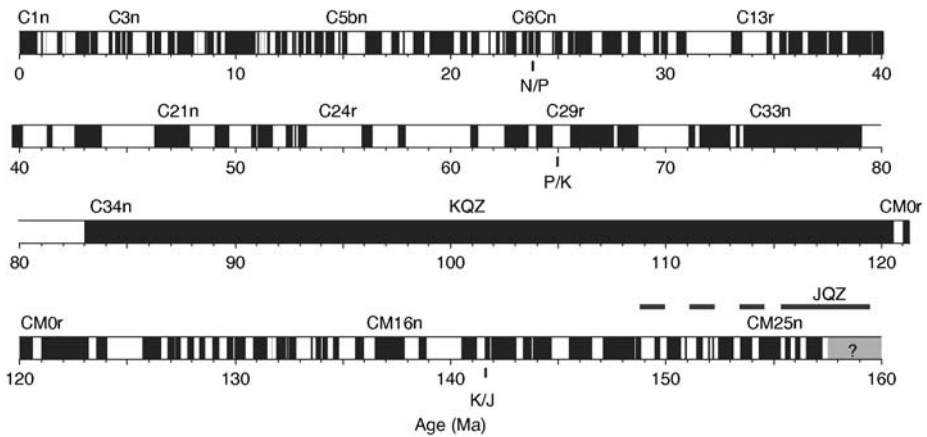


Fig. 13 Geomagnetic polarity timescale from marine magnetic anomalies for 0–160 Ma, after Lowrie and Kent (2004); largely based on Cande and Kent (1995) and Channell et al. (1995). Filled and open blocks represent intervals of normal and reverse geomagnetic field polarity. Those intervals, known as “chrons”, are labelled in an elaborate way to account for the fact that shorter chrons (subchrons) and possible but not firmly identified even shorter chrons (cryptochrons) have progressively been included (for details see e.g. Gee and Kent 2007). Only key chrons that were used as calibration tiepoints are identified by their names above the bar graph (C1n, C3n, etc.). Correlated positions of geologic period boundaries are otherwise indicated by ticks below the bar graph (N/P, Neogene/Paleogene; P/K, Paleogene/Cretaceous; K/J, Cretaceous/Jurassic). KQZ is the Cretaceous Quiet Zone, an unusually long chron also known as the Cretaceous Normal Superchron. JQZ is the Jurassic Quiet Zone, corresponding to times with low field strength (see Sect. 4.3.2)

data selection (by selecting night-time data when ionospheric sources are weakest, see however Gillet et al. 2009b), or by using so-called comprehensive modeling approaches (see e.g. Sabaka et al. 2004).

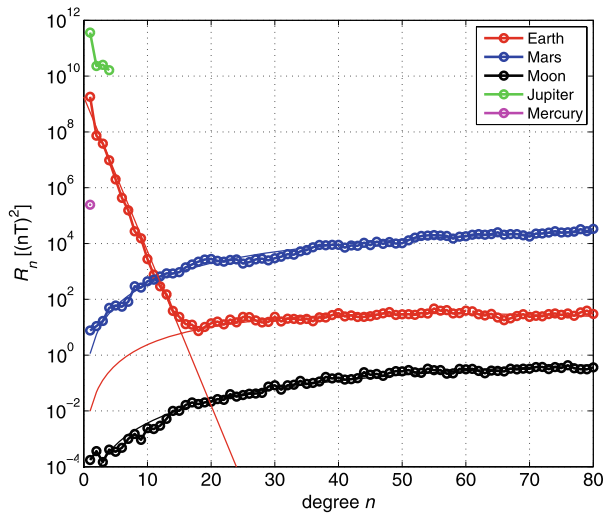
The time change of the field of truly internal origin is then modeled either by a Taylor expansion of each Gauss coefficient g_l^m, h_l^m around a given epoch

$$g_l^m(t) = g_l^m|_{t_0} + \dot{g}_l^m|_{t_0} \cdot (t - t_0) + \frac{1}{2} \ddot{g}_l^m|_{t_0} \cdot (t - t_0)^2 + \dots \quad (2)$$

(and similar for h_l^m) or by means of a spline representation (see next section where this representation is further discussed). The time variation of the external field (i.e. of the expansion coefficient q_l^m, s_l^m) is typically parameterized by proxies of the large-scale magnetospheric field variations like the Dst index (which is a measure of the strength of the dynamic magnetospheric ring-current) derived from observatory data. Those proxies are also used to correct the field of internal origin for signals produced by externally induced currents within the slightly conducting mantle. The model parameters (i.e. the expansion coefficients $g_l^m, h_l^m, q_l^m, s_l^m$ including their temporal representation) are finally estimated from the magnetic field observations using standard inverse methods (e.g. Parker 1994; Tarantola 2005).

Such procedures then lead to Gauss coefficients g_l^m, h_l^m describing the field of internal origin, with sources in the core and the crust. Potential theory does not provide any further formal way of separating the signal of each of those two sources. However, as demonstrated from models derived from MAGSAT data in particular (Langel and Estes 1982), plotting the so-called spatial Lowes-Mauersberger power spectrum of the field of internal origin (Fig. 14, which shows the contribution of each degree l to the surface average value of

Fig. 14 Lowes-Mauersberger power spectra of the field of internal origin for the Earth (after Olsen et al. 2009a and Maus et al. 2008), Mars (after Cain et al. 2003), Jupiter, Mercury (after Connerney 2008) and the Moon (after Purucker 2008) at their respective surface reference radius. Also shown are theoretical crustal spectra (thin curves, Voorhies et al. 2002) for the Earth, Mars and the Moon. Note the lack of any significant core field in the case of Mars and the Moon, which display pure crustal types of spectra



B^2 at a given reference radius, Lowes 1974) clearly suggests that its large-scale decreasing segment up to spherical harmonic degree $l = 13$ is dominated by the field from the remote core, while its fairly flat segment beyond degree $l = 16$ is dominated by the field of the nearby crust (which indeed is expected to produce such a spectrum, see e.g. Jackson 1994; Voorhies et al. 2002 and Fig. 14). Likewise, it can be argued that detectable time changes in the large scale field of internal origin most certainly reflect core field changes, while yet undetected crustal field changes likely dominate the signal beyond degree 22 (Hulot et al. 2009a; Thébaud et al. 2009).

This natural separation of the field of internal origin into a large scale component mainly produced by the core, and a small scale component mainly produced by the crust, is an essential property. It implies that only the largest scales of the field of internal origin can be associated with the core field and down-continued to the core-mantle boundary (CMB) with the help of (1a), which only holds where no sources lie. Thus models of the field of internal origin inferred from satellite data can be used to infer the core field at the CMB where it originates, provided however that one restricts those models to degree $l = 13$ or less for the field, to degree 22 or less for its first-time derivative.

Several core field models derived from Ørsted, CHAMP and SAC-C satellites data have recently been published, for which the first time derivative is now determined up to perhaps degree $l = 14-16$ (e.g. Maus et al. 2006; Lesur et al. 2008; Olsen et al. 2009a). Current efforts are directed towards also better constraining the higher derivatives of the field, to better detect possible fast core field changes (see e.g. Olsen and Mandea 2008). Figure 15 shows maps of the radial component of the present core field and of its first time-derivative at the Earth’s surface and at the CMB.

3.2 Time-Dependent Models Over Historical and Archeological Times

Building geomagnetic field models that span longer time intervals presents additional technical challenges. The simplest procedure, which has for example been used in the construction of the International Geomagnetic Reference Field (IGRF) model series (see Barton 1997 and Macmillan and Maus 2005 for the most recent revision), consists of a series of snapshots of

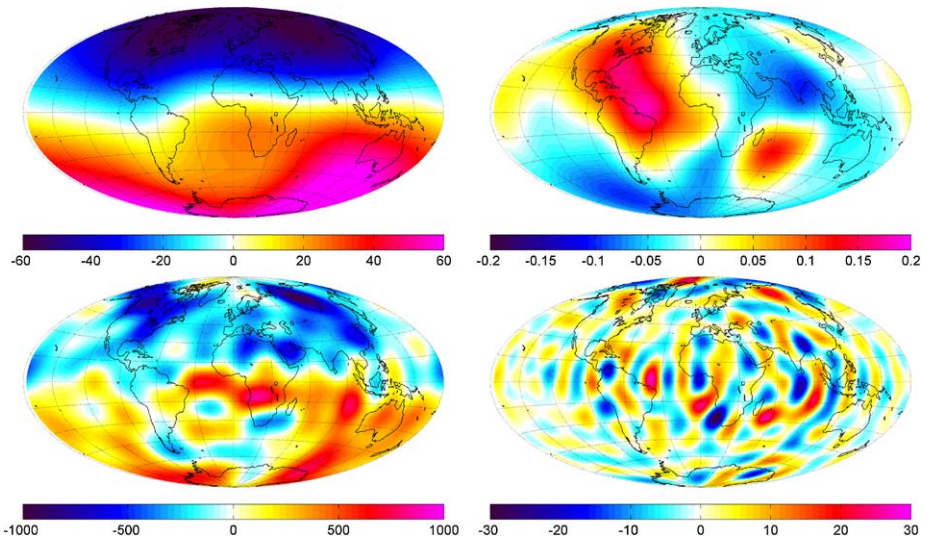


Fig. 15 Maps of B_r (left column, in units of μT), resp. dB_r/dt (right column, in units of $\mu\text{T}/\text{yr}$) at the Earth's surface (top row), and at the CMB (bottom row), according to model CHAOS-2s Olsen et al. 2009a for epoch 2004. B_r is tapered at degree $n = 13$ (8) of Olsen et al. 2009a with $\mu = 1.4 \cdot 10^{-8}$), while dB_r/dt is tapered at degree $n = 16$ ($\mu = 3.5 \cdot 10^{-10}$)

the internal field. These snapshots are available at five year intervals since 1900 and are updated every five years. The IGRF model is designed to estimate robustly the internal (core) field and is used for a wide variety of industrial and societal applications. However, due to the limitations of its linear interpolation temporal representation, it is not suitable for detailed scientific study of secular variation.

A more sophisticated approach is to invert for core field models that are by construction continuously time-dependent. Early such models relied on polynomial representations of time (e.g. Bloxham 1987; Bloxham and Jackson 1989). However the most widely used historical core field model *gufml* (Jackson et al. 2000) is based on a cubic (4th order) spline temporal representation of the Gauss coefficients first introduced by Bloxham and Jackson (1992). Under this framework each spherical harmonic coefficient g_l^m is considered to be time-dependent and is expanded as

$$g_l^m(t) = \sum_n g_l^{mn} M_n(t), \quad (3)$$

where the $M_n(t)$ are B-spline basis functions (e.g. Lancaster and Salkauskas 1986) and g_l^{mn} are the coefficients defining the time-dependency of the Gauss coefficients that must be determined from the observations.

Adopting a B-spline temporal representation has several advantages. In particular, the B-splines provide a natural basis for a smoothly varying description of noisy data. It can be shown that of all the interpolators passing through a time-series of points (say $f(t_i)$, $i = 1, N$), an expansion in B-splines of order 4 ($\hat{f}(t)$ say) is the unique interpolator which minimizes the following measure of roughness (see for example De Boor 2001)

$$\int_{t_s}^{t_e} \left[\frac{\partial^2 \hat{f}(t)}{\partial t^2} \right]^2 dt. \quad (4)$$

This form of optimally smooth representation is designed to avoid that too extra detail be present in the solution other than that truly demanded by the data.

The inverse problem of determining the model parameters g_l^{mn} can then be addressed in several ways. In the case of *gufm1* Jackson et al. (2000) rely on a regularized least-squares approach that involves minimizing an objective function of the form,

$$\Theta(\mathbf{m}) = [\mathbf{d} - \mathbf{f}(\mathbf{m})]^T \mathbf{C}_e^{-1} [\mathbf{d} - \mathbf{f}(\mathbf{m})] + \mathbf{m}^T \mathbf{C}_m^{-1} \mathbf{m}, \tag{5}$$

where \mathbf{d} is a vector of the magnetic observations, $\mathbf{f}(\mathbf{m})$ is a vector of the observations predicted by the field model, \mathbf{C}_e is the data covariance matrix and \mathbf{C}_m is a model covariance matrix that includes norms measuring the spatial and temporal complexity of the field

$$\mathbf{C}_m^{-1} = (\lambda_S \mathbf{S}^{-1} + \lambda_T \mathbf{T}^{-1}), \tag{6}$$

where λ_S and λ_T are spatial and temporal damping parameters. But other objective functions than (5) can be used, assuming e.g. Laplace rather than Gaussian error distributions (e.g. Walker and Jackson 2000), or maximum entropy rather than quadratic regularisation in both space (Jackson et al. 2007a) and time (Gillet et al. 2007a). In the case of *gufm1*, the temporal norm is further chosen to be the square of the temporal curvature of the radial magnetic field integrated over the CMB and over time,

$$\mathbf{m}^T \mathbf{T}^{-1} \mathbf{m} = \frac{1}{t_e - t_s} \int_{t_s}^{t_e} \oint_{CMB} (\partial_t^2 B_r)^2 d\Omega dt. \tag{7}$$

Here t_s and t_e are the start and end of the time interval being modeled. Note the close correspondence of this norm with the roughness measure mentioned above; this illustrates that choice of a cubic B-spline temporal basis is optimal when the temporal curvature norm is employed.

In addition to temporal regularization, spatial regularization is also an essential ingredient in historical core field modeling where data spatial coverage can be very sparse. Bloxham and Jackson (1992) and later Jackson et al. (2000) employed a measure of model spatial complexity based on minimizing the Ohmic heating due to poloidal magnetic field inferred at the CMB (since we are dealing with core sources),

$$\mathbf{m}^T \mathbf{S}^{-1} \mathbf{m} = \frac{4\pi}{t_e - t_s} \int_{t_s}^{t_e} \sum_{l=1}^L f(l) \sum_{m=0}^l [(g_l^m)^2 + (m_l^m)^2] dt, \tag{8}$$

$$\text{with } f(l) = \frac{(l+1)(2l+1)(2l+3)}{l} \left(\frac{a}{c}\right)^{2l+4}. \tag{9}$$

The optimization problem of minimizing Θ can then be solved numerically via an iterative quasi-Newton scheme (LSQN); an iterative approach is necessary when using inclination, declination and intensity data because these depend non-linearly on the model parameters g_l^{mn} . This methodology has been successfully applied by Bloxham and Jackson (1992) and Jackson et al. (2000) to compute core field models from the historical data sources described in Sect. 2.3, together with more recent observatory, survey and satellite data.

Most historical field models including the IGRF series and *gufm1* (Jackson et al. 2000) rely heavily on survey and observatory data collected at Earth’s surface. Since such observations are made below the ionosphere in an approximately source free environment the

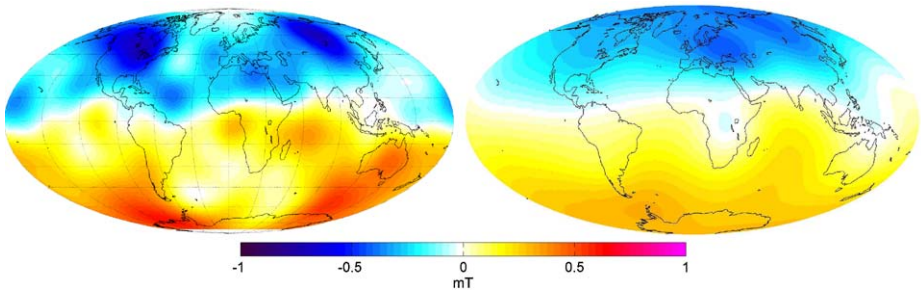


Fig. 16 Maps of time-averaged B_r at the CMB, averaged over the historical 1590–1990 period (*left*, as inferred from the *gufm1* model of Jackson et al. 2000), and over the past 7000 years (*right*, as inferred from model CALS7K.2 of Korte and Constable 2005). Units in mT

modeling strategies invert only for the Gauss coefficients of the internal field. To avoid signal from externally induced currents within the slightly conducting mantle, data selection procedures are used (such as choosing magnetically quiet days), together with temporal filtering (possible because observatories are fixed points in space) where monthly or annual means are employed. In addition to careful data selection, error budget assessment (particularly to account for the non-modelled crustal contributions) and spatial and temporal regularizations are found to be essential in the production of structurally simple, smoothly evolving, field models.

One weakness of historical core field models is that they only rely on directional observations prior to AD1840; before this no intensity observations were carried out. Directional observations alone provide enough information to constrain the core field morphology, but not its absolute magnitude (Hulot et al. 1997). Historical models such as *gufm1* have thus far assumed a simple linear trend for the axial dipole (which effectively defines the magnitude of the field model) from AD1590 to AD1840. This assumption is however rather arbitrary and attempts have recently been made to directly constrain the trend from archeomagnetic intensity data covering AD1590–1840 (see Sect. 4.1.3). Figure 16 (left), shows a map of the radial component of the average core field between AD1590 and AD1990, as inferred from the *gufm1* historical model.

Models describing the core field evolution before AD1590 can also be built using analogous modeling strategies and using the declination, inclination and intensity provided by archeomagnetic records. The magnetic field recording process in archeological artifacts and young volcanic flows is indeed fast (a few days at most). It provides a good record of past core field values. Again, however, contributions from external and crustal fields must be considered as part of the error budget. An important additional specificity of such records is the fairly large uncertainty (50 years, if not more) with which the age of each sample is known, from historical accounts, or isotopic methods. Those uncertainties are usually converted into additional contributions to the error budget. But they also imply that observations from different locations cannot be used to constrain phenomena occurring on time scales of less than say, a century. Similar dating errors affect sediment data which further suffer the effect of temporal smoothing associated with their magnetic recording process. This sets an important intrinsic limit to our ability to recover information about medium to small scale core field variations, which mainly occur on such time scales (see Fig. 19 in Sect. 4.1). This issue only mildly affects the recovery of the largest scales of the core field, which are also those best resolved by the still limited geographical distribution of data.

Early archeomagnetic field models were built as a sequence of snapshots and restricted to only the first few degrees of the field (Hongre et al. 1998) and next to somewhat higher degrees (by introducing some spatial regularization, Constable et al. 2000). More recently, the B-spline technique described above has also been introduced. But the problems in producing trustworthy field models are even more challenging than in the case of historical data. Iterative data rejection together with strong spatial and temporal regularization were key ingredients used to combat these difficulties in producing the most widely used CALS7K.2 field model spanning the interval BC5000 to AD1950 (Korte and Constable 2005). CALS7K.2 is believed to be a good representation of Earth's magnetic field up to perhaps spherical harmonic degree $l = 4$, with temporal resolution of approximately 300 years and agrees satisfactorily with a spatially truncated and temporally smoothed version of *gufm1* during the time when the models overlap. Figure 16 (right), shows a map of the radial component of the average core field over the 5000 BC to AD 1950 time period as inferred from CALS7K.2. Unfortunately the scarcity of data from low latitudes and the southern hemisphere, and a general bias of data towards Europe and the near-East makes the study of global patterns of field evolution difficult at present. In recent years the available of suitable data sources has expanded considerably and associated new field models have recently been published (Donadini et al. 2009; Korte et al. 2009).

3.3 Paleomagnetic Field Models

When moving back in time deterministic, time-dependent, spherical harmonic field modeling is usually no longer possible, because dating errors become larger than the dominant time-scales of the secular variation (see Fig. 19). Each data must then be seen as a sample of the core field value at a given known location and at a roughly known time. Fortunately this time is often known with enough accuracy that the data belonging to a common chron in the geomagnetic polarity times scale (GPTS, recall Fig. 13) can still be used for some statistical analysis of the field at times of stable polarity. Of course, not all data correspond to such stable polarity periods and some will correspond to times of transitional (reversals) or unstable polarity (excursions). Fortunately these times can be identified and the behavior of the field during such events investigated separately (see Sect. 4.2).

3.3.1 The Geocentric Axial Dipole Hypothesis and Related Concepts

A very useful concept since the early days of paleomagnetism has been the “Virtual Geomagnetic Pole” (VGP). Its usefulness is related to the fact that the core field happens to always have been essentially consistent with the so-called “Geocentric Axial Dipole” (GAD) hypothesis which states that the field has always been dominated by its axial dipole component (g_1^0), with either the present (“normal”) or opposite (“reverse”) polarity. Starting from any paleodirectional data which provides a record of I and D at a given location, the corresponding VGP is defined as being the pole of the pure dipole field that would have produced the observed I and D at this location (see e.g. Merrill et al. 1996; McElhinny 2007 for details and formulae). Figure 10 shows an example of such a conversion of directional data into VGPs for data covering the 0–5 Ma period. As can be seen, VGPs do cluster about the location of either the North or the South geographical pole as expected from the GAD hypothesis. Scatter about those poles can then be understood in terms of additional contributions from equatorial dipole and non-dipole components, each datum

being affected by different amounts of such fields as a result of secular variation acting during the time elapsed between the various data samples. This scatter can be measured and is usually referred to as the “VGP scatter”.

The fact that VGPs do cluster about the geographical poles is confirmed by all igneous directional data that are young enough to not have been affected by any significant plate tectonic motions. This provides support for the GAD hypothesis up to at least 5 Ma. For earlier epochs, and not surprisingly, VGPs from different sites will usually cluster about different poles. But extensive work has shown that those different paleopoles can be reconciled, and brought back to the geographical poles, if appropriate motions and rotations are applied to the tectonic plates to which the various sites belong. It is important to stress that such paleopoles are part of the input data used to carry out such plate motion reconstructions, and that the validity of the GAD hypothesis stems from the internal consistency of those reconstructions with all observed paleopoles, and with independent information recovered from ocean magnetic anomalies. These directly provide an image of the history of ocean floor spreading associated with plate motions (for more details see e.g. McElhinny and McFadden 2000). For even earlier epochs, testing the GAD hypothesis becomes much more difficult. But it is fair to state along with McElhinny (2007), that all tests done so far suggest that the GAD hypothesis is a reasonable first-order approximation for the time-averaged field at least for the past 400 My (see also Perrin and Shcherbakov 1997) and probably for the whole of the geological time. It will thus not come as a surprise to the reader that when investigating the times of stable polarity, much of the paleomagnetic field modeling strategy is being geared towards first, quantifying the relative amount of additional non GAD field component needed to properly account for the time-averaged field (TAF), and second, quantifying the amplitude of field fluctuations about this TAF, the so-called PaleoSecular Variation (PSV).

Before getting into the details of these TAF and PSV modeling strategies, it is useful to introduce a number of other GAD related concepts. Paleointensity data are for instance often converted into so-called Virtual Dipole Moment (VDM) values, a concept closely related to that of VGP in that it also converts local observations into information about the virtual dipole field that would have produced those observations. Whereas the VGP is the pole of this virtual dipole field, the VDM is its dipole moment. Its computation requires the knowledge of both the paleointensity B and the inclination I . Then indeed the angular distance λ_{VGP} from the sampling site to the VGP can be inferred from (see e.g. Merrill et al. 1996):

$$\tan \lambda_{VGP} = \frac{1}{2} \tan I \quad (10)$$

and the VDM from

$$VDM = \frac{4\pi a^3}{\mu_0} B (1 - 3 \sin^2 \lambda_{VGP})^{-1/2} \quad (11)$$

where μ_0 is the magnetic permeability and a the Earth’s mean radius. Note that both λ_{VGP} and the VDM can be computed without any knowledge of the declination D . This is an important property that makes it possible to compute VDMs even when considering old samples from sites that may have experienced considerable (possibly unknown) plate tectonic displacement and be affected by systematic declination (but hopefully no inclination) biases. VDMs provide estimates of the dipole moment $M_D = (4\pi a^3/\mu_0)((g_1^0)^2 + (g_1^1)^2 + (h_1^1)^2)^{1/2}$ of the paleomagnetic field to within the (quite large) uncertainty introduced by the non-dipole field contributions to the data.

Equation (10) can also be used to recover an estimate of the paleolatitude of a sampling site from directional data, if enough such data are available, so that an average direction can

be computed, hopefully reflecting the local direction of the TAF at the site under consideration (possibly to within some systematic declination bias due to plate tectonic motion, which again is not an issue). Using the inclination of this average direction in (10) then leads to an estimate of the paleogeographic latitude of the site, under the assumption that the averaging properly removed the effect of the secular variation, and that the TAF of the time was very close to satisfy the GAD hypothesis. This estimate is known as the paleomagnetic latitude of the site.

When paleointensities are available alone, neither VDMs nor paleomagnetic latitudes can be computed. But if the geographic latitude of the site happens to be known directly (when the data is young enough) or can be recovered by independent means (thanks to plate tectonic reconstruction, for instance), then a so-called Virtual Axial Dipole Moment (VADM) can still be computed with the help of (11) by just changing λ_{VGP} into the geographic latitude. Such VADM's are quite similar to VDMs, except for the fact that they now provide local estimates of the axial (and not the full) dipole moment $M_{AD} = (4\pi a^3/\mu_0)|g_1^0|$ of the paleomagnetic field to within the (larger) uncertainties introduced by both the non-dipole field and the equatorial dipole field contribution to the data.

Both VDMs and VADM's are commonly used to compare paleointensity data from distant sites, to calibrate sedimentary relative paleointensity records such as the one shown in Fig. 12, and to reconstruct the past variations of the dipole moments of the geomagnetic field.

3.3.2 Time-Averaged Field and Paleosecular Variation Models

Current time-average field (TAF) and paleosecular variation (PSV) modeling strategies are best understood in terms of the so-called Giant Gaussian Process (GGP) statistical description of the field, first introduced by Constable and Parker (1988) and next generalized by Hulot and Le Mouél (1994). The GGP description consists of considering that at times of stable polarity, the core field can be described in terms of a multidimensional stationary random Gaussian process governing a point of coordinates $\mathbf{x}(t)$ defined by the time-varying Gauss coefficients $g_l^m(t)$ and $h_l^m(t)$ in a multidimensional space. At any given instant t , this point completely characterizes the core field (by virtue of (1a)). It evolves through time about a mean point $\mu = E\{\mathbf{x}(t)\}$ with coordinates (i.e. Gauss coefficients) fluctuating about their mean values $G_l^m = E\{g_l^m(t)\}$ (resp. $H_l^m = E\{h_l^m(t)\}$). These fluctuations are statistically described by a covariance matrix $\gamma(t' - t) = E\{[\mathbf{x}(t) - \mu][\mathbf{x}(t') - \mu]^T\}$ defining the correlation times $\tau(g_l^m)$ (resp. $\tau(h_l^m)$) and variances $\sigma^2(g_l^m)$ (resp. $\sigma^2(h_l^m)$) of those fluctuations, as well as the possible cross-correlations two different Gauss coefficients may experience (see Bouligand et al. 2005 for details).

Such a GGP formalism provides a very decent statistical description of the field produced by geodynamo numerical simulations (McMillan et al. 2001; Kono et al. 2000a; Bouligand et al. 2005) and analysis of such simulations have even shown that interesting symmetry breaking properties can be detected (Hulot and Bouligand 2005). But paleomagnetic data are not as numerous as synthetic data provided by simulations and in practice a number of simplifying assumptions must be introduced. Even so, simplified GGP analysis of the historical, archeomagnetic and paleomagnetic fields have proven very useful. Hulot and Le Mouél (1994) and Hongre et al. (1998) have for instance shown that the dominant correlation time scales in the historical and archeomagnetic fields is on the order of a few centuries and decreases fast as a function of the degree l of the Gauss coefficients (as illustrated in e.g. Fig. 19). Since paleomagnetic data, and particularly those from igneous rocks, are frequently separated in time by more than a millenium, temporal correlations and time issues

are often ignored altogether. Each such data (say D_i, I_i) can then be seen as a local measure of a single independent field realization \mathbf{x}_i from a Gaussian distribution with means G_l^m (resp. H_l^m) and covariance matrix $\gamma = E\{[\mathbf{x} - \mu][\mathbf{x} - \mu]^T\}$. Additional simplifications are usually introduced by further assuming a lack of cross-correlations among different Gauss coefficients. Then γ becomes diagonal and is entirely defined by just the variances $\sigma^2(g_l^m) = E\{(g_l^m - G_l^m)^2\}$ and $\sigma^2(h_l^m) = E\{(h_l^m - H_l^m)^2\}$. Although reasonable to first order, this simplification carries a number of hidden assumptions, and one should be aware of these (see Bouligand et al. 2005; Hulot and Bouligand 2005).

Within the GGP framework, and assuming the above simplifications, all TAF and PSV modeling carried out so far can then be understood in terms of attempts to recover the mean Gauss coefficients (G_l^m, H_l^m) which define the TAF over the period considered, and the variances ($\sigma^2(g_l^m), \sigma^2(h_l^m)$) which characterize the PSV.

TAF and PSV Models for the Past 5 My Lava flows less than 5 My old, which have not significantly been affected by plate tectonic motions, are particularly well suited for this type of modeling since they directly comply with the underlying assumptions of the above simplified GGP approach. This is the time period most extensively investigated so far and the one we will now focus on. Provided enough such data are available at a given site, local statistical distributions of field parameters (usually D, I and occasionally B) can be computed. Those reflect the underlying parameters of the TAF and PSV.

In particular, the distribution of vector field values \mathbf{B}_i observed at a given location during a given chron is expected to be that of a 3D Gaussian distribution centered on the vector field value $\overline{\mathbf{B}}$ the TAF would produce (see e.g. Khokhlov et al. 2001). In this ideal situation, exactly the same modeling methods can be used as in the case of historical data, to recover estimates of G_l^m and H_l^m . In addition, moments of the local 3D Gaussian distributions of the \mathbf{B}_i values at each site can also be inverted for the variances ($\sigma^2(g_l^m), \sigma^2(h_l^m)$) of the PSV, at least in principle. In practice however, this turns out to be a difficult endeavor and only one study so far has looked into this (Kono et al. 2000b). In fact, even just inverting for the TAF turns out to be problematic, both because of the limited amount of such data, and because of the still large uncertainties affecting paleointensity data (again, see Kono et al. 2000b).

Most investigations of the TAF over the past 5 My have therefore focused on the much more numerous and accurately recovered paleodirectional data. Those studies again consist in computing averages \overline{D} and \overline{I} of the declination and inclination values available at each sampling site, and assuming that those averages reflect the declination and inclination the TAF would predict at those sites. Then the G_l^m and H_l^m can again be recovered, as if dealing with historical data (see e.g. Gubbins and Kelly 1993). Because, as already noted in Sect. 3.2, such directional data can only define the morphology of the field, the absolute value of the field is usually defined by assuming $G_1^0 = -30.000$ nT (roughly the modern value of g_1^0) when considering TAF models for normal polarity chrons, and the opposite value when considering TAF models for reverse polarity chrons. This choice is arbitrary and has in fact been challenged (Tauxe and Kent 2004) (see Sect. 4.3.2). Such models have been built for the present normal chron (Bruhnes, up to roughly 780 kyr ago), the previous reverse chron (Matuyama, between 780 ky and 990 ky ago), and for all combined normal or reverse chrons over the past 5 Ma, under the assumption that the Earth's dynamo is likely to have produced the same normal (resp. reverse) TAF during this period of time. Some models have also been built by combining all chrons (reversing the orientation of data for reverse chrons), under the additional assumption that the reverse TAF must exactly be the opposite of the normal TAF.

Not all models have been built in the same way and based on the same data basis (usually one of the two data basis set by Quidelleur et al. 1994 and Johnson and Constable 1996,

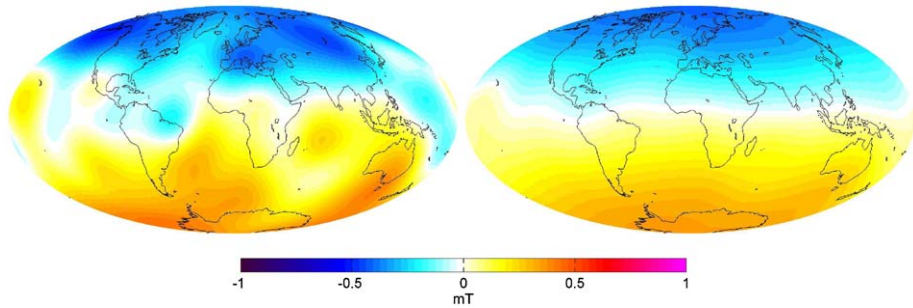


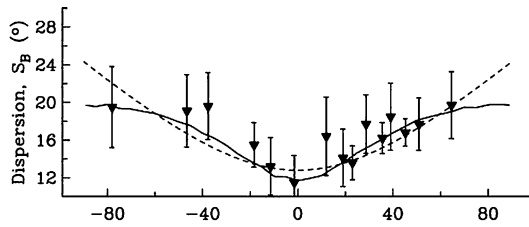
Fig. 17 Maps of the Time-Averaged Field B_r at the CMB for the past 5 My, as inferred from normal lava flow data (*left*, model LN1 of Johnson and Constable 1995), and as inferred from both normal lava flow data and additional normal marine sediment data (*right*, model LSN1 of Johnson and Constable 1997). Units in mT

both of which have been reanalyzed and updated to form the most recent TAFI database of Johnson et al. 2008). Several TAF models have been developed since the work of Gubbins and Kelly (1993) (see Johnson and Constable 1995, 1997, 1998; Kelly and Gubbins 1997; Carlot and Courtillot 1998 and the recent review of Johnson and McFadden 2007). Some of those models have also used additional marine sediment data (such as those compiled by Schneider and Kent 1988, 1990) to improve the geographical coverage of the sampling sites, in which case only average inclinations are considered (because of coring related orientation issues with respect to the declination). Figure 17 shows maps of the radial component B_r for two such TAF models plotted at the core surface: model LN1 of Johnson and Constable (1995) built from normal lava flow data for the past 5 My, and model LSN1 of Johnson and Constable (1997) built with additional normal marine sediment data. The comparison of these two maps perfectly illustrates the difficulty of recovering TAF models. Whereas LN1 would suggest fairly strong non-zonal structures in the TAF (as originally suggested by Gubbins and Kelly 1993), LSN1 clearly suggests far less structure. In fact a number of authors have argued that no significant non-zonal features can yet be recovered from normal lava flow data (McElhinny et al. 1996b; Carlot and Courtillot 1998). Clearly, the exact amount of non-zonal structure present in the TAF over the past 5 My is still a matter of debate.

Most of the problem lies in the relatively poor geographical coverage of sites and the non-uniform temporal sampling associated with volcanic processes (see e.g. Johnson and McFadden 2007). But one must also be aware that computing \overline{D} and \overline{I} independently from one another (as is done by most authors) can introduce some biases, even if the original directional data distribution can be assumed isotropic (see e.g. Love and Constable 2003). In addition, GGP models usually predict local directional distributions that are not isotropic, and this may introduce further biases (Khokhlov et al. 2001). Relying on just \overline{D} and \overline{I} for TAF modeling is thus a questionable choice. Recent methodological progress have however been made by Khokhlov et al. (2006) who showed how a given joint TAF and PSV model could be tested against any directional data without having to resort to questionable averaging procedures. They too concluded that no non-zonal structures are needed in the TAF to account for the Quidelleur et al. (1994) data they tested.

It thus seems safe to conclude that for the time being, and as far as the past 5 My are concerned, only the zonal (axisymmetric) structure of the TAF can be recovered with some certainty, suggesting a TAF with at least a G_2^0 component of 2–4% of G_1^0 and perhaps some G_3^0 of similar or less relative magnitude. Still, there are some good reasons to believe that

Fig. 18 VGP scatter over the past 5 My as a function of site latitude, as inferred from normal lava flow data selected within the PSVRL database of McElhinny and McFadden (1997). Also shown the prediction from the TK03 GGP model of Tauxe and Kent (2004) (solid line) and model G of McFadden et al. (1988) (dashed line). After Johnson et al. (2008)



some amount of non-zonal structure must be present in the TAF (see Sect. 4.3.1) and it may be that the one seen in Fig. 17, though not proven robust yet, provides some hints of it. Also of fundamental interest is the fact that the most recent investigation of Johnson et al. (2008) suggests that significantly different relative magnitudes might hold for G_2^0 and G_3^0 when considering the Bruhnes normal TAF and the Matuyama reverse TAF (a challenging result also to be discussed in Sect. 4.3).

What about the PSV over the past 5 My? Studies of this PSV have usually been carried out by investigating the way lava flow paleodirectional data scatter about their mean direction at each site. Because, as we have described, the TAF is found to mainly be axisymmetric, the PSV is also most often assumed to only be a function of the site latitude. It is traditionally measured in either of two ways: by measuring the dispersion of the direction of the field at each site, the “directional scatter”, or by measuring the dispersion of the corresponding VGPs, the “VGP scatter” already introduced in Sect. 3.3.1. Both are measured by assuming that the corresponding dispersions follow a Fisherian distribution (for details see e.g. Merrill et al. 1996). Unfortunately the transformation of field directions into VGPs does not transform a Fisherian distribution into another Fisherian distribution (Cox 1970) and this has led to quite some discussion about which measure of PSV is most appropriate (again, see e.g. Merrill et al. 1996). More recent work based on the GGP formalism has however brought very useful clarification. In particular, and as already mentioned, this formalism predicts that the distribution of field directions will usually not be Fisherian. In contrast VGP scatter, though not strictly Fisherian, can formally (albeit approximately) be related to the variances ($\sigma^2(g_l^m)$, $\sigma^2(h_l^m)$) defining the PSV (Kono and Tanaka 1995; Hulot and Gallet 1996). Figure 18 shows a typical VGP scatter curve for normal polarity lava flow data over the past 5 My. This figure clearly suggests an increase of the VGP scatter with latitude. Although perhaps exaggerated by some possible inclusion of low-quality data (as the recent investigation of Johnson et al. 2008 suggests might have been the case, at least to some extent), such a trend brings important information: it shows that the PSV produced by the geodynamo somewhat “senses” the Earth’s rotation axis, and breaks the spherical symmetry (Hulot and Gallet 1996). Although this does not come as a surprise, it nevertheless shows that VGP scatter curves can be used to investigate how and how strongly this symmetry is broken. This is not a trivial exercise, as the geodynamo, and the many variances ($\sigma^2(g_l^m)$, $\sigma^2(h_l^m)$) of a PSV model, have plenty of options for producing such a curve.

Two alternative PSV models have been proposed to account for this curve. Both start from the a priori assumption that the present field has little reason to be significantly different from the field over the past 5 My. This field must then be seen as one realization \mathbf{x} of the GGP process that has been governing the field over the recent past. Since the observed TAF contributes little beyond the axial dipole, it is reasonable to assume

that the core field Lowes-Mauersberger power spectrum shown in Fig. 14 reflects the PSV. This spectrum can then be used to construct a simple baseline PSV model by setting $\sigma(g_l^m) = \sigma(h_l^m) = \sigma_l$ and appropriately scaling σ_l , as originally proposed by Constable and Parker (1988). By construction, such a PSV satisfies the spherical symmetry (see Hulot and Bouligand 2005). It predicts the right order of magnitude for the VGP scatter curve, but not surprisingly fails to account for its increasing trend with latitude. However, just increasing the relative contribution of order one ($m = 1$) variances (Hulot and Gallet 1996), possibly mainly in the degree two ($l = 2$) (Kono and Tanaka 1995; Quidelleur and Courtillot 1996) can account for this trend. Alternatively, as originally proposed by McFadden et al. (1988) (though via some different more empirical means) and recently discussed by Tauxe and Kent (2004), one may also increase the relative contributions from the so-called “Dipole family” (or “antisymmetric family”, with $l - m$ odd) and decrease those from the “Quadrupole family” (or “symmetric family”, with $l - m$ even) variances. This too leads to a satisfactory fit to the VGP Scatter curve (Fig. 18). More detailed joint TAF and PSV tests by Khokhlov et al. (2006) however suggest that the increased degree two order one assumption is more compatible with the normal lava flow data set (at least as provided by the Quidelleur et al. 1994 database). These alternative suggestions will be discussed further in Sect. 4.3.1.

VGP scatter curves assume the PSV to be axisymmetric. But just as in the case of the TAF, some amount of non-axisymmetric structure might also affect the PSV. Can this be assessed? This is clearly an even more challenging task (see discussion in e.g. Constable and Johnson 1999; Hulot and Bouligand 2005; Bouligand et al. 2005). Indeed, even though some claims are regularly made that regionally low PSV might have affected the Pacific (e.g. Lawrence et al. 2006), those claims are just as often refuted on the basis that the data analyzed might not have properly sampled the PSV (McElhinny et al. 1996a; Johnson and McFadden 2007). This issue is also still rather open.

TAF and PSV Models Prior to 5 Ma Inferring departures of the TAF from the GAD geometry and recovering the PSV for even earlier epochs is severely limited by both the fewer data available within a given reasonably narrow time period, and the fact that plate tectonic motions must be taken into account. But the internal consistency of the TAF geometry required for plate tectonic reconstruction does provide some constraints. We already pointed out that these constraints provide the main proof that the TAF has always been dominated by a GAD in the geological past. In fact these constraints further suggest that on average over the past 200 My, some G_2^0 is also present, on order of 3% of G_1^0 (Besse and Courtillot 2002; Courtillot and Besse 2004). A number of claims have also been made that at least on some occasions in the past, the TAF could have also included additional terms (e.g. Thomas et al. 1993; Chauvin et al. 1996), and in particular some axial octupole (G_3^0) component (Kent and Smethurst 1998; Van der Voo and Torsvik 2001; Si and Van der Voo 2001; Torsvik and Van der Voo 2002). Quite a few of those claims are however based on data coming from Central Asia that can also be interpreted in terms of extreme internal deformation of the Eurasian plate (Cogne et al. 1999; Hankard et al. 2007). They also very often rely on data recovered from sediments (in particular redbeds) which may suffer from so-called inclination flattening. This flattening tends to bias inclinations towards shallower values (as a result of compaction in the sedimentation process, see e.g. Dunlop and Özdemir 2007) and map into a G_3^0 signature in the TAF (e.g. Gilder et al. 2003). Elegant methods developed by Kodama and Sun (1992) and Tauxe and Kent (2004) to detect and correct for such inclination flattening tend to confirm this interpretation (Tauxe 2005; Tauxe et al. 2008). But it should be emphasized that no such explanation can account for

shallow inclinations observed in igneous rocks (e.g. Kent and Smethurst 1998). It thus is still unclear whether the ancient TAF truly involves more than a G_2^0 of relative amount similar to that required for the recent TAF. (Note, as a final comment, that as all the above results are derived from directional data, they only constrain the relative value of the TAF with respect to G_1^0 , the long term variations of which will be discussed in Sect. 4.3.2).

Recovering information about the ancient PSV is also of prime interest. This is achieved by building VGP scatter curves similar to the one seen in Fig. 18. But just as in the case of the TAF, one has to deal with the fact that site latitudes must first be recovered. For most of the past 20 years, the reference work for such PSV studies has been the one by McFadden et al. (1991), who investigated the PSV over the 0–195 Ma time period with the help of the now rather out of date Lee (1983) lava flow data set. Site latitudes were reconstructed by directly inferring continental drift from the same data set. Recent studies either rely on more recent and precise plate motion reconstructions (when e.g. simultaneously investigating the TAF and the PSV), or directly recover the paleolatitude from the mean inclination (as described in Sect. 3.3.1), the latter option being the only one available when investigating the very ancient (e.g. Archean) PSV. This then leads to VGP scatter curves similar in shape to the one shown in Fig. 18, with a minimum scatter at the equator, and a maximum at the poles, though those extrema, and the resulting trend in between, may differ. Most investigations have followed the lead of McFadden et al. (1991) and characterized those curves via a best fit to the so-called model G of McFadden et al. (1988), which assumes a VGP scatter of the form:

$$S^2 = (\alpha\lambda)^2 + \beta^2 \quad (12)$$

Although the rationale behind this empirical model is now known to be questionable (Hulot and Gallet 1996), it does provide a very useful means (via the two parameters α and β) of quantifying the changes of the PSV through geological times (see Sect. 4.3.2).

4 Geophysical Interpretation

4.1 Core Field Changes on the Annual to Millennial Time Scales

Interpreting the manner in which the core field has changed over annual to millennial time scales requires consideration of how motional induction occurs in the outer core, where liquid iron alloy is undergoing vigorous convection driven by the cooling of the planet. The theoretical framework for describing these processes, magnetohydrodynamics, is described in some detail by Gubbins and Roberts (1987).

The fluid is assumed to satisfy the Navier-Stokes equation (in the Boussinesq approximation)

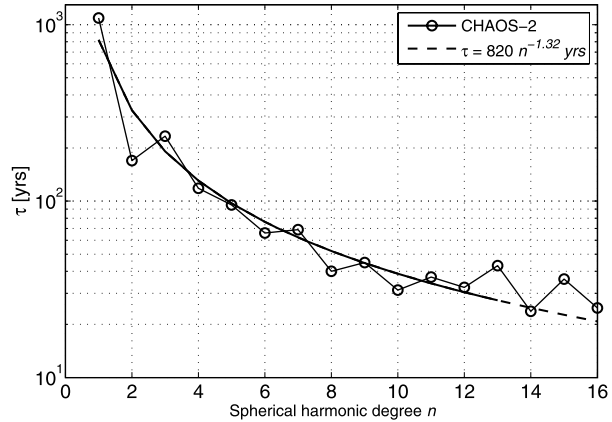
$$\rho_0 \left(\frac{\partial \mathbf{u}}{\partial t} + \mathbf{u} \cdot \nabla \mathbf{u} + 2\boldsymbol{\Omega} \wedge \mathbf{u} \right) = -\nabla p + \rho' \mathbf{g} + \mathbf{J} \wedge \mathbf{B} + \rho_0 \nu \nabla^2 \mathbf{u} \quad (13)$$

where ρ_0 and ρ' are the hydrostatic density and departure from hydrostatic density respectively, \mathbf{u} is the fluid velocity, \mathbf{B} is the magnetic field, $\boldsymbol{\Omega}$ is the Earth's rotation vector, p is the non-hydrostatic part of the pressure, \mathbf{g} the acceleration due to gravity, ν the kinematic viscosity, and \mathbf{J} the current density.

The evolution of the magnetic field is assumed to follow the magnetic induction equation

$$\frac{\partial \mathbf{B}}{\partial t} = \nabla \wedge (\mathbf{u} \wedge \mathbf{B}) + \eta \nabla^2 \mathbf{B} \quad (14)$$

Fig. 19 Time-scales of the secular variation, as defined by Hulot and Le Mouél (1994), using $\tau_n = (W_n/W'_n)^{1/2}$ where W_n and W'_n are the degree n contributions to the Lowes-Mauersberger spectra of the core field and its first time derivative. Estimates derived from the CHAOS-2 model of Olsen et al. (2009a) for epoch 2004. *Solid line* shows a two-parameter exponential fit to the data



where $\eta = 1/(\mu_0\sigma)$ the magnetic diffusivity, with μ_0 the magnetic permeability and σ the electrical conductivity of the core fluid. This equation follows from Maxwell’s equations of electrodynamics and Ohm’s law applied to moving conductors, under the magnetohydrodynamic approximation that we are considering fluid motions much slower than the speed of light.

Interpretation of the changes in Earth’s magnetic field is often simplified by neglecting the contribution of magnetic diffusion (last term on the RHS of (14))—this is known as the Frozen Flux Hypothesis (Roberts and Scott 1965; Backus 1968). This hypothesis turns out to be a good approximation if the length scale of the magnetic field feature is sufficiently large and the time scale of their variations sufficiently short. This is reasonably the case when considering changes in the observed core field that occur on the dominant secular variation time scales (as characterized by $\tau_n = (W_n/W'_n)^{1/2}$ where W_n and W'_n are the degree n contributions to the Lowes-Mauersberger spectra of the core field and its first time derivative, see Hulot and Le Mouél 1994 and Fig. 19). Then, the time evolution of the down-continued radial component B_r of the field at the CMB can be understood as the consequence of the equation

$$\frac{\partial B_r}{\partial t} = -\nabla_H \cdot (\mathbf{u}B_r) \tag{15}$$

where ∇_H is the horizontal component of the gradient operator ∇ , and \mathbf{u} is the flow at the top of the core. This equation is derived from the radial component of (14), assuming $\eta = 0$ and that the flow \mathbf{u} is tangent to the CMB. It also assumes that B_r is continuous across the CMB. This indeed is the only component of the field that can be assumed continuous across the CMB (Jault and Le Mouél 1991b). Note more generally that because of (1a), all the core field behavior we may witness at the Earth’s surface is the direct consequence of the way B_r behaves at the core surface, which is where the core field must therefore be investigated.

4.1.1 Large Scale Core Flows

In Earth’s core because the viscosity of liquid iron alloys at high pressures and temperatures is small, and because the rotation time scale is much faster than the time scale of observed field changes, the influences of viscosity and inertia are often neglected in (13). This leads to the so-called magnetostrophic approximation of core dynamics (Taylor 1963; Moffatt 1978)

$$\rho_0 (2\boldsymbol{\Omega} \wedge \mathbf{u}) = -\nabla p + \rho' \mathbf{g} + \mathbf{J} \wedge \mathbf{B} \tag{16}$$

The term $\mathbf{J} \wedge \mathbf{B}$ on the right hand side represents the Lorentz force through which the magnetic field influences the fluid motions. It is also often assumed to be reasonable to further neglect the Lorentz force in the horizontal force balance at the core surface, because the horizontal component of the magnetic field and its radial gradient will likely be small at this location. This is known as the tangentially geostrophic assumption (Le Mouél 1984; Bloxham and Jackson 1991).

Both the frozen-flux and the tangentially geostrophic assumptions imply some constraints on the way the radial component of the field behaves at the core surface (Backus 1968; Gubbins 1991; Jackson and Hide 1996; Jackson 1996; Chulliat and Hulot 2001; Chulliat 2004), and in principle some estimates of the amount of diffusion and of the strength of the Lorentz force can thus be computed to check the validity of those assumptions (see e.g., Hulot and Chulliat 2003). Indeed, various attempts have been made to quantify the amount of diffusion that may have occurred through historical times (see e.g. Bloxham et al. 1989). But the issue is complicated by our lack of knowledge of the small scales of the core field, and it has been argued that diffusion detected in this way remains within the error bounds implied by the quality of the available core field models (Backus 1988, see also Gillet et al. 2009a). As a matter of fact, several recent studies have shown that models describing the core field evolution over the past century can be built that comply with the frozen-flux constraints (Constable et al. 1993; O'Brien et al. 1997; Jackson et al. 2007b, but see also Chulliat and Olsen 2010). Over the past four centuries however, the growth of the large reversed field patch currently seen below the South Atlantic (recall Fig. 15) and which was much smaller in the early historical period (Bloxham et al. 1989; Jackson et al. 2000), is not compatible with the frozen-flux constraints (which imply the field flux to be conserved within such a patch). As first noted by Gubbins (1987) (see also Gubbins 1996), it must involve some mechanism of flux expulsion from within the core. This suggests that although negligible when considering decade to century time scales, diffusion must play a significant role when longer time scales are considered (see also Jackson and Finlay 2007 where this issue is discussed in some detail).

Adopting the frozen flux hypothesis and a core dynamic assumption (most commonly the tangentially geostrophic assumption), it is then possible to use (15) to estimate the large scale motions at the core surface that can account for observed geomagnetic secular variation (see e.g., Bloxham and Jackson 1991; Chulliat and Hulot 2000; Holme 2007). This is a highly non-unique inverse problem—regularisation is required to produce large scale flows and several choices of dynamic constraint are possible. Furthermore there are difficulties concerning the large scale secular variation produced by the small scale field and flow (Hulot et al. 1992; Eymin and Hulot 2005).

Nonetheless, the dominant features that emerge from such inversion seem fairly robust (Amit and Olson 2006; Holme 2007); a typical example of a large scale core surface flow is presented in Fig. 20. Note the intense westward gyre that runs from under west of Australia, under southern Africa through to under southern America. Another prominent feature is the anticyclonic vortex below Asia. There is also some evidence for the existence of vortices in the polar regions (Olson and Aurnou 1999; Pais and Hulot 2000; Hulot et al. 2002).

It is important to stress that such computations only give access to (estimates of) the large scale core surface flows. An important question is the extent to which the inferred core surface flows reflect deeper core flows. Early attempts of down-continuing this flow within the rest of the core were based on the assumption that the Lorenz force could also be neglected (or balanced by pressure forces) within the deep core and essentially organized along so-called Busse (1970) rolls parallel to the Earth's rotation axis (Hulot et al. 1990). Recently Jault (2008), building on the ideas of Hide (1966), suggested that for flows evolving

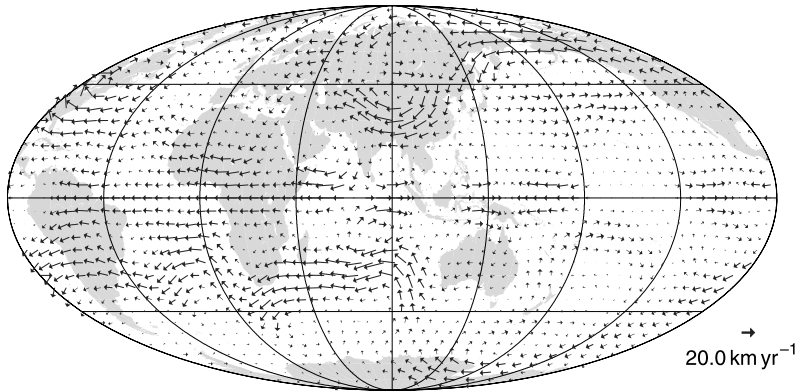
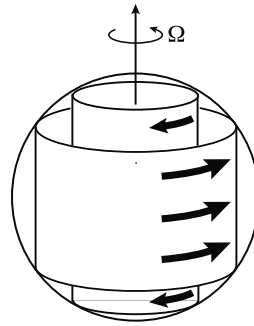


Fig. 20 Large-scale core surface flow constructed by Holme and Olsen (2006) under the frozen-flux and tangential geostrophy assumptions from a satellite observation-derived secular variation model

on time scales much shorter than the diffusive time $\tau_D = r_c^2/\eta$, where r_c is the radius of Earth's core, similar down-continuation in the form of quasi-geostrophic flows could also be performed in the presence of a relatively strong magnetic field, provided the so-called Lehnert number (Lehnert 1954) $\lambda = B/(\Omega(\mu_0\rho_0)^{1/2}r_c)$ is small enough, which is indeed likely the case in the Earth's core. Note that such assumptions also imply that the flow should then be symmetric with respect to the equator, an assumption that has the advantage of further reducing the non-uniqueness of the core surface flow determination, and which indeed seems to comply with the observations when considering fast changing flows (Pais and Jault 2008; Gillet et al. 2009a). On longer time scales, however, the dynamics may very well be different, and it has indeed been pointed out that core surface flows averaged over centuries might rather reflect some influence of the asymmetric thermal boundary conditions imposed by the (very slowly) convecting mantle (Aubert et al. 2007; Amit et al. 2008, see also Sect. 4.3.1).

One important aspect of the magnetostrophic approximation (see (16)) is that it requires the average torque exerted by the Lorentz force on each axisymmetric cylinder (about the Earth's rotation axis, see Fig. 21) to be exactly zero. This is known as the Taylor constraint (Taylor 1963). But the dynamo may very well produce magnetic fields that do not exactly comply with that constraint. Furthermore, slight departures of the CMB shape and of the gravitational field \mathbf{g} from axisymmetry may also lead to additional torques. If such torques arise, the cylinders will start accelerating. This is a mechanism by which the core and the mantle can exchange axial angular momentum on short time scales (Braginsky 1970, 1984; Jault and Le Mouél 1991a), with the solid inner core possibly also playing an important role (Mound and Buffett 2005). Because the surface expression of such cylindrical accelerations must show up as part of the estimated core surface flows, those can be used to infer the amount of axial angular momentum the core is exchanging with the mantle (Jault et al. 1988). Indeed, numerous studies have shown that observed length of day variations on decade time scales can be accounted for by this mechanism (Jault et al. 1988; Jackson et al. 1993; Jackson 1997; Holme 1998; Pais and Hulot 2000). Note that core-mantle exchange of equatorial angular momentum must of course also occur. But because equatorial torques do not break the Taylor constraint, their consequence on the core surface flow cannot be easily identified. Nonetheless their magnitude can be roughly estimated and shown to also be compatible with the weak and poorly resolved decade

Fig. 21 Torsional oscillations after Dumberry (2008b): coaxial cylinders on which torsional oscillations occur



time-scale motion of the Earth's pole of rotation (Hide et al. 1996; Hulot et al. 1996; Dumberry 2008a).

4.1.2 Torsional Oscillations and Magnetostrophic Waves

The axisymmetric cylindrical differential rotation produced by the breaking of the Taylor condition within the fluid core cannot act for too long, as this stretches the magnetic field lines (by virtue of (14)) and leads to electromagnetic restoring torques. This interplay between (13) and (14) then leads to so-called torsional oscillations (Taylor 1963; Braginsky 1970). These are a special type of Alfvén wave that propagate along the cylindrically radial component of the magnetic field perpendicular to Earth's rotation axis (see e.g. Dumberry 2008b where an accessible introductory account is given). Figure 21 shows schematically the geometrical form of torsional oscillations.

The fundamental period T_M of Alfvén waves propagating as torsional oscillation in Earth's core scales as $T_M \sim r_c \sqrt{\rho_0 \mu_0 / \{B_s^2\}}$ where $\{B_s^2\}$ is the average value of the square of the cylindrically radial component of the magnetic field in Earth's core. This quantity is poorly known; if $\sqrt{\{B_s^2\}}$ is 0.2 mT (roughly the order of magnitude of the observed rms amplitude of the large scale radial field at the core surface) then $T_A \sim 60$ years which is compatible with the observed timescale of decadal changes in zonal core flows. On the other hand if $\sqrt{\{B_s^2\}}$ is 5 mT, as might be the case if there is a strong toroidal field in the core, then $T_A \sim 2.5$ years, and torsional oscillations would be involved in more rapid core dynamics. Most tentative observations of torsional oscillations in Earth's core have to date been based on an interpretation of decadal variations of the equatorially symmetric, axisymmetric component of the core surface flow inversions, precisely to investigate the unknown $\sqrt{\{B_s^2\}}$ quantity (see e.g. Zatman and Bloxham 1997, 1999; Buffett et al. 2009). More detailed, dynamically-consistent, models of torsional oscillations are now being developed and promise exciting insights in the next few years.

Torsional oscillations have also been proposed as the origin of a peculiar phenomena known as geomagnetic jerks (Bloxham et al. 2002). These jerks are traditionally defined as sudden changes of trends in the secular variation recorded in observatories (recall Fig. 3, Courtillot et al. 1978). They often occur worldwide, though slightly earlier (by one or two years) in the northern than in the southern hemisphere (Alexandrescu et al. 1996b). This delay might be caused by the slightly conducting mantle, though this has recently been shown to be unlikely (Pinheiro and Jackson 2008). It is still unclear what may cause those jerks, and a variety of instability mechanisms have been proposed (Desjardins et al. 2001; Bellanger et al. 2001). However it seems unavoidable that geomagnetic jerks must be related to core surface flows (Hulot et al. 1993) and involve sudden changes in the acceleration of

part of those flows (Le Huy et al. 1998), including flows associated with torsional oscillations. This could explain why the occurrence of geomagnetic jerks appear to be associated with changes of trends in the length of day variations (Holme and de Viron 2005).

Another variety of hydromagnetic wave can arise from the coupling of (13) and (14) when the Magnetic (Lorentz) forces act to oppose the restoring action of the Coriolis forces. In this scenario rather slow oscillations of fluid parcels can occur and the resulting waves are referred to as magnetostrophic (Lehnert 1954; Acheson and Hide 1973). Magnetostrophic waves are also sometimes referred to in the literature as MC or magneto-inertial waves. In the simplest (plane layer) models, magnetostrophic waves have a period T_{MC} that scales as $T_{MC} \sim \Omega \rho \mu_0 r_c / B_0^2 m^2$ where Ω is the rotation rate of the fluid, B_0 is the background magnetic field strength and m is the azimuthal wavenumber of the disturbance. Taking $m = 8$ and $B_0 = 5$ mT yields a period of 300 years, while taking a weaker field strength of $B_0 = 0.5$ mT yields a period of 30,000 years. For comparable strengths of magnetic fields, magnetostrophic waves are thus typically much slower than either torsional oscillations or simple inertial waves; in geomagnetism they are therefore sometimes called ‘slow waves’. As first noted by Hide (1966) and Braginsky (1967) magnetostrophic waves possess the correct timescale to contribute to the observed secular variation. For a review of the diverse forms of wave motion possible in rapidly-rotating MHD fluids see Finlay (2008b).

The advent of modern core field models has led to observational evidence consistent with the presence of magnetostrophic waves in Earth’s core. Using high quality satellite data Jackson (2003) pinpointed the existence of wave-like features at low latitudes under the Atlantic hemisphere. Finlay and Jackson (2003) investigated the historical evolution of these wave-like features in more detail (building on the earlier work of Bloxham et al. 1989 and Jackson et al. 2000) and found a particularly distinct westward moving wave pattern centered on the equator with period of approximately 270 years and azimuthal wavenumber of $m = 5$ (Fig. 22). This spatially and temporally coherent feature possesses a significant equatorially symmetric component that is not usually reproduced in numerical simulations of the geodynamo.

Despite this recent progress, precise models of hydromagnetic waves in Earth’s core remain elusive. The primary difficulty is our ignorance of the structure and magnitude of the magnetic field within Earth’s core. Knowledge of this is a prerequisite for calculating hydromagnetic wave properties that can be compared to observations; perhaps methods of data assimilation (such as proposed by e.g., Fournier et al. 2007; Kuang et al. 2008; Canet et al. 2009, see also Fournier et al. 2010 for a review) may in the future allow a resolution of such issues. Another major unknown is the precise mechanism generating the waves in the Earth’s core. These could be driven by convection (as originally proposed by Braginsky 1964, 1967—he called such motions MAC waves), but also by shear instability, magnetic instability, hydromagnetic boundary layer instability, or forced by core-mantle topography.

4.1.3 Interpretation of Archeomagnetic Field Behaviour

Interpretations of the archeomagnetic field behaviour in terms of large scale core flows have also been proposed (Dumberry and Bloxham 2006; Wardinski and Korte 2008). Such interpretations must acknowledge the fact that archeomagnetic field models only give information about the very large scale core field and cannot account for temporal variations with time scales less than a century (recall Sect. 3.2). As a result most geophysical assumptions used in the context of the investigation of the historical field must also be reconsidered with care. Dumberry and Bloxham (2006) for instance used the frozen-flux approximation to account for the archeomagnetic field behavior in terms of the superposition of a stationary

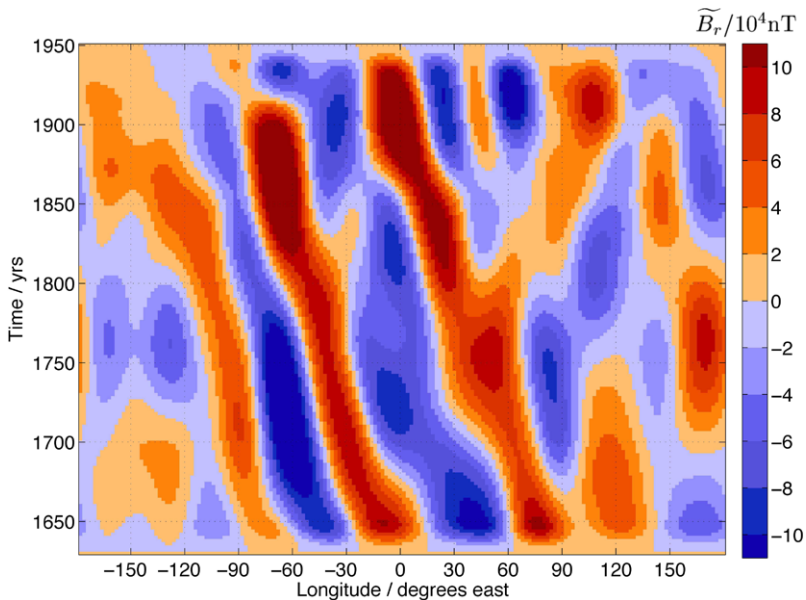


Fig. 22 Time-longitude plot of historical wave-like variations in B_r . This plot presents B_r at the equator after removal of both the time-averaged axisymmetric field and signals with time-scales larger than 400 years as a function of longitude and time. The analysis reveals oblique bands indicating the westward motion of an equatorial wave-like structure with azimuthal wavenumber $m = 5$. After Finlay and Jackson (2003)

flow and of time-dependent axisymmetric zonal flows. Those were then interpreted in terms of axial cylindrical motions to predict the possible contribution of the core to the length of day variations on millennial time scales (in very much the same way core flows derived from historical field models had successfully been used to predict length of day variations on decade time scales, recall Sect. 4.1.1). This led to a prediction with the correct amplitude, suggesting that the core could indeed be responsible for some of the length of day variations also on those time scales. However the prediction also appeared not to be correlated with the observed length of day variations. As noted by Dumberry and Bloxham (2006), this could precisely be because assuming axial cylindrical motions when investigating such long time scales is questionable, though we further note that the frozen-flux assumption could also be an issue (recall Sect. 4.1.1).

Interpreting the archeomagnetic field behaviour without invoking any of those two assumptions is also possible. Dumberry and Finlay (2007) for instance used the same type of analysis as Finlay and Jackson (2003) to directly investigate the drift of prominent magnetic field features at the core surface in the CALS7K.2 model of Korte and Constable (2005) over the past 3000 yr. They noted some wave-like westward motions close to the equator, akin to those found by Finlay and Jackson (2003) in the historical field (recall Fig. 22), mainly in the Atlantic hemisphere, but somewhat weaker and slower. They also noted a much stronger signal at mid- to high latitudes in the Northern hemisphere, where eastward and westward motions occur. These motions appear to correspond to the slow displacements and distortions of the two main high-latitude Northern normal magnetic flux patches best seen in the radial component of the time-average historical field at the core surface (Fig. 16). Those flux patches are thought to be the consequence of core downwelling flows associated with prograde vortices that concentrate the field in those regions, as suggested by both high reso-

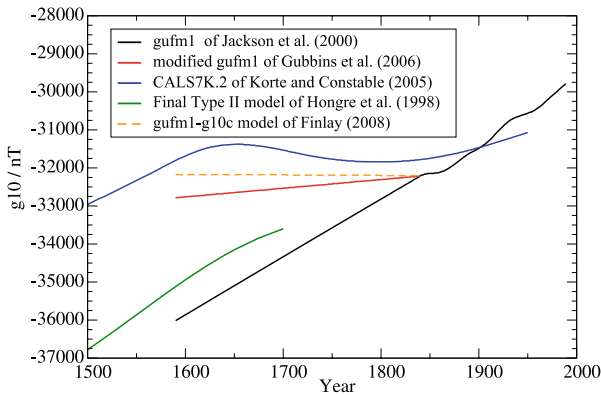


Fig. 23 Estimates of the g_1^0 Gauss coefficient over the past 500 years, from the gufm1 historical model of Jackson et al. (2000) which linearly extrapolates between 1590 and 1840 the well-constrained 1840 to 1990 historical trend (black); from the modified gufm1 models of Gubbins et al. (2006) (red) and Finlay (2008a) (dashed yellow), which use the Korte et al. (2005) archeomagnetic data to rescale the 1590–1840 gufm1 g_1^0 linear trend; from the CAL57K.2 archeomagnetic field model of Korte and Constable (2005) (blue), which only relies on the Korte et al. (2005) archeomagnetic data; and by the earlier Hongre et al. (1998) archeomagnetic field model (green). Note that the most recent models of Korte et al. (2009) based on the latest archeomagnetic data of Donadini et al. (2009) again predict a trend close to that of Hongre et al. (1998) (not shown). After Finlay (2008a)

lution core surface flow estimates (e.g. Hulot et al. 2002) and dynamo numerical simulations (e.g. Olson et al. 1999). Interestingly, Dumberry and Finlay (2007) also noted that changes in the motions they detected could be associated with so-called “archeomagnetic jerks” (Gallet et al. 2003), i.e. sharp changes, or cusps, in directional archeomagnetic plots such as the one shown in Fig. 6. In a more recent analysis of the same CAL57K.2 model, Gallet et al. (2009) further showed that such archeomagnetic jerks tend to occur at times when a simple description of the core field in terms of an eccentric (i.e. off-center) dipole reveals the center of this eccentric dipole to be at a maximum distance away from the Earth’s center. They noted this could be a consequence of the high latitude normal flux patches drifting closer to each other, and producing a field stronger in one hemisphere (say the Pacific hemisphere, as is presently the case), and weaker in the opposite hemisphere. More generally, and despite the limited resolution of the CAL57K.2 model, it is clear that high latitude normal flux patches must have undergone significant motions over the past millennia, as is apparent from the very weak signature they leave when the archeomagnetic field is averaged over thousands of years (recall Fig. 16). On the million year time scale however, and as will later be discussed in more detail (see Sect. 4.3.1), high latitude flux patches seem to display a statistical preference for being located where they presently stand.

A number of studies have also looked into the interpretation of the recent variations in the axial dipole moment of the core field. We know for sure that this moment (proportional to the absolute value $|g_1^0|$ of the g_1^0 Gauss coefficient, recall Sect. 3.3.1) has been decreasing fast since 1840, when systematic direct observations of the magnetic field intensity were first introduced. Its earlier evolution however can only be estimated from archeomagnetic data and is much harder to resolve accurately (Fig. 23). Some studies (e.g. Hongre et al. 1998; Genevey et al. 2008; Valet et al. 2008; Korte et al. 2009) would suggest a general decreasing trend over the past millenium (amounting to an increasing trend in the presently negative g_1^0 coefficient), while others (Korte and Constable 2005; Gubbins et al. 2006; Finlay 2008a) would favor a more stable behavior over the AD1500–1800 time period, if not an oscillatory

behavior (Genevey et al. 2009). Whatever the exact long-term trend, there is little doubt that the axial dipole moment decrease observed since 1840 is related to the evolution of the reverse patch currently seen below the South Atlantic (recall Fig. 15, Gubbins 1987; Bloxham and Jackson 1992). How such a large reverse patch can develop is still an open issue. Hulot et al. (2002) noted that it is located where retrograde vortices are to be seen in their detailed core surface flow calculations and pointed out that such vortices are found to indeed be associated with flux expulsions in many numerical simulations. More recently, however, Olson and Amit (2006) pointed out that more complex mechanisms must be at work, involving both flux expulsion and meridional advection of magnetic flux by the core flow.

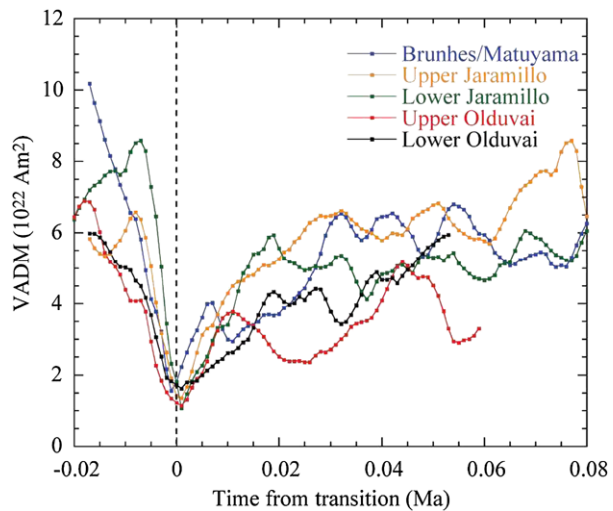
4.2 Reversals and Excursions

One of the motivations for investigating the current fast decrease of the axial dipole is that, were it to go on for another two millennia, it would result in a polarity reversal. Whether this has any chance of happening has been the subject of much speculation (see e.g. Constable and Korte 2006 for a review). Although a very recent investigation of a numerical dynamo simulation suggests that some reversal precursors could possibly be found by inspection of the field morphology at the core surface, no such candidate precursor was found when inspecting the present field (Olson et al. 2009). This might not be a surprise since results from a more systematic scaling study of the limit of predictability of dynamos suggest that no reversal can possibly be predicted so far ahead of time (Hulot et al. 2009b). In fact, as can be seen in Fig. 12, it often happened in the past that the Earth's dipole field experienced similar fast drops without undergoing a reversal.

Paleomagnetic data more generally bring important information about the way the field behaves during a reversal. For the most recent reversals (over the past few My) sediment data can provide relatively high-resolution time series of the inclination, declination and relative intensity at given locations, with some reasonable time-control. Lava flow data are quite complementary. They can provide ordered sequences (as defined by the flow stratification) of spot readings of the absolute intensity (though not always), inclination and declination. But the time elapsed between two successive flows is impossible to measure with enough accuracy. Synchronizing information from various types of data and sites is thus extremely difficult. Interesting attempts to produce time-varying spherical harmonic field models of reversals analogous to those produced from archeomagnetic data have recently been published (Leonhardt and Fabian 2007; Ingham and Turner 2008; Leonhardt et al. 2009). Such models can account for the data used to build them, and provide interesting insight (see below). But they rely on many free parameters and involve arbitrary adjustments for precise synchronization of data from different sites and to ensure uniqueness of the model. Less detailed, but perhaps more robust information about reversals can be recovered by relying on simpler tools, such as the VADM value and the VGP position that can be computed from any time series or sequence available at a given site (recall Sect. 3.3.1).

Considerable work has been devoted to this type of investigation, and the interested reader is referred to reviews such as those by Merrill and McFadden (1999), Coe and Glen (2004) or Glatzmaier and Coe (2007). Here we will focus on what appears to be the most important characteristics of reversals inferred so far. The first of these is that reversals only occur once the field intensity has already dropped to a value on order 10–20% of its present value, comparable to the average intensity we would witness if the axial dipole field was to vanish, keeping the rest of the non-dipole field to its current magnitude. The intensity might drop to an even lower value, but this is difficult to assess because of the intrinsic

Fig. 24 Field intensity variations at times of reversals, across the five last reversals, as estimated from sediment data, after Valet et al. (2005)



limitations of paleointensity records. The way the field decreases to such a low value has been found to be complicated. Relative sedimentary paleointensity records built in very much same way as the one shown in Fig. 12d, but for the 0–4 Ma time period, initially suggested that just after recovering from a previous reversal, the VADM (a measure of the dipole field strength), would start to progressively decrease in a staggered manner until the next reversal, resulting in a so-called saw-tooth pattern (Valet and Meynadier 1993; Meynadier et al. 1994). However, this has been much disputed ever since (see e.g. Valet 2003 and Tauxe and Yamazaki 2007 for recent discussions). Although there is still some evidence of a weak correlation between the average intensity of the field during a given chron, and the length of the chron (Tauxe and Hartl 1997; Constable et al. 1998), more recent data suggest that conditions for a reversal to occur are usually met only after some rather erratic intensity decline ending with a final drop over several millennia. This can be seen in Fig. 24, which would also suggest that the recovery of the field strength after the reversal is perhaps somewhat quicker (though this also happens to be disputed see e.g. Tauxe and Yamazaki 2007). Note that this figure also shows that the time-scales involved in the reversal process are short compared to the time (on order 40 ky, see e.g. Gubbins and Roberts 1987) it would take for the dipole field to freely decay because of core convection becoming quiescent for some time (with just the diffusive term on the RHS of (14) governing the field evolution). This already shows that reversals are the result of some active dynamo process.

The second important characteristic of reversals is that the field appears to go on being dominated by its axial dipole component until quite close to the reversal itself. Recent investigations of the four most recent reversals, again from sedimentary records, clearly show that the VGP latitudes remain close to the geographical pole until they suddenly switch to the opposite geographical pole, within a matter of 2000 years for sites close to the equator, but substantially more slowly, within 10,000 years, for sites closer to the geographic poles (Fig. 25, Clement 2004). This dependence of the length of the reversal event on the site latitude is a manifestation of the third important characteristic, namely that, the field is usually not dominated by its dipole component during the reversal itself.

This finding is also evident from the observation that VGP paths (i.e. the sequence of successive VGP locations as recovered from both continuous sedimentary records and lava flow irregular sequences) inferred from different sites will usually be very different. Obvi-

Fig. 25 Estimates of the local duration of reversals as a function of site latitude for the four last reversals: Bruhnes-Matuyama (*solid squares*), Upper Jaramillo (*open circles*), Lower Jaramillo (*open squares*), Upper Oluvai (*solid circles*), as inferred from sediment data. After Clement (2004)

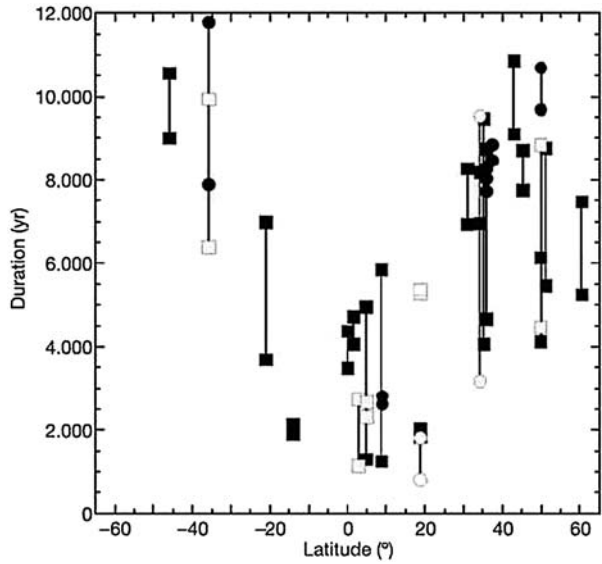
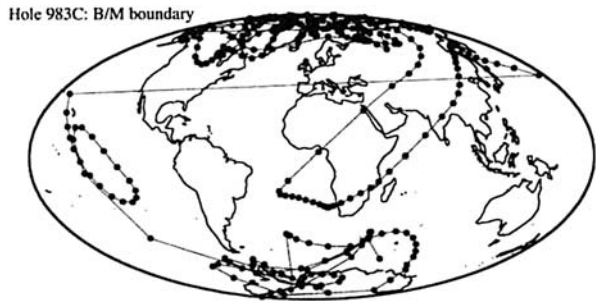


Fig. 26 Example of a VGP path for the last (Bruhnes-Matuyama) reversal, as inferred from sediment data (ODP hole 983C). After Channell and Lehman (1997)



ously, had the field remained mainly dipolar, all VGP paths would follow roughly (to within accuracy, and because of the non-negligible contribution of the non-dipole field) the same paths. This is not the case. Furthermore, even when analyzing data from a single site, VGP paths can be very complicated (Fig. 26). There is thus no doubt that the field becomes much less dipolar and has a very dynamical behavior during a reversal, presumably because of the fast changing non-dipole components of the field (as the present dominant short time scales of the non-dipole field would suggest, recall Fig. 19). This is also what tentative time-varying spherical harmonic models of the last reversal (Leonhardt and Fabian 2007; Ingham and Turner 2008), and simple forward analysis (Brown et al. 2007; Valet and Pleinier 2008) would suggest.

Complex VGP paths reaching low latitudes are not observed only at times of reversals, but also each time the field intensity gets low enough. From a pure observational point of view it is usual to define such events as “excursions” as soon as latitudes reached by VGPs are less than 45° (Jacobs 2007), to distinguish them from the regular VGP scatter associated with PSV at times of stable polarity (recall Sect. 3.3.2). But this is obviously an arbitrary choice which can lead to the classification of one such event as being an excursion when the data analyzed come from one site, and not when they come from another site. This issue is well recognized and more sophisticated ways of distinguishing excursions from regular

PSV have been proposed (e.g. Vandamme 1994). It also raises the interesting question of the pertinence of considering excursions differently from regular PSV. When excursions are unambiguously identified in many sites, this is usually because all VGP paths go way below the 45° latitude limit, often reaching the opposite hemisphere and getting close to the opposite geographical pole, suggesting that such excursions could then amount to failed reversals.

To better understand the origin of reversals and excursions, and the possible link between excursions and PSV, the fast growing body of 3D numerical simulations initiated by Glatzmaier and Roberts (1995) turns out to be particularly useful. Those simulations model thermo-chemical dynamos driven by the slow cooling of the Earth. Heat extracted at the core surface, and crystallization of the inner-core (which releases both latent heat and light elements at the base of the outer core) provide the conditions required for maintaining the liquid outer core in convective motion. These motions then interact in a constructive way with the magnetic field (via (13) and (14)) to permanently regenerate it, despite magnetic diffusion (i.e., ohmic dissipation). The detailed way such self-consistent simulations are carried out can be found in e.g. Christensen and Wicht (2007). Although these simulations are run in parameter regimes that are still very remote from that of the geodynamo (see also Dormy et al. 2000), they show in particular that by varying the control parameters, but keeping the same fundamental equations, a wide range of different dynamo behaviors can be found. Some regimes display no reversal at all. Others display so many reversals that the distinction between PSV, excursions and reversals is virtually irrelevant (see e.g. Christensen and Aubert 2006). This then suggests that the geodynamo regime could currently be intermediate, with excursions and reversals simply rare enough that periods of stable polarity can be defined from an observational point of view, without necessarily implying that PSV, excursions and reversals result from distinctly different processes. Detailed analysis of numerical simulations indeed suggest that reversals occur when in the course of their spontaneous evolution dynamos reach a state that meets specific conditions. Those conditions are found to be subtle (e.g. Wicht and Olson 2004; Aubert et al. 2008a), so subtle that even marginally perturbing a dynamo that is apparently bound to reverse can change the course of the field evolution, produce an excursion, or even prevent any such event (Hulot et al. 2009b). This then suggests that reversals could result from a late option sometimes taken by the field when a particularly extreme excursion is already under way. What then makes a reversal a reversal and not just an excursion is that the subsequent evolution of the geodynamo enables the new polarity to establish itself in the entire core, and in particular within the inner core, as suggested by e.g. Gubbins (1999) following Hollerbach and Jones (1993, 1995) (though for an alternative view of the importance of magnetic diffusion in the inner core, see Wicht 2002). This would explain why substantially more excursions are observed than reversals, as is also found in numerical simulations (e.g. Wicht 2005). Finally, simulations also show that other events that would qualify as excursions from an observational point of view are in fact manifestations of extreme PSV (Wicht 2005). Numerical simulations thus suggest that excursions could indeed form an intermediate class of phenomena ranging from an extreme expression of PSV to failed reversals.

Reversals produced by numerical dynamo simulations can also be used to produce plots such as those shown in Figs. 24–26 (see e.g. Coe et al. 2000; Coe and Glen 2004; Wicht 2005). One particularly important lesson learned from such investigations is that reversals do not always occur in the same way, even within a single dynamo run with fixed parameters and boundary conditions (Coe et al. 2000). VGP paths are site dependent, and generally as complicated as the one shown in Fig. 26. In addition two successive reversals

can lead to very different paths even when considering a given fixed site, as is observed in the data (see e.g. Channell and Lehman 1997). In contrast however, when heterogeneous thermal boundary conditions are imposed on such dynamos, some statistical preference for specific (but rather broad) bands of longitudes can be found in the VGP paths (e.g. Coe et al. 2000; Kutzner and Christensen 2004). When the imposed thermal boundary conditions are inferred from seismic tomography of the present lower-most mantle (such as that of Masters et al. 1996) assuming more heat than average flows out the core into seismically faster-than-average and therefore cooler regions of the mantle (but note that this is not a trivial assumption, as some of the seismic structure may well be of compositional, rather than thermal, origin), those bands roughly lie at American and East Asian longitudes. This result is interesting because it shows that some signature of the mantle influence on the core might be obtained by investigating the statistics of VGP paths. Such preferential bands have been reported by several authors when analyzing sediment data (Laj et al. 1991; Clement 1991), and some lava flow data have even provided evidence of temporary clustering of VPGs within more specific regions inside those bands (Hoffman 1992). But the robustness of those early results has since been questioned (e.g. Langereis et al. 1992; Valet et al. 1992; McFadden et al. 1993; Prévot and Camps 1993; Barton and McFadden 1996) and even though particularly careful more recent analysis of reversals and excursions recorded in lava flows over the past 20 My do lend support to some of those earlier results (Love 1998), it is perhaps best to view the question of the two preferred longitudinal bands as still open from an observational perspective (Mazaud 2007).

4.3 Core Field Long-Term Behavior

4.3.1 *The Past 5 My*

Guidance from numerical simulation has also proven very useful for the interpretation of the long-term behavior of the Earth's dynamo. Many simulations have for instance looked into the possible influence of heterogeneous thermal boundary conditions on the structure of the TAF, for comparisons with the 0–5 Ma TAF inferred from paleomagnetic data (recall Sect. 3.3.2 and Fig. 17). This has led to very stimulating results (e.g. Bloxham 2000; Olson and Christensen 2002; Christensen and Olson 2003; Gubbins et al. 2007; Willis et al. 2007; Aubert et al. 2008b; Davies et al. 2008). Such simulations usually impose heterogeneous thermal (heat flux) boundary conditions based on the Masters et al. (1996) shear-wave mantle tomography model (as in the VGP preferred longitudinal bands investigations mentioned in the previous section). They do however differ in both their choice of the magnitude of the thermal contrast to be applied with this morphology, and in their choice of dynamo control parameters (which we stress are anyway very remote from those of the geodynamo). Such differences can lead to a variety of geomagnetic field behaviors. Interestingly, all such “tomographic” simulations lead to a TAF with some amount of non-zonal structure, reminiscent of what can be seen in Fig. 17. To our knowledge however, none have yet succeeded in recovering the G_2^0 Gauss coefficient considered most robust in the observations (recall Sect. 3.3.2). In fact, the only simulation so far that did produce a TAF with G_2^0 and G_3^0 coefficients of the right sign and magnitude is one which simply assumes a Y_1^0 thermal boundary condition at the core surface, forcing a higher heat flow in the northern hemisphere, than in the southern hemisphere (Olson and Christensen 2002). Perhaps this is a suggestion that a more antisymmetric heat flow component is imposed by the mantle than suggested by the Masters et al. (1996) tomography model.

Another intriguing result to come from dynamo simulations is model *g* of Glatzmaier et al. (1999), run with perfectly homogeneous thermal boundary conditions and analyzed

in detail by Bouligand et al. (2005). This simulation also produced a G_2^0 of a relative magnitude comparable to that of the observed TAF, but with the wrong sign. This wrong sign might lead one to reject such a simulation as being unrealistic. But it turns out that for such homogeneous dynamos, if a solution is found with a TAF displaying a mix of G_1^0 and G_2^0 coefficients, then a “mirror symmetry” solution can always be found with a TAF displaying the same G_1^0 , but the opposite G_2^0 (see Hulot and Bouligand 2005 for details). Thus simulation *g* of Glatzmaier et al. (1999) actually shows that even homogeneous thermal boundary conditions can produce a TAF with the right G_2^0 coefficient. It is worth further pointing out that the existence of “mirror symmetries” in such dynamos more generally implies that four different fundamental states can be sustained (Hulot and Bouligand 2005). To see this, first recall that changing \mathbf{B} into $-\mathbf{B}$ in a solution always leads to a second solution (since such a sign change is compatible with (13) and (14), and all other dynamo equations, see e.g. Christensen and Wicht 2007). This is formally why dynamos may experience magnetic field reversals. But as noted by Hulot and Bouligand (2005), “mirror symmetries”, when applicable, imply in much the same way that a third and a fourth state can also be found by either changing the sign of all coefficients of the “Dipole family” (as defined in Sect. 3.3.2) or changing the sign of all coefficients of the “Quadrupole family”. Of course, it may be argued that mirror symmetries cannot strictly apply to the geodynamo, which does not see exactly homogeneous boundary conditions. But it could be that two closely related pairs of equivalent states exist, leading to the possibility of observing “Dipole family” dominated and “Quadrupole family” dominated reversals, in addition to the better known full field reversals. As explained by Hulot and Bouligand (2005), this could provide a natural explanation for the fact that observed normal and reverse TAF field models, computed by ignoring the possibility of such partial reversals, seem to differ.

Several important recent studies indicate that the non-zonal structure in the Masters et al. (1996) tomography model perhaps captures some of the true heat flow pattern imposed by the mantle on the geodynamo. Aubert et al. (2008b) noted that such boundary conditions would lead to a TAF displaying some of the non-zonal features found in TAF models (particularly that of Kelly and Gubbins 1997), as well as to a statistical preference for core flow patterns bearing some resemblance with the time-averaged core surface flow inferred from historical data (Amit and Olson 2006). In their simulations, the preferred convection patterns are further shown to be associated with some asymmetric growth of the inner core, compatible with the asymmetric pattern seismically observed in the upper layers of the inner core (e.g. Tanaka and Hamaguchi 1997; Cao and Romanowicz 2004).

Strong locking of the geomagnetic field morphology itself can also be achieved if appropriate thermal contrasts and control parameters are imposed. Such simulations produce high-latitude patches strikingly similar to those found in the time-averaged historical field shown in Fig. 16 (see e.g. Gubbins et al. 2007; Willis et al. 2007). Whether such strong locking of the field actually occurs is however debatable as it would also imply that the archeomagnetic field and the TAF be very similar to the time-averaged historical field. This does not seem to be the case (compare maps in Figs. 16 and 17). Although one could argue that this is simply because the archeomagnetic field and TAF models are not yet sufficiently resolved, it seems more likely that no strong locking has permanently been at work. One possible scenario is that the field can often be temporarily locked in the configuration it has had over the past centuries (with characteristic high-latitude patches below the Americas, Asia and South of Australia), while still regularly moving away from that preferred configuration on millennial timescales, as CALS7K.2 suggests has been the case over the previous six millennia. This would explain why some weaker high-latitude flux patches can be found in some of the TAF

models (most strikingly in the Gubbins and Kelly (1993) model, and to a lesser extent in model LN1 shown in Fig. 17) at locations close to those seen in the time-averaged historical field. Several numerical dynamo simulations also display such behavior (e.g. Bloxham 2002; Amit et al. 2010).

Paleosecular variation produced by numerical simulations have also been investigated for comparison with the PSV recovered from paleomagnetic data over the past 5 My. A few publications have also looked into the possible influence of heterogeneous thermal boundary conditions, particularly with the aim of assessing how much non-zonal PSV those conditions could lead the geodynamo to produce (e.g. Bloxham 2000; Christensen and Olson 2003; Bouligand et al. 2005; Davies et al. 2008). Those studies show that quite different types of signature can be expected. For the time being however, comparisons with observations are much less conclusive than in the case of the TAF, not least because observational evidence of a non-zonal PSV pattern is still much debated (recall Sect. 3.3.2). More generally, all numerical dynamo simulations seem to fail to reproduce the observed magnitude of the VGP scatter. They do however often predict an increase of the scatter with the latitude, as observed (recall Fig. 18). Understanding the cause of this trend in those simulations does provide valuable insight into the origin of such trends found in the data.

As noted in Sect. 3.3.2, the behavior of VGP scatter curves is entirely dictated by the way each Gauss coefficient of the field contributes to the Lowes-Mauersberger power spectrum (Fig. 14). We also noted that the VGP scatter curve for the past 5 My could be accounted for by either assuming a stronger than average contribution from the order 1 Gauss coefficients, possibly mainly in the degree 2 (as proposed by e.g. Kono and Tanaka 1995; Hulot and Gallet 1996; Quidelleur and Courtillot 1996), or a significant imbalance between contributions from the “Dipole” and “Quadrupole” family Gauss coefficients (as proposed by e.g. McFadden et al. 1988; Tauxe and Kent 2004). Most numerical dynamos in a dipole-dominated regime have a Lowes-Mauersberger power spectrum roughly similar to that of the Earth shown in Fig. 14 (though the dipole field itself is then often too dominant, see e.g., Christensen and Wicht 2007). But the detailed way each Gauss coefficient contributes changes significantly from one simulation to the next. Interestingly, in a number of simulations, those differences arise in the form of a stronger contribution from the “Dipole” family than from the “Quadrupole” family (Bouligand et al. 2005; Coe and Glatzmaier 2006), confirming that interpreting VGP scatter curves in terms of “Dipole” versus “Quadrupole” family contributions is a possibility.

Interpreting the recent PSV (0–5 Ma) along these lines is however not without controversy. As noted by Hulot and Gallet (1996) and Tauxe and Kent (2004), this would imply a non-dipole contribution of the “Dipole” family to the field spectrum of about an order of magnitude larger than that of the “Quadrupole” family. Yet, no such imbalance is to be found in the present geomagnetic field (Hulot and Gallet 1996) which would thus have to be considered as being in a very unusual state (as also pointed out by Tauxe and Kent 2004). In contrast, the alternative suggestion that over the past 5 My the field has experienced a stronger than average contribution from the order 1 Gauss coefficients is compatible with the historical field, which displays such an imbalance (Hulot and Gallet 1996). In addition, as noted by Gallet et al. (2009), interpreting archeomagnetic field behavior in terms of high-latitude flux patches dynamics (recall Sect. 4.1.3) can provide an explanation for what may cause this imbalance, particularly in the degree 2 coefficients. It will be of great interest in the future to investigate whether this scenario can be realized in numerical dynamo simulations.

4.3.2 Geological Time Scales

Evidence for very long time scale changes in geomagnetic field behavior is primarily provided by three different types of paleomagnetic observations: the sequence of reversals as provided by the GPTS over the past 160 My (recall Fig. 13) and by additional more ancient, but more sparse magnetostratigraphic sequences (see e.g. Pavlov and Gallet 2005, 2010); a collection of paleointensity measurements (see e.g. Biggin et al. 2009), a few of which date back to 3.2 Ga (e.g. Tarduno et al. 2007); and PSV estimates (up to 2.8 Gy ago, see e.g. Smirnov and Tarduno 2004; Biggin et al. 2008a). As noted in Sect. 3.3, very little is otherwise known with respect to the geometry of the very ancient TAF, except for the fact that it must have been dominated by its GAD component since at least 400 My ago. There is no compelling evidence that this was not the case for earlier epochs. Of course, this should not be taken as evidence that the TAF has always had the same geometry, particularly as the TAF is apparently sensitive to the boundary conditions imposed by the mantle on the core (see previous section). Rather, it illustrates that current paleomagnetic data are still too few to reveal the subtle changes that are likely to have occurred in the TAF.

There are many reasons to expect the geomagnetic field to have experienced long-term changes in its behavior over geological times. The Earth is known to be ~ 4.5 Gy old (Allègre et al. 1995) and its core is thought to have formed very early on (to within roughly 100 My, see e.g. Allègre et al. 2008). But thermal models of the Earth show that the heat extracted from the core must have significantly evolved since that time (e.g. Gubbins et al. 1979; Buffett et al. 1996; Labrosse et al. 2007; Nimmo 2007). They also suggest that the inner core only started its growth (by crystallization of the central part of the core (Jacobs 1953)) quite late, probably not earlier than 1 Gy ago (Buffett et al. 1992; Labrosse et al. 2001, but see Buffett 2003). In addition, mantle convection must have always imposed time-varying heterogeneous thermal boundary conditions at the top of the core. Finally the Earth's rotation rate is known to have slowly decreased over geological times (see e.g. Varga et al. 1998). Since all of those changes affect parameters that are important in defining planetary dynamo behavior (see e.g. Christensen and Wicht 2007), it is inevitable that they must have produced some signature in the paleomagnetic data. Both the GPTS (recall Fig. 13) and the temporal power spectrum shown in Fig. 27, reveal long-term changes in the field behavior over periods of time commensurate with mantle convection timescales (Schubert et al. 2001).

The possibility that mantle convection could control the geomagnetic reversal rate has been proposed more than thirty years ago (Jones 1977) and much investigated since (for a review of the early work, see e.g. Merrill et al. 1996). Most recent investigations rely on the statistical tools introduced by McFadden (1984) (but see also Marzocchi 1997; Constable 2000; McFadden and Merrill 2000). Those have led McFadden and Merrill (1984, 1993) to conclude that reversals within the GPTS behave as if produced by a Gamma process (as originally proposed by Naidu 1971) characterized by a time-varying statistical reversal rate, defining the probability for a reversal to occur at any time, and an inhibition time, defining the short period of time after a reversal during which no other reversal can occur. The inhibition time was initially estimated to be of order 40 ky by McFadden and Merrill (1993). But this might well be an artifact linked to the limited resolution of the GPTS. Marzocchi (1997), and most recently Lowrie and Kent (2004), indeed concluded that no significant inhibition time seems to be required by the data, if additional relevant short polarity chrons (cryptochrons) are taken into account. In this case the GPTS could simply be described in terms of a time-varying Poisson process, as originally proposed by Cox (1968) and in agreement with the fact that reversals happen to be unpredictable until very shortly before they occur (recall Sect. 4.2). Such a description has the advantage

Fig. 27 Estimate of the temporal power spectrum of the Earth's dipole moment for the time interval 0–160 Ma, as inferred from a composite analysis of the GPTS (including cryptochrons, *black and grey*), of various slowly depositing ocean sediment cores (*blue, red*), of faster depositing sediment cores (*blue, brown, orange*), and of the archeomagnetic field (*pink*). After Constable and Johnson (2005) where details can be found. Note that this spectrum focusses on the dipole moment and does not include historical data, which is dominated by the much shorter time-scales of the secular variation (recall Fig. 19)

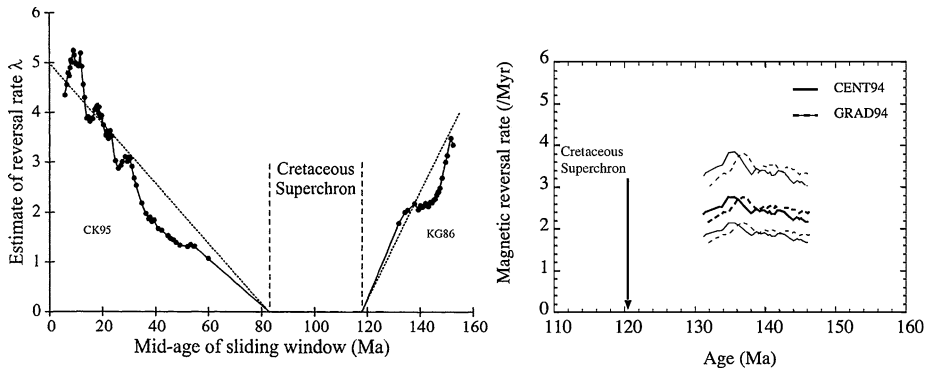
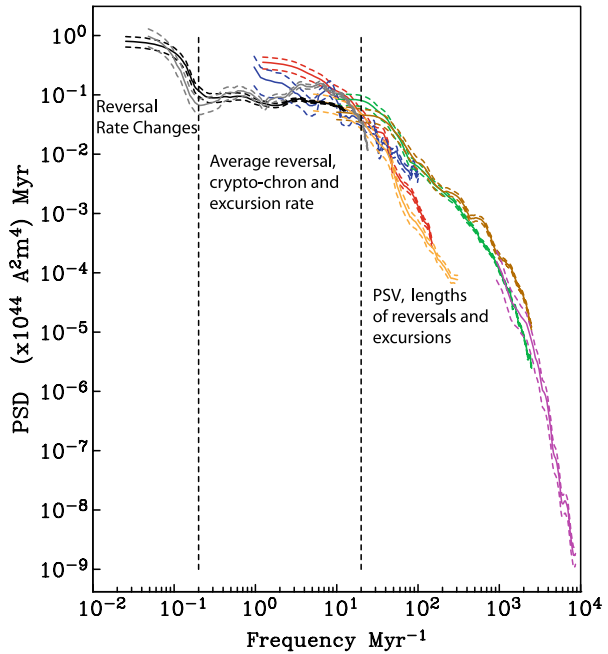


Fig. 28 Estimates of the reversal rate (in Myr^{-1}) for the time interval 0–160 Ma, following the method of McFadden (1984) and using a sliding window over 50 successive intervals. *Left*: estimate based on the Cande and Kent (1995) GPTS (CK95) for the Upper Cretaceous to Cenozoic and on the Kent and Gradstein (1986) GPTS (KG86) for the Upper Jurassic to Lower Cretaceous, with the simple linear model for the evolution of this rate proposed by McFadden and Merrill (2000) (after which the plot is adapted); *Right*: Revised estimates for the Upper Jurassic to Lower Cretaceous reversal rate based on the GPTS of Gradstein et al. (1994) (GRAD94) and Channell et al. (1995) (CENT94), with 2σ curves between which the true reversal rate lies, after Hulot and Gallet (2003)

that estimates of the reversal rate can then be readily computed (see e.g. McFadden 1984; Merrill et al. 1996). Note that such calculations usually involve some averaging of the raw information provided by the GPTS which may smooth out important sudden changes in the GPTS behavior.

Figure 28 (left) shows such a smooth estimate of the reversal rate based on an early version of the GPTS, using a sliding window over 50 successive intervals and following the method of McFadden (1984). This estimate progressively decreases between 160 Ma and the onset of the Cretaceous Normal Superchron, when the reversal process ceased, and then progressively increases again after the superchron. As noted by most authors, following McFadden and Merrill (1984, 2000), this behavior suggests that slow changes in the boundary conditions imposed by the mantle on the core could have progressively led the geodynamo to reach a non-reversing regime, and next led the geodynamo to progressively return to a frequently reversing regime. That this could have been the case is supported by some numerical simulations which show that the tendency of dynamos to produce reversals is indeed sensitive to the pattern of inhomogeneous thermal boundary conditions imposed at the core surface (Glatzmaier et al. 1999). However, an alternative interpretation of the observed transition to the superchron can also be proposed, based on the more recent reversal rate estimate proposed by Hulot and Gallet (2003) for the Upper Jurassic to Lower Cretaceous time period (Fig. 28 (right)), consistent with the GPTS shown in Fig. 13). As can be seen, this revised estimate no longer shows any unambiguous sign of decrease before the superchron. A careful look at the GPTS itself (Fig. 13) shows that the transition to the superchron may well have been very sudden. This suggests an alternative interpretation that the geodynamo could have entered the superchron as a result of a sudden change in its boundary conditions (for example, following the rapid arrival of a cold subducted slab at the core surface, the most effective way of quickly and significantly changing thermal boundary conditions at the core surface (Gallet and Hulot 1997)), or perhaps as a result of a spontaneous transition from a reversing to a non-reversing state (as proposed by Hulot and Gallet 2003 and supported by the analysis of Lowrie and Kent 2004). Although no such transition has yet been observed in numerical simulations (possibly because no very long runs displaying as many reversals as observed in the GPTS have yet been simulated), it is worth noting that numerical dynamos displaying occasional transitions between two distinctly different states have recently been found (Simitev and Busse 2009), and that simplified dynamo models can indeed spontaneously produce superchrons (Ryan and Sarson 2007, 2008). This interpretation does not deny that mantle convection could modulate the reversal rate of the geodynamo while in its reversing state (though some have argued that all of the temporal power spectrum of the field, shown in Fig. 27, from the shortest to the superchron time scales, could result from pure core dynamics, see e.g., Jonkers 2007).

Further interesting insight into the possible cause of superchrons can be gained from inspection of more ancient magnetostratigraphic data. These data reveal that at least four other superchrons have occurred over the past 1.4 Ga: the ~ 50 My long Kiaman reverse superchron, from ~ 310 to ~ 260 Ma (Opdyke and Channell 1996); the ~ 30 My long Moyero reversed superchron, from ~ 490 to ~ 460 Ma (Pavlov and Gallet 2005); and two more recently recognized (and not yet baptized) even older superchrons, one dated ~ 1 Ga and at least 16 My long (if not 30 My or more) (Pavlov and Gallet 2010), and another one dated ~ 1.4 Ga and ~ 30 My long (Elston et al. 2002). Some information is also often available with respect to the sequence of reversals that preceded or followed these superchrons. For the past 550 My, this information is summarized in Fig. 29, analogous to Fig. 28, except for the fact that reversal rates have been estimated by geological stage, rather than by relying on a moving window average, to harmonize post- and pre- 150 Ma data for which much less data is available. This figure shows that superchrons tend to occur with a rough periodicity of about 200 My, again suggesting a possible global link between the occurrence of superchrons, mantle convection and related phenomena, such as true polar wander, mantle plumes, exceptional volcanism, and even mass species extinctions

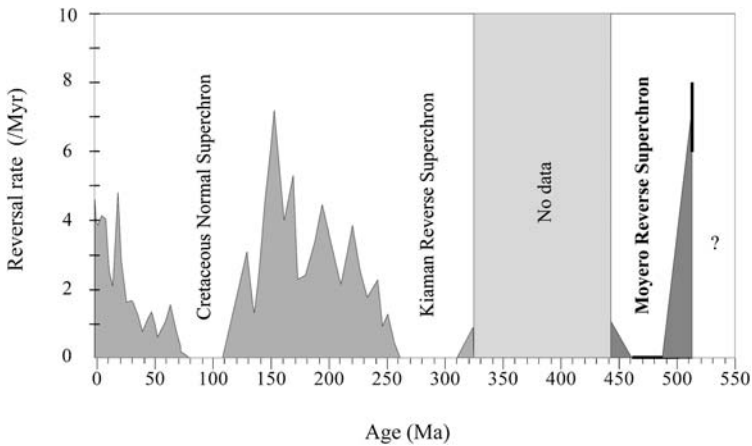


Fig. 29 Estimate of the reversal rate (in Myr^{-1}) for the time interval 0–500 Ma, where reversal rates are estimated by geological stage, rather than by using a moving window average (as in Fig. 28), to harmonize post- and pre- 150 Ma data for which much less data is available. After Pavlov and Gallet (2005)

(see e.g. Loper and McCartney 1986; Courtillot and Besse 1987; Larson and Olson 1991; Courtillot and Olson 2007).

When considering the possible cause of such a succession of superchrons over a period of time of 1.4 Gy, one should also consider the possible consequences of changes in the size of the inner core, in the global amount of heat extracted from the core, and in Earth's rotation rate. Although rather few simulation studies have looked into this so far (Driscoll and Olson 2009b, 2009a; Aubert et al. 2009), they all conclude that to produce superchrons as a result of mantle control, the geodynamo must have operated in a regime close to a transition between reversing and non-reversing regimes, as had been proposed by Courtillot and Olson (2007). Then, the time-varying heterogeneous thermal boundary conditions produced by mantle convection, combined with the slow thermal evolution of the Earth, growth of the inner core, and increase of the Earth's rotation rate, could have conspired to occasionally shift the geodynamo from a reversing regime to a non-reversing regime. However, this scenario is not without difficulties. As noted by Aubert et al. (2009), models of the thermal evolution of the Earth also likely imply that the transition from the reversing to the non-reversing regime was very close to the transition from the non-reversing regime to the non-dynamo regime, particularly over the past 500 My, making it quite remarkable that superchrons could have been produced in this way without shutting down the dynamo altogether. Furthermore this scenario predicts a progressive decrease in the reversal rate before reaching each superchron, followed by a progressive increase after the superchron. In contrast, the transition to the Cretaceous Normal Superchron seems to have been sudden and, although little is known about the reversal rate before the Kiaman reverse superchron, there also are clear indications that the transition towards the Moyero reverse superchron could have been as sudden (Pavlov and Gallet 2001). Finally, and as noted by Pavlov and Gallet (2010), both of the two previous superchrons strongly suggest even more sudden transitions between periods of frequent reversals and superchrons. Such sudden transitions seem to favor a spontaneous origin of superchrons, as proposed by Hulot and Gallet (2003).

As noted earlier, the sequence of reversals is not the only information available to investigate the very long term behavior of the geomagnetic field. Additional important information can be recovered from the investigation of the ancient PSV. As explained in Sect. 3.3.2,

this information is usually recovered in the form of VGP scatter curves formally converted into best fits to the model G (see (12)). This was first done by McFadden et al. (1991) who produced model G estimates for six broad epochs covering the past 195 My. Figure 30 shows the evolution of the α and β best-fit parameters defining the evolution of those VGP scatter curves, as originally proposed by McFadden et al. (1991). As noted by these authors, comparing this Figure to Fig. 28 suggests a connection between the changes in the VGP scatter and in the reversal rate over the past 160 My. Quite a few investigations have since been conducted (e.g. Cronin et al. 2001; Tarduno et al. 2002; Mankinen 2008; Biggin et al. 2008b) and it now appears that this connection is not as clear-cut as initially envisioned by McFadden et al. (1991) (see e.g. Biggin et al. 2008b). All these investigations nevertheless confirm the most striking fact that the PSV has been behaving very differently during the Cretaceous Normal Superchron compared to other times when the field was reversing, particularly compared to the best documented past 5 My. As can be seen in Fig. 30, the parameter β (a direct measure of the VGP scatter at the equator, recall (12)) was low. This result is interesting because VGP scatter at the equator can only be produced by Gauss coefficients belonging to the “Quadrupole” family (e.g. Kono and Tanaka 1995; Hulot and Gallet 1996). At this time, the contribution of the “Quadrupole” family to the Lowes-Mauersberger spectrum (relative to the axial dipole) must thus have been significantly less than over the past 5 My. Parameter α , a measure of the increasing trend of the scatter with latitude, was high. This corresponds to the fact that the VGP scatter at high latitudes was then about the same as over the past 5 My (as confirmed by the more recent studies of Tarduno et al. 2002; Biggin et al. 2008b). This now implies that contributions from the “Dipole” family must have remained large enough. Whereas the most plausible explanation for the VGP scatter curve over the past 5 My seems related to the order one Gauss coefficients behavior (recall Sect. 4.3.1), it now seems much more natural to invoke an imbalance between the “Dipole” and “Quadrupole” families to account for the VGP scatter curve during the Cretaceous Normal Superchron, as envisioned by McFadden et al. (1991).

Two additional lines of evidence support such an interpretation. First, the few numerical dynamos displaying such a strong imbalance (with a weak “Quadrupole” family field) are particularly stable with respect to reversals (Coe and Glatzmaier 2006). Second, the VGP scatter during the previous Kiaman Reverse Superchron was quite similar to the one observed during the Cretaceous Normal Superchron (Haldan et al. 2009). Taken together the above results suggest that during superchrons the geodynamo operated in a very different way than at other times, with no reversals and a significantly depleted “Quadrupole” family field.

Just as in the case of the reversal rate, some PSV observations are also available for even earlier epochs. But the data are sparse and those most appropriate for investigating the sequence of reversals rarely provide suitable information for PSV studies. In addition, rather contradictory results have been reported so far. Smirnov and Tarduno (2004) have for instance found that Late Archean-Early Proterozoic data from dikes dated ~ 2.5 Ga and ~ 2.7 Ga would favor a VGP scatter comparable to that observed over the past 5 My while Biggin et al. (2008a) concluded that the VGP scatter was similar to that observed during the Cretaceous Normal Superchron. Biggin et al. (2008a) argued that the reasons for the discrepancy were the stricter selection criteria they applied and the larger data set they investigated, sampling the 2.82 to 2.45 Ga time period. As noted by Hulot (2008) this time period is indeed so long (longer than 190 My) that some time evolution should be expected (recall Fig. 30) which could result in such disagreement between the two studies. The results of Biggin et al. (2008a) nevertheless indicate that during the Late Archean-Early Proterozoic the geodynamo produced a PSV much more often comparable to that of the Cretaceous

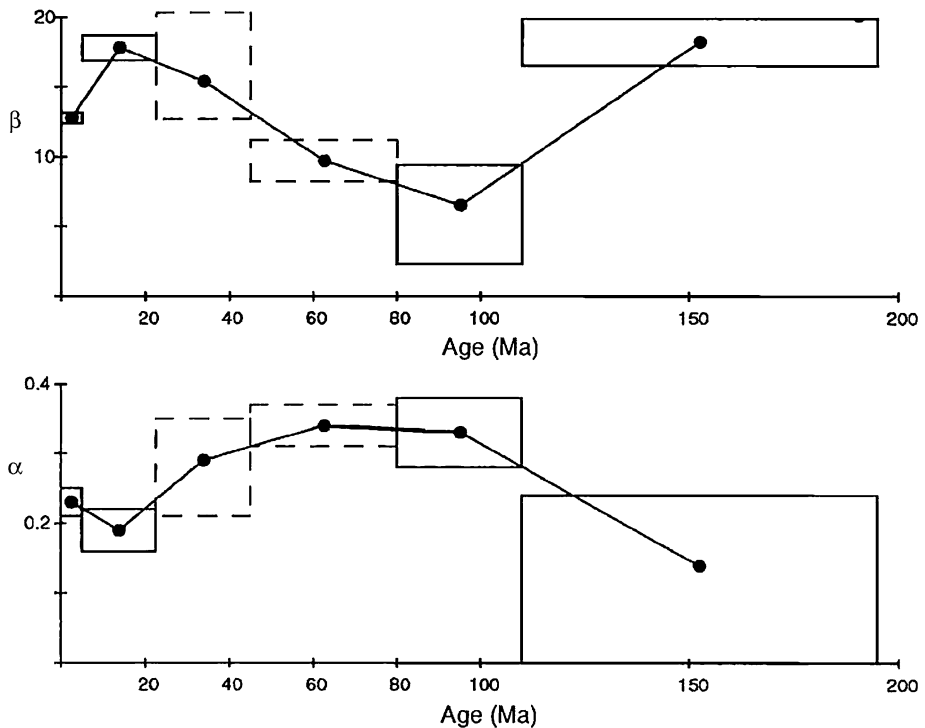
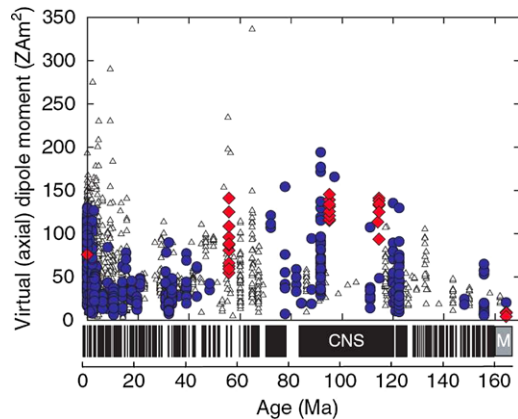


Fig. 30 VGP scatter Model G parameters as a function of time over the past 190 My. Parameters α (*lower panel*, dimensionless) and β (*top panel*, in degrees), as defined by (12). Boxes define range of age contributing to the estimated parameter and 95% confidence limits, dotted boxes indicates that the fit to (12) was poor. After McFadden et al. (1991)

Normal Superchron, than to that of other recent epochs when the field was reversing. This observation led Biggin and co-workers to speculate that the geodynamo could have been less prone to reversals during the Late Archean-Early Proterozoic. Their hypothesis is consistent with the data available over the 2.775 to 1.05 Ga time period (Halls 1991; Gallet et al. 2000; Elston et al. 2002; Strik et al. 2003) during which the few time intervals investigated so far, totaling 225–250 My, document only 45 reversals and suggest an average reversal rate of only 0.2 My^{-1} (Coe and Glatzmaier 2006).

Both Coe and Glatzmaier (2006) and Biggin et al. (2008a) interpret their observations as a consequence of the inner core being smaller (or even absent) at the time, based on results from a very stable small inner-core simulation by Roberts and Glatzmaier (2001), which also displayed the weak “Quadrupole” family field characteristic that we saw could account for the PSV at times of superchrons. But it should be noted that reversing dynamo with no inner core can also be found (e.g. Sakuraba and Kono 1999), and that other factors may have influenced the dynamo on such long time scales. Indeed Aubert et al. (2009) recently confirmed that small inner-core dynamo can reverse frequently. They also noted that the thermal evolution of the Earth (and changes in the rotation rate) could have led the geodynamo to lie closer to the transition between the reversing and non-reversing regimes at the time. If superchrons are caused by the geodynamo occasionally crossing this transition, they could then have occurred more often in the past. If superchrons are spontaneous, it could alternatively be that the regime was more prone to superchrons at the time. Whatever the

Fig. 31 Paleointensities over the past 170 My, expressed in terms of Virtual Axial Dipole Moments (VADM, see Sect. 3.3.1). Data extracted from the PINT06 database of Tauxe and Yamazaki (2007) after some minimum quality criteria selection. Blue dots are submarine basaltic glass data. Red diamonds are single-crystal results. Triangles are all other data (whole rocks). Units ZAm^2 stand for $10^{21} Am^2$. After Tauxe and Yamazaki (2007) where more details can be found



cause of superchrons, it is finally worth recalling that both the data used by Coe and Glatzmaier (2006) to estimate a low 0.2 My^{-1} reversal rate, and the more recent data published by Pavlov and Gallet (2010) primarily reveal transitions between periods with frequent reversals and superchrons. The main cause of the apparent low reversal rate observed by Coe and Glatzmaier (2006) and of the superchron type of VGP scatter found by Biggin et al. (2008a) could thus be the more frequent occurrence of superchrons before 1 Ga than during the past 160 My (or even 300 My, recall Figs. 28–29).

Finally we turn to the paleointensity observations. As already mentioned in Sect. 2.5, these data are particularly difficult to recover and most prone to artifacts, especially when very ancient. Essentially four different types of data can be used: relative paleointensity records from sediments, absolute intensity estimates from whole igneous rocks, submarine basaltic glass samples, or single silicate crystals extracted from igneous rocks. Relative paleointensity records have already been much discussed in Sect. 4.2 where we noted that they suggest some weak correlation between the average field intensity during a chron and the length of the chron (Tauxe and Hartl 1997; Constable et al. 1998, Sect. 4.2). Do the other types of paleointensity data confirm this correlation or reveal other correlations with e.g., the reversal rate or the paleosecular variation?

Answers to these questions unfortunately remain rather unclear. Figure 31 perfectly illustrates the complexity of the information provided by these various types of data over the past 170 My. This figure was plotted from the PINT06 database of Tauxe and Yamazaki (2007) after some minimum quality criteria selection and conversion of the data in terms of VADM (as defined in Sect. 3.3.1). It first shows that much more data are available for recent epochs than for ancient epochs (with roughly 40% of the data younger than 1 My). It also suggests that the field intensity experienced considerable variability at all times and shows that defining long-term trends in the geomagnetic field intensity is no simple matter. Considerable effort has been put into deciphering the messages possibly embedded in these data.

Selecting data from six polarity intervals of known durations (with ages ranging from 3.3 Ma to 121 Ma), Tauxe and Yamazaki (2007) for instance argued that a weak correlation between the average field intensity during a chron and the length of the chron could again be found. But the correlation is very weak (as is in fact obvious from the fact that the Cretaceous Normal Superchron, the longest of all chrons by far, does not display such an outstanding VADM, see Fig. 31). It also is not clear why such a correlation should apply between 3.3 Ma

and 121 Ma, and not to more recent data, when both short intervals and large intensities are to be found.

Identifying epochs when the field was high or low on average has also been the subject of many studies. Some authors (e.g. Juárez et al. 1998; Selkin and Tauxe 2000; Juárez and Tauxe 2000), relying on submarine basaltic glasses, have argued that significantly higher values are found only when considering data younger than 300 ky. [This, incidentally, is the reason why Tauxe and Kent (2004) chose a weaker value for the G_1^0 TAF Gauss coefficient than usually assumed in their GGP model for the past 5 My, recall Sect. 3.3.2]. But this view is not supported by the latest basaltic glass data plotted in Fig. 31, which now suggest that the average VADM during the Normal Cretaceous Superchron was quite similar to today's dipole moment (Tauxe 2006). These findings are more consistent with previous results based on whole igneous rock data (e.g. Prévot et al. 1990; Tanaka et al. 1995; Perrin and Shcherbakov 1997) which suggested that the only time the field was truly low was during the Mesozoic (before 120 Ma, as is suggested by Fig. 31). Interestingly, independent indications that this may well have been the case can also be found in marine magnetic anomaly profiles which happen to be particularly weak during the 167–155 Ma time period (e.g., Tivey et al. 2006; Tominaga et al. 2008). This portion of the magnetic anomaly record, found in the Pacific, displays many small amplitude fluctuations and is known as the Pacific Jurassic Quiet Zone (JQZ in Fig. 13). However, this is also an epoch for which magnetostratigraphic evidence for polarity reversals is ambiguous (as reflected by the grey area in the GTPS of Fig. 13, also reproduced below the intensity plot in Fig. 31), and it is still unclear whether the observed anomalies truly reflect fluctuations of a weak field with few reversals, or a rapid succession of reversals (Tivey et al. 2006; Tominaga et al. 2008).

More recently Heller et al. (2002, 2003), following earlier work by Perrin and Shcherbakov (1997), pointed out an intriguing property of whole igneous rock data selected using their own criteria. Investigating the longer 320–0 Ma time period, which they split in time intervals of up to a few tens of millions of years, they noted that the distribution of intensities could be fit by a bimodal distribution with the same two (broad) peaks (at roughly 9×10^{22} Am² and $4\text{--}5 \times 10^{22}$ Am²). The only temporal variation they could find over the corresponding 320 My was in the relative distribution of the data within this distribution, which reduced to a unimodal distribution on only two occasions: over the past 5 My, when it only displayed the high 9×10^{22} Am² peak; between ~ 250 Ma and ~ 20 Ma, when it only displayed the low $4\text{--}5 \times 10^{22}$ Am² peak. The reason for such a behavior is unclear. Heller et al. (2003) suggests that perhaps the geodynamo has the choice to operate in two different states, each defined by a different (either high, or low) average dipole moment, and constantly switched (at an unknown rate) between those two states over the past 320 My, except during the 250–120 Ma and 5–0 Ma time periods. But it is puzzling that such a change of behavior could have remained unaffected by the occurrence of the Cretaceous Normal Superchron. More likely, and as also noted by Heller et al. (2003), this observation may result from some artifacts related to the selection criteria, undersampling of the data for the earliest epochs, and possibly unidentified rock magnetic issues. That the most recent and much more numerous data only display a unimodal distribution is perhaps an indication that this is the more likely explanation.

Particularly suspicious of whole rock data, Tarduno (2009) (see also Tarduno et al. 2006) argues that perhaps one should rather concentrate on single-silicate crystal data (red diamonds in Fig. 31). These data show the same kind of general trends as the other data, but in a clearer way, with a maximum during the Cretaceous Normal Superchron, and a somewhat weaker field at times of frequent reversals. That the field could usually be strong at times

of superchrons is also supported by the single-silicate crystal results recently published by Cottrell et al. (2008), who found VADM estimates on order 9×10^{22} Am² during the Kiaman Reverse Superchron. It should however be emphasized that so far only two (mutually consistent) data points have been obtained in this way and that the inferred VADM is similar to that of the recent frequently reversing field. Perhaps what controls the average field paleointensity is simply unrelated to what controls the occurrence of superchrons.

Some information concerning the very ancient field intensity is also available. Most of the data are from whole rock studies, though quite a few, among which the oldest data, are from single crystal silicates (up to 3.2 Ga, see Tarduno et al. 2007). These data have also been scrutinized for long-term evolution, particularly in view of identifying some possible signature associated with the onset of the inner-core crystallization (see e.g. Hale 1987; Labrosse and Macouin 2003; Macouin et al. 2004 and most recently Biggin et al. 2009). Unfortunately, this has again led to rather contradicting results and interpretations. This is because of the still very limited database currently available. It may also be because, as illustrated by the recent numerical simulations of Aubert et al. (2009), only weak long-term changes in the paleointensity should be expected as a result of the Earth's thermal history and inner core growth. Such a scenario is consistent with the undisputed fact that the field has always been of the same order of magnitude and displaying the same kind of fluctuations, since at least 3.2 Gy ago (the earliest record Tarduno et al. 2007).

5 Concluding Remarks

As must now be obvious to the reader, the past decade has been a remarkable period of progress in our knowledge and understanding of the magnetic field of the Earth. This we largely owe to the considerable success of recent magnetic satellite missions, to the emergence of new archeomagnetic and paleomagnetic measurement techniques, to the development of advanced geomagnetic, archeomagnetic and paleomagnetic modeling methods, and to the coming of age of fully consistent numerical dynamo simulations. Of course, much remains to be done, and many issues are still open.

From an observational point of view, there is little doubt that a lot could be learned from more, ideally uninterrupted, magnetic observations from space, combined with synchronous observations from an improved network of ground based observatories. Such observations are crucial for better characterizing and understanding the sometimes surprisingly fast changing phenomena that occur within the core. Fortunately, more such missions are now scheduled (such as the ESA *Swarm* mission, Friis-Christensen et al. 2006, 2009) or in preparation, and more observatories are joining the INTERMAGNET worldwide network standards.

Technical progress is also under way in archeomagnetism and paleomagnetism, and databases are continually building up, thanks to patient collective endeavors. Such improvements are still badly needed to improve geographical coverage, to enable better documentation of field variations at all time scales, to enable more reliable reconstructions of the detailed behavior of the field during excursions and reversals, and to better assess the influence of the heterogeneous mantle. A major challenge is also to further improve our understanding of paleointensity data and of the temporal filtering involved in sedimentary data, not to mention the permanent need to improve the time control on the age of those samples.

From a field modeling point of view the next step, already initiated (recall Sect. 4.1.3), is to introduce dynamical considerations in the currently purely descriptive time varying spherical harmonic models of the geomagnetic and archeomagnetic fields, using e.g. data

assimilation techniques. This is crucial to better taking advantage of the recent increase in data quality, and for improved understanding of the short to medium-term dynamics inside the core. Also of importance in relation to better understanding the links between decadal field fluctuations and variations in Earth's rotation, is the still unclear role of gravitational coupling between the inner core and the mantle. Gravitational coupling may both prevent the inner core from freely rotating within the outer core on the long term and be an important ingredient in the short-term dynamics of the core (see Buffett 2007 for a recent discussion).

Possibly just as important is the fact, that we did not discuss, that the Earth is not an isolated body within the solar system. Its mechanical interactions with the Moon and the Sun, but also with other planets, are responsible for phenomena such as tides and precession which affect the coupled (because of the slight ellipticity of the structure of the Earth) inner-core—core-mantle system. It has indeed been suggested that the energy provided by such precession phenomena could play a significant role in the geodynamo process (see e.g. Tilgner 2007 for a recent review), and it may even be that some resonance arose in the geological past, which could have very significantly affected the geodynamo (Greff-Lefftz and Legros 1999). Evidence for possible orbital influence in the magnetic field data (in sediment data) has been searched for, but only with rather contradicting results so far (see e.g. Roberts et al. 2003; Xuan and Channell 2008; Thouveny et al. 2008). The manner in which precession and related phenomena (such as so-called parametric instabilities, see e.g. Aldridge and Baker 2003) could interfere with the main geodynamo process (driven by thermo-chemical convection) needs to be assessed more precisely.

More progress is also to be expected in the numerical simulation of the geodynamo. Running simulations with more Earth-like control parameters remains a permanent challenge, particularly because of the extremely high resolution required by the very small viscosity of the outer core liquid iron. Several avenues are currently being explored, with some taking advantage of the latest advances in computer power (e.g. Kageyama et al. 2008), while others look for advanced ways of dealing with unresolved length-scales (e.g. Matsui and Buffett 2005, 2007; Matsushima 2006), or investigate whether using more appropriate boundary conditions could be important with improving numerical resolution (Sakuraba and Roberts 2009). Further exploration and development of dynamo scaling laws derived from simulations with more moderate numerical resolution is also an interesting avenue (e.g. Christensen 2009).

But perhaps the next great advances will come instead from laboratory experiments. Although running such experiments is very challenging, a number of teams now have operational set-ups that have already brought very interesting results (see the recent reviews of Cardin and Olson 2007 and Verhille et al. 2009). Some of these have succeeded at producing magnetic fields from energy drawn from conducting fluids. But the way this has been achieved so far is by mechanically forcing the conducting fluid (liquid sodium) through well-designed pipes (e.g. Gailitis et al. 2001; Stieglitz and Müller 2001), or by using counter-rotating propellers in a cylinder (Monchaux et al. 2007). No experimental dynamo has yet been found that directly compares to the geodynamo (though some experiments already brought interesting insight into the way reversals can occur, see Berhanu et al. 2007; Petrelis et al. 2009). Whether fast-rotating, convecting, experimental dynamos can be achieved some day remains an open question. Nonetheless other set-ups are available that already make it possible to investigate the specific dynamics of fast rotating flows (in particular in connection with precession, see Tilgner 2007 for a review), sometimes in the presence of thermal convection (see Cardin and Olson 2007 for a review), and with imposed magnetic fields (e.g. Brito et al. 1995; Aurnou and Olson 2001; Nataf et al. 2006, 2008; Gillet et al. 2007b;

Schmitt et al. 2008). Such experiments bring very interesting insight into the dynamics relevant for the investigation of the historical field behavior (recall Sect. 4.1.2).

No doubt the combination of results from such improved experiments, more advanced numerical simulations, and better modeling of more high-quality observations promises to make the next decade just as productive as the one covered by the present review.

Acknowledgements The authors are very grateful to Nicolas Gillet for his very thorough review of the present paper and to Andre Balogh, Roger-Maurice Bonnet, and the International Space Science Institute for inviting them to take part in the Planetary Magnetism Workshop held in Bern in September 2008. CC acknowledges support from US National Science Foundation Geophysics Program Grants EAR-0537986 and EAR-0809709. This is IGP contribution 2602.

Open Access This article is distributed under the terms of the Creative Commons Attribution Noncommercial License which permits any noncommercial use, distribution, and reproduction in any medium, provided the original author(s) and source are credited.

References

- D.J. Acheson, R. Hide, *Rep. Prog. Phys.* **36**, 159–221 (1973)
- K. Aldridge, R. Baker, *Phys. Earth Planet. Int.* **140**(1–3), 91–100 (2003). doi:[10.1016/j.pepi.2003.07.005](https://doi.org/10.1016/j.pepi.2003.07.005)
- M. Alexandrescu, V. Courtillot, J.L. Le Mouél, *Phys. Earth Planet. Int.* **98**, 321–360 (1996a)
- M. Alexandrescu, D. Gibert, G. Hulot, J.L. Le Mouél, G. Saracco, *J. Geophys. Res.* **101**(B10), 21975–21994 (1996b)
- C.J. Allègre, G. Manhès, C. Göpel, *Geochim. Cosmochim. Acta* **59**(8), 1445–1456 (1995)
- C.J. Allègre, G. Manhès, C. Göpel, *Earth Planet. Sci. Lett.* **267**(1–2), 386–398 (2008). doi:[10.1016/j.epsl.2007.11.056](https://doi.org/10.1016/j.epsl.2007.11.056)
- H. Amit, P. Olson, *Phys. Earth Planet. Int.* **155**, 120–139 (2006)
- H. Amit, J. Aubert, G. Hulot, P. Olson, *Earth Planets Space* **60**(8), 845–854 (2008)
- H. Amit, J. Aubert, G. Hulot, *J. Geophys. Res.* (2010). doi:[10.1029/2009JB006542](https://doi.org/10.1029/2009JB006542)
- J. Aubert, H. Amit, G. Hulot, *Phys. Earth Planet. Int.* **160**, 143–156 (2007)
- J. Aubert, J. Aurnou, J. Wicht, *Geophys. J. Int.* **172**(3), 945–956 (2008a). doi:[10.1111/j.1365-246X.2007.03693.x](https://doi.org/10.1111/j.1365-246X.2007.03693.x)
- J. Aubert, H. Amit, G. Hulot, P. Olson, *Nature* **454**(7205), 758–80 (2008b). doi:[10.1038/nature07109](https://doi.org/10.1038/nature07109)
- J. Aubert, S. Labrosse, C. Poitou, *Geophys. J. Int.* **179**, 1414–1428 (2009). doi:[10.1111/j.1365-246X.2009.04361.x](https://doi.org/10.1111/j.1365-246X.2009.04361.x)
- J.M. Aurnou, P.L. Olson, *J. Fluid Mech.* **430**, 283–307 (2001)
- H. Auster, M. Manda, A. Hemshorn, E. Pulz, M. Korte, *Earth Planets Space* **59**(9), 1007–1014 (2007)
- V. Auster, O. Hillenmaier, R. Kroth, M. Weideman, in *XIIIth IAGA Workshop on Geomagnetic Observatory Instruments, Data Acquisition and Processing*, Abstract volume 21, 2006
- G. Backus, *Philos. Trans. R. Soc. Lond. A* **263**, 239–266 (1968)
- G.E. Backus, *J. Geophys. Res.* **75**(31), 6339–6341 (1970)
- G.E. Backus, *Geophys. J.* **92**, 125–142 (1988)
- D. Barraclough, *Trans. R. Soc. Edinb. Earth Sci.* **85**, 239–252 (1995)
- C.E. Barton, *J. Geomagn. Geoelectr.* **49**, 123–148 (1997)
- C.E. Barton, P.L. McFadden, *Earth Planet. Sci. Lett.* **140**(1–4), 147–157 (1996)
- W. Baumjohann, M. Blanc, A. Fedorov, K.H. Glassmeier, *Space Sci. Rev.* (2010). doi:[10.1007/s11214-010-9629-z](https://doi.org/10.1007/s11214-010-9629-z)
- E. Bellanger, J.L. Le Mouél, M. Manda, S. Labrosse, *Phys. Earth Planet. Int.* **124**(1–2), 95–103 (2001)
- E. Ben-Yosef, L. Tauxe, H. Ron, A. Agnon, U. Avner, M. Najjar, T.E. Levy, *J. Archeol. Sci.* **35**(11), 2863–2879 (2008a). doi:[10.1016/j.jas.2008.05.016](https://doi.org/10.1016/j.jas.2008.05.016)
- E. Ben-Yosef, H. Ron, L. Tauxe, A. Agnon, A. Genevey, T.E. Levy, U. Avner, M. Najjar, *J. Geophys. Res.* **113**(B8), B08101 (2008b). doi:[10.1029/2007JB005235](https://doi.org/10.1029/2007JB005235)
- E. Ben-Yosef, L. Tauxe, T.E. Levy, R. Shaar, H. Ron, M. Najjar, *Earth Planet. Sci. Lett.* **287**(3–4), 529–539 (2009). doi:[10.1016/j.epsl.2009.09.001](https://doi.org/10.1016/j.epsl.2009.09.001)
- M. Berhanu, R. Monchaux, S. Fauve, N. Mordant, F. Petrelis, A. Chiffaudel, F. Daviaud, B. Dubrulle, L. Marie, F. Ravelet, M. Bourgoin, P. Odier, J.F. Pinton, R. Volk, *Europhys. Lett.* **77**(5), 59001 (2007). doi:[10.1209/0295-5075/77/59001](https://doi.org/10.1209/0295-5075/77/59001)

- J. Besse, V. Courtillot, *J. Geophys. Res.* **107**(B11), 2300 (2002). doi:[10.1029/2000JB000050](https://doi.org/10.1029/2000JB000050)
- A.J. Biggin, G.H.M.A. Strik, C.G. Langereis, *Nat. Geosci.* **1**(6), 395–398 (2008a). doi:[10.1038/ngeo181](https://doi.org/10.1038/ngeo181)
- A.J. Biggin, D.J.J. van Hinsbergen, C.G. Langereis, G.B. Straathof, M.H.L. Deenen, *Phys. Earth Planet. Int.* **169**(1–4, Sp. Iss.), 3–19 (2008b). doi:[10.1016/j.pepi.2008.07.004](https://doi.org/10.1016/j.pepi.2008.07.004)
- A.J. Biggin, G.H.M.A. Strik, C.G. Langereis, *Earth Planets Space* **61**(1), 9–22 (2009)
- J. Bloxham, *J. Geophys. Res.* **92**(B11), 11597–11608 (1987)
- J. Bloxham, *Philos. Trans. R. Soc. Lond. A* **358**(1768), 1171–1179 (2000)
- J. Bloxham, *Geophys. Res. Lett.* **29**(18), 1854 (2002). doi:[10.1029/2001GL014543](https://doi.org/10.1029/2001GL014543)
- J. Bloxham, A. Jackson, *J. Geophys. Res.* **94**(B11), 15753–15769 (1989)
- J. Bloxham, A. Jackson, *Rev. Geophys.* **29**, 97–120 (1991)
- J. Bloxham, A. Jackson, *J. Geophys. Res.* **97**, 19537–19563 (1992)
- J. Bloxham, D. Gubbins, A. Jackson, *Philos. Trans. R. Soc. Lond. A* **329**(1606), 415–502 (1989)
- J. Bloxham, S. Zaitman, M. Dumberry, *Nature* **420**, 685–687 (2002)
- C. Bouligand, G. Hulot, A. Khokhlov, G.A. Glatzmaier, *Geophys. J. Int.* **161**(3), 603–626 (2005). doi:[10.1111/j.1365-246X.2005.02613.x](https://doi.org/10.1111/j.1365-246X.2005.02613.x)
- C. Bouligand, J. Dyment, Y. Gallet, G. Hulot, *Earth Planet. Sci. Lett.* **250**(3–4), 541–560 (2006). doi:[10.1016/j.epsl.2006.06.051](https://doi.org/10.1016/j.epsl.2006.06.051)
- N.E. Bowers, S.C. Cande, J.S. Gee, J.A. Hildebrand, R.L. Parker, *J. Geophys. Res.* **106**(B11), 26379–26396 (2001)
- S.I. Braginsky, *Geomagn. Aeron.* **4**, 698–712 (1964)
- S.I. Braginsky, *Geomagn. Aeron.* **7**, 851–859 (1967)
- S.I. Braginsky, *Geomagn. Aeron.* **10**, 1–8 (1970)
- S.I. Braginsky, *Geophys. Astrophys. Fluid Dyn.* **30**, 1–78 (1984)
- D. Brito, P. Cardin, H.C. Nataf, G. Marollet, *Phys. Earth Planet. Int.* **91**(1–3), 77–98 (1995)
- M.C. Brown, R. Holme, A. Bargery, *Geophys. J. Int.* **168**(2), 541–550 (2007). doi:[10.1111/j.1365-246X.2006.03234.x](https://doi.org/10.1111/j.1365-246X.2006.03234.x)
- B.A. Buffett, *Science* **299**(5613), 1675–1677 (2003)
- B.A. Buffett, in *Treatise on Geophysics*, vol. 8, ed. by P. Olson (Elsevier, Amsterdam, 2007)
- B.A. Buffett, H.E. Huppert, J.R. Lister, A.W. Woods, *Nature* **356**(6367), 329–331 (1992)
- B.A. Buffett, H.E. Huppert, J.R. Lister, A.W. Woods, *J. Geophys. Res.* **101**(B4), 7989–8006 (1996)
- B. Buffett, J. Mound, A. Jackson, *Geophys. J. Int.* **177**, 878–890 (2009)
- F.H. Busse, *J. Fluid Mech.* **44**, 441 (1970)
- L. Cafarella, A. De Santis, A. Meloni, *Phys. Earth Planet. Int.* **73**, 206–221 (1992)
- J.C. Cain, B.B. Ferguson, D. Mozzoni, *J. Geophys. Res.* **108**, 2 (2003). doi:[10.1029/2000JE001487](https://doi.org/10.1029/2000JE001487)
- S.C. Cande, D.V. Kent, *J. Geophys. Res.* **100**(B4), 6093–6095 (1995)
- E. Canet, A. Fournier, D. Jault, *J. Geophys. Res.* **114**(B11), 11101 (2009). doi:[10.1029/2008JB006189](https://doi.org/10.1029/2008JB006189)
- A. Cao, B. Romanowicz, *Earth Planet. Sci. Lett.* **228**(3–4), 243–253 (2004). doi:[10.1016/j.epsl.2004.09.032](https://doi.org/10.1016/j.epsl.2004.09.032)
- P. Cardin, P. Olson, in *Treatise on Geophysics*, vol. 8, ed. by P. Olson (Elsevier, Amsterdam, 2007)
- J. Carlot, V. Courtillot, *Geophys. J. Int.* **134**(2), 527–544 (1998)
- J. Carlot, D.V. Kent, *Earth Planet. Sci. Lett.* **183**(3–4), 389–401 (2000)
- J.E.T. Channell, B. Lehman, *Nature* **389**(6652), 712–715 (1997)
- J.E.T. Channell, E. Erba, M. Nakanishi, T. Tamaki, in *Geochronology, Timescales, and Stratigraphic Correlation*, ed. by W.A. Berggren, D.V. Kent, M. Aubry, J. Hardenbol (SEPM, Tulsa, 1995), pp. 51–64
- S. Chapman, J. Bartels, *Geomagnetism*, vol. I, II (Clarendon Press, Oxford, 1940)
- A. Chauvin, H. Perroud, M.L. Bazhenov, *Geophys. J. Int.* **126**(2), 303–313 (1996)
- U.R. Christensen, *Space Sci. Rev.* (2009). doi:[10.1007/s11214-009-9553-2](https://doi.org/10.1007/s11214-009-9553-2)
- U.R. Christensen, J. Aubert, *Geophys. J. Int.* **166**(1), 97–114 (2006). doi:[10.1111/j.1365-246X.2006.03009.x](https://doi.org/10.1111/j.1365-246X.2006.03009.x)
- U.R. Christensen, P. Olson, *Phys. Earth Planet. Int.* **138**(1), 39–54 (2003). doi:[10.1016/S0031-9201\(03\)00064-5](https://doi.org/10.1016/S0031-9201(03)00064-5)
- U.R. Christensen, J. Wicht, in *Treatise on Geophysics*, vol. 8, ed. by P. Olson (Elsevier, Amsterdam, 2007)
- A. Chulliat, *Geophys. J. Int.* **157**(2), 537–552 (2004). doi:[10.1111/j.1365-246X.2004.02216.x](https://doi.org/10.1111/j.1365-246X.2004.02216.x)
- A. Chulliat, G. Hulot, *Phys. Earth Planet. Int.* **117**(1–4), 309–328 (2000)
- A. Chulliat, G. Hulot, *Geophys. J. Int.* **147**(2), 237–246 (2001)
- A. Chulliat, N. Olsen, *J. Geophys. Res.* (2009). doi:[10.1029/2009JB006994](https://doi.org/10.1029/2009JB006994)
- B.M. Clement, *Earth Planet. Sci. Lett.* **104**(1), 48–58 (1991)
- B.M. Clement, *Nature* **428**(6983), 637–640 (2004). doi:[10.1038/nature02459](https://doi.org/10.1038/nature02459)
- R.S. Coe, G.A. Glatzmaier, *Geophys. Res. Lett.* **33**(21), L21311 (2006). doi:[10.1029/2006GL027903](https://doi.org/10.1029/2006GL027903)
- R.S. Coe, J.M.G. Glen, in *Timescales of the Paleomagnetic Field*, ed. by J.E.T. Channell, D.V. Kent, W. Lowrie, J.G. Meert, *Geophysical Monograph Series*, vol. 145 (2004), pp. 221–232. 0-87590-410-6. doi:[10.1029/145GM16](https://doi.org/10.1029/145GM16)
- R.S. Coe, L. Hongre, G.A. Glatzmaier, *Philos. Trans. R. Soc. Lond. A* **358**(1768), 1141–1170 (2000)

- J.P. Cogne, J. Francheteau, V. Courtillot, R. Armijo, M. Constantin, J. Girardeau, R. Hekinian, R. Hey, D.F. Naar, R. Searle, *Earth Planet. Sci. Lett.* **136**(3–4), 213–222 (1995)
- J.P. Cogne, N. Halim, Y. Chen, V. Courtillot, *J. Geophys. Res.* **104**(B8), 17715–17734 (1999)
- J. Connerney, in *Treatise on Geophysics*, vol. 10, ed. by T. Spohn (Elsevier, Amsterdam, 2008). Chap. 7
- C. Constable, *Phys. Earth Planet. Int.* **118**(3–4), 181–193 (2000)
- C. Constable, C. Johnson, *Phys. Earth Planet. Int.* **153**(1–3, Sp. Iss.), 61–73 (2005). doi:[10.1016/j.pepi.2005.03.015](https://doi.org/10.1016/j.pepi.2005.03.015)
- C.G. Constable, in *Treatise on Geophysics*, vol. 5, ed. by M. Kono (Elsevier, Amsterdam, 2007)
- C.G. Constable, C.L. Johnson, *Phys. Earth Planet. Int.* **115**(1), 35–51 (1999)
- C. Constable, M. Korte, *Earth Planet. Sci. Lett.* **246**(1–2), 1–16 (2006). doi:[10.1016/j.epsl.2006.03.038](https://doi.org/10.1016/j.epsl.2006.03.038)
- C.G. Constable, R.L. Parker, *J. Geophys. Res.* **93**(B10), 11569–11581 (1988)
- C.G. Constable, R.L. Parker, P.B. Stark, *Geophys. J. Int.* **113**(2), 419–433 (1993)
- C.G. Constable, L. Tauxe, R.L. Parker, *J. Geophys. Res.* **103**(B8), 17735–17748 (1998)
- C.G. Constable, C.L. Johnson, S.P. Lund, *Philos. Trans. R. Soc. Lond. A* **358**, 991–1008 (2000)
- R.D. Cottrell, J.A. Tarduno, *Earth Planet. Sci. Lett.* **169**(1–2), 1–5 (1999)
- R.D. Cottrell, J.A. Tarduno, J. Roberts, *Phys. Earth Planet. Int.* **169**(1–4, Sp. Iss.), 49–58 (2008). doi:[10.1016/j.pepi.2008.07.041](https://doi.org/10.1016/j.pepi.2008.07.041)
- V. Courtillot, J. Besse, *Science* **237**(4819), 1140–1147 (1987)
- V. Courtillot, J. Besse, in *Timescales of the Paleomagnetic Field*, ed. by J. E.T. Channell, D.V. Kent, W. Lowrie, J.G. Meert, Geophysical Monograph Series, vol. 145 (2004), pp. 59–74. 0-87590-410-6. doi:[10.1029/145GM05](https://doi.org/10.1029/145GM05)
- V. Courtillot, J.L. Le Mouél, *Rev. Geophys.* **45**(3), RG3008 (2007). doi:[10.1029/2008GC002295](https://doi.org/10.1029/2008GC002295)
- V. Courtillot, P. Olson, *Earth Planet. Sci. Lett.* **260**(3–4), 495–504 (2007). doi:[10.1016/j.epsl.2007.06.003](https://doi.org/10.1016/j.epsl.2007.06.003)
- V. Courtillot, J. Ducruix, J.L. Le Mouél, C. R. Acad. Sci. D **287**(12), 1095–1098 (1978)
- A. Cox, *J. Geophys. Res.* **73**(10), 3247 (1968)
- A. Cox, *Geophys. J. R. Astron. Soc.* **20**(3), 253 (1970)
- M. Cronin, L. Tauxe, C. Constable, P. Selkin, T. Pick, *Earth Planet. Sci. Lett.* **190**(1–2), 13–30 (2001)
- C.J. Davies, D. Gubbins, A.P. Willis, P.K. Jimack, *Phys. Earth Planet. Int.* **169**(1–4, Sp. Iss.), 194–203 (2008). doi:[10.1016/j.pepi.2008.07.021](https://doi.org/10.1016/j.pepi.2008.07.021)
- C. De Boor, *A Practical Guide to Splines* (Springer, New York, 2001)
- C. DeMets, R.G. Gordon, D.F. Argus, S. Stein, *Geophys. Res. Lett.* **21**(20), 2191–2194 (1994)
- B. Desjardins, E. Dormy, E. Grenier, *Phys. Earth Planet. Int.* **123**(1), 15–26 (2001)
- F. Donadini, K. Korhonen, P. Riisager, L. Pesonen, *EOS Trans. AGU* **87**(14), 137 (2006)
- F. Donadini, M. Korte, C. Constable, *Geochem. Geophys. Geosyst.* **10**(6), Q06007 (2009). doi:[10.1029/2008GC002295](https://doi.org/10.1029/2008GC002295)
- E. Dormy, J.P. Valet, V. Courtillot, *Geochem. Geophys. Geosyst.* **1**(10), 2000GC000062 (2000)
- P. Driscoll, P. Olson, *Geophys. J. Int.* **178**(3), 1337–1350 (2009a). doi:[10.1111/j.1365-246X.2009.04234.x](https://doi.org/10.1111/j.1365-246X.2009.04234.x)
- P. Driscoll, P. Olson, *Earth Planet. Sci. Lett.* **282**(1–4), 24–33 (2009b). doi:[10.1016/j.epsl.2009.02.017](https://doi.org/10.1016/j.epsl.2009.02.017)
- M. Dumberry, *Geophys. J. Int.* **172**(3), 903–920 (2008a). doi:[10.1111/j.1365-246X.2007.03653.x](https://doi.org/10.1111/j.1365-246X.2007.03653.x)
- M. Dumberry, in *Les Houches Proceedings: Session LXXXVIII—Dynamos*, ed. by P. Cardin, L. Cugliandolo (Elsevier, Amsterdam, 2008b), pp. 383–401
- M. Dumberry, J. Bloxham, *Geophys. J. Int.* **165**(1), 32–46 (2006). doi:[10.1111/j.1365-246X.2006.02903.x](https://doi.org/10.1111/j.1365-246X.2006.02903.x)
- M. Dumberry, C.C. Finlay, *Earth Planet. Sci. Lett.* **254**(1–2), 146–157 (2007). doi:[10.1016/j.epsl.2006.11.026](https://doi.org/10.1016/j.epsl.2006.11.026)
- D.J. Dunlop, Y. Yu, in *Timescales of the Paleomagnetic Field*, ed. by J.E.T. Channell, D.V. Kent, W. Lowrie, J.G. Meert, Geophysical Monograph Series, vol. 145 (2004), pp. 85–100. 0-87590-410-6. doi:[10.1029/145GM07](https://doi.org/10.1029/145GM07)
- D. Dunlop, Ö. Özdemir, in *Treatise on Geophysics*, vol. 5, ed. by M. Kono (Elsevier, Amsterdam, 2007), pp. 277–336
- D.P. Elston, R.J. Enkin, J. Baker, D.K. Kisilevsky, *Bull. Geol. Soc. Am.* **114**(5), 619–638 (2002)
- C. Eymin, G. Hulot, *Phys. Earth Planet. Int.* **152**(3), 200–220 (2005)
- C.C. Finlay, *Phys. Earth Planet. Int.* **170**, 1–14 (2008a). doi:[10.1016/j.pepi.2008.06.029](https://doi.org/10.1016/j.pepi.2008.06.029)
- C.C. Finlay, in *Les Houches Proceedings: Session LXXXVIII—Dynamos*, ed. by P. Cardin, L. Cugliandolo (Elsevier, Amsterdam, 2008b), pp. 407–447
- C.C. Finlay, A. Jackson, *Science* **300**, 2084–2086 (2003)
- A. Fournier, C. Eymin, T. Alboussiere, *Nonlinear Process. Geophys.* **14**(2), 163–180 (2007)
- A. Fournier, G. Hulot, D. Jault, W. Kuang, A. Tangborn, N. Gillet, E. Canet, J. Aubert, F. Lhuillier, *Space Sci. Rev.* (2010)
- E. Friis-Christensen, H. Lühr, G. Hulot, *Earth Planets Space* **58**, 351–358 (2006)

- E. Friis-Christensen, H. Lühr, G. Hulot, R. Haagmans, M. Purucker, EOS Trans. AGU **90**(25), 213–215 (2009)
- A. Gailitis, O. Lielausis, E. Platacis, S. Dement'ev, A. Cifersons, G. Gerbeth, T. Gundrum, F. Stefani, M. Christen, G. Will, Phys. Rev. Lett. **86**(14), 3024–3027 (2001)
- Y. Gallet, G. Hulot, Geophys. Res. Lett. **24**(15), 1875–1878 (1997)
- Y. Gallet, V.E. Pavlov, M.A. Semikhatov, P.Y. Petrov, J. Geophys. Res. **105**(B7), 16481–16499 (2000)
- Y. Gallet, A. Genevey, M. Le Goff, Phys. Earth Planet. Int. **131**(1), 81–89 (2002)
- Y. Gallet, A. Genevey, V. Courtillot, Earth Planet. Sci. Lett. **214**(1–2), 237–242 (2003). doi:[10.1016/S0012-821X\(03\)00362-5](https://doi.org/10.1016/S0012-821X(03)00362-5)
- Y. Gallet, G. Hulot, A. Chulliat, A. Genevey, Earth Planet. Sci. Lett. **284**(1–2), 179–186 (2009). doi:[10.1016/j.epsl.2009.04.028](https://doi.org/10.1016/j.epsl.2009.04.028)
- J.S. Gee, D.V. Kent, in *Treatise on Geophysics*, vol. 5, ed. by M. Kono (Elsevier, Amsterdam, 2007)
- J.S. Gee, S.C. Cande, J.A. Hildebrand, K. Donnelly, R.L. Parker, Nature **408**(6814), 827–832 (2000)
- A. Genevey, Y. Gallet, J. Geophys. Res. **107**(B11), 2285 (2002)
- A. Genevey, Y. Gallet, G. Boudon, Earth Planet. Sci. Lett. **201**(2), 369–382 (2002)
- A. Genevey, Y. Gallet, J.C. Margueron, J. Geophys. Res. **108**(B5), 2228 (2003). doi:[10.1029/2001JB001612](https://doi.org/10.1029/2001JB001612)
- A. Genevey, Y. Gallet, C.G. Constable, M. Korte, G. Hulot, Geochem. Geophys. Geosyst. **9**(4), Q04038 (2008). doi:[10.1029/2007GC001881](https://doi.org/10.1029/2007GC001881)
- A. Genevey, Y. Gallet, J. Rosen, M. Le Goff, Earth Planet. Sci. Lett. **284**(1–2), 132–143 (2009). doi:[10.1016/j.epsl.2009.04.024](https://doi.org/10.1016/j.epsl.2009.04.024)
- S. Gilder, Y. Chen, J.P. Cogne, X.D. Tan, V. Courtillot, D.J. Sun, Y.G. Li, Earth Planet. Sci. Lett. **206**(3–4), 587–600 (2003)
- N. Gillet, A. Jackson, C.C. Finlay, Geophys. J. Int. **171**(3), 1005–1016 (2007a)
- N. Gillet, D. Brito, D. Jault, H.C. Nataf, J. Fluid Mech. **580**, 123–143 (2007b). doi:[10.1017/S00222121007005289](https://doi.org/10.1017/S00222121007005289)
- N. Gillet, M.A. Pais, D. Jault, Geochem. Geophys. Geosyst. **10**(6), Q06004 (2009a). doi:[10.1029/2008GC002290](https://doi.org/10.1029/2008GC002290)
- N. Gillet, V. Lesur, N. Olsen, Space Sci. Rev. (2009b). doi:[10.1007/s11214-009-9586-6](https://doi.org/10.1007/s11214-009-9586-6)
- G.A. Glatzmaier, R.S. Coe, in *Treatise on Geophysics*, vol. 8, ed. by P. Olson (Elsevier, Amsterdam, 2007)
- G.A. Glatzmaier, P.H. Roberts, Phys. Earth Planet. Int. **91**(1–3), 63–75 (1995)
- G.A. Glatzmaier, R.S. Coe, L. Hongre, P.H. Roberts, Nature **401**(6756), 885–890 (1999)
- F.M. Gradstein, F.P. Agterberg, J.G. Ogg, S. Hardenbol, P. Vanveen, J. Thierry, Z.H. Huang, J. Geophys. Res. **99**(B12), 24051–24074 (1994)
- O. Gravrand, A. Khokhlov, J.L. Le Mouél, J.M. Léger, Earth Planets Space **53**, 949–958 (2001)
- M. Greff-Lefftz, H. Legros, Science **286**(5445), 1707–1709 (1999)
- D. Gubbins, Nature **326**(6109), 167–169 (1987)
- D. Gubbins, Phys. Earth Planet. Int. **68**(1–2), 170–182 (1991)
- D. Gubbins, Phys. Earth Planet. Int. **98**, 193–206 (1996)
- D. Gubbins, Geophys. J. Int. **137**(1), 1–3 (1999)
- D. Gubbins, P. Kelly, Nature **365**(6449), 829–832 (1993)
- D. Gubbins, N. Roberts, Geophys. J. R. Astron. Soc. **73**, 675–687 (1983)
- D. Gubbins, P.H. Roberts, Geomagnetism **2**, 1–183 (1987)
- D. Gubbins, T.G. Masters, J.A. Jacobs, Geophys. J. R. Astron. Soc. **59**(1), 57–99 (1979)
- D. Gubbins, A. Jones, C.C. Finlay, Science **312**, 900–902 (2006)
- D. Gubbins, A.P. Willis, B. Sreenivasan, Phys. Earth Planet. Int. **162**(3–4), 256–260 (2007). doi:[10.1016/j.pepi.2007.04.014](https://doi.org/10.1016/j.pepi.2007.04.014)
- Y. Guyodo, J.P. Valet, Earth Planet. Sci. Lett. **143**(1–4), 23–36 (1996)
- Y. Guyodo, J.P. Valet, Nature **399**(6733), 249–252 (1999)
- M.M. Haldan, C.G. Langereis, A.J. Biggin, M.J. Dekkers, M.E. Evans, Geophys. J. Int. **177**(3), 834–848 (2009). doi:[10.1111/j.1365-246X.2009.04124.x](https://doi.org/10.1111/j.1365-246X.2009.04124.x)
- C.J. Hale, Nature **329**(6136), 233–237 (1987)
- H.C. Halls, Earth Planet. Sci. Lett. **105**(1–3), 279–292 (1991)
- F. Hankard, J.P. Cogne, V.A. Kravchinsky, L. Carporzen, A. Bayasgalan, P. Lkhagvadorj, J. Geophys. Res. **112**(B2), 02101 (2007). doi:[10.1029/2006JB004488](https://doi.org/10.1029/2006JB004488)
- R. Heller, R.T. Merrill, P.L. McFadden, Phys. Earth Planet. Int. **131**(3–4), 237–249 (2002)
- R. Heller, R.T. Merrill, P.L. McFadden, Phys. Earth Planet. Int. **135**(2–3), 211–223 (2003). doi:[10.1016/S0031-9201\(03\)00002-5](https://doi.org/10.1016/S0031-9201(03)00002-5)
- R. Hide, Philos. Trans. R. Soc. Lond. A **259**, 615–647 (1966)
- R. Hide, D.H. Boggs, J.O. Dickey, D. Dong, R.S. Gross, A. Jackson, Geophys. J. Int. **125**(2), 599–607 (1996)
- K.A. Hoffman, Nature **359**(6398), 789–794 (1992)
- R. Hollerbach, C.A. Jones, Nature **365**(6446), 541–543 (1993)

- R. Hollerbach, C.A. Jones, *Phys. Earth Planet. Int.* **87**(3–4), 171–181 (1995)
- R. Holme, *Geophys. J. Int.* **132**(1), 167–180 (1998)
- R. Holme, in *Treatise on Geophysics*, vol. 8, ed. by P. Olson (Elsevier, Amsterdam, 2007), pp. 107–130
- R. Holme, O. de Viron, *Geophys. J. Int.* **160**(2), 435–439 (2005). doi:[10.1111/j.1365-246X.2004.02510.x](https://doi.org/10.1111/j.1365-246X.2004.02510.x)
- R. Holme, N. Olsen, *Geophys. J. Int.* **166**(2), 518–528 (2006). doi:[10.1111/j.1365-246X.2006.03033.x](https://doi.org/10.1111/j.1365-246X.2006.03033.x)
- R. Holme, M.A. James, H. Lühr, *Earth Planets Space* **57**, 1203–1209 (2005)
- L. Hongre, G. Hulot, A. Khokhlov, *Phys. Earth Planet. Int.* **106**, 311–335 (1998)
- Y. Hueda-Tanabe, A.M. Soler-Arechalde, J. Urrutia-Fucugauchi, L. Barba, L. Manzanilla, M. Rebolledo-Vieyra, A. Goguitchaichvili, *Phys. Earth Planet. Int.* **147**(2–3), 269–283 (2004). doi:[10.1016/j.pepi.2004.06.006](https://doi.org/10.1016/j.pepi.2004.06.006)
- G. Hulot, *Nat. Geosci.* **1**(6), 345–346 (2008). doi:[10.1038/ngeo213](https://doi.org/10.1038/ngeo213)
- G. Hulot, C. Bouligand, *Geophys. J. Int.* **161**(3), 591–602 (2005). doi:[10.1111/j.1365-246X.2005.02612.x](https://doi.org/10.1111/j.1365-246X.2005.02612.x)
- G. Hulot, A. Chulliat, *Phys. Earth Planet. Int.* **135**(1), 47–54 (2003)
- G. Hulot, Y. Gallet, *Phys. Earth Planet. Int.* **95**(1–2), 37–53 (1996)
- G. Hulot, Y. Gallet, *Earth Planet. Sci. Lett.* **210**(1–2), 191–201 (2003). doi:[10.1016/S0012-821X\(03\)00130-4](https://doi.org/10.1016/S0012-821X(03)00130-4)
- G. Hulot, J.L. Le Mouél, *Phys. Earth Planet. Int.* **82**, 167–183 (1994). doi:[10.1016/0031-9201\(94\)90070-1](https://doi.org/10.1016/0031-9201(94)90070-1)
- G. Hulot, J.L. Le Mouél, D. Jault, J. Geomagn. Geoelectr. **42**(7), 857–874 (1990)
- G. Hulot, J.L. Le Mouél, J. Wahr, *Geophys. J. Int.* **108**, 224–246 (1992)
- G. Hulot, M. Le Huy, J.L. Le Mouél, C. R. Acad. Sci. II **317**(3), 333–341 (1993)
- G. Hulot, M. Le Huy, J.L. Le Mouél, *Geophys. Astrophys. Fluid Dyn.* **82**(1–2), 35–67 (1996)
- G. Hulot, A. Khokhlov, J.L. Le Mouél, *Geophys. J. Int.* **129**, 347–354 (1997)
- G. Hulot, C. Eymmin, B. Langlais, M. Manda, N. Olsen, *Nature* **416**, 620–623 (2002)
- G. Hulot, T.J. Sabaka, N. Olsen, in *Treatise on Geophysics*, vol. 5, ed. by M. Kono (Elsevier, Amsterdam, 2007)
- G. Hulot, N. Olsen, E. Thébault, K. Hemant, *Geophys. J. Int.* **177**, 361–366 (2009a). doi:[10.1111/j.1365-246X.2009.04119.x](https://doi.org/10.1111/j.1365-246X.2009.04119.x)
- G. Hulot, F. Lhuillier, J. Aubert, *Geophys. Res. Lett.* (2009b). doi:[10.129/2009GL041869](https://doi.org/10.129/2009GL041869)
- M. Ingham, G. Turner, *Phys. Earth Planet. Int.* **168**(3–4), 163–178 (2008). doi:[10.1016/j.pepi.2008.06.008](https://doi.org/10.1016/j.pepi.2008.06.008)
- A. Jackson, *Geophys. J. Int.* **119**, 991–998 (1994)
- A. Jackson, *Philos. Trans. R. Soc. Lond. A* **452**(1953), 2195–2201 (1996)
- A. Jackson, *Phys. Earth Planet. Int.* **103**, 293–311 (1997)
- A. Jackson, *Nature* **424**, 760–763 (2003)
- A. Jackson, C.C. Finlay, in *Treatise on Geophysics*, vol. 5, ed. by M. Kono (Elsevier, Amsterdam, 2007)
- A. Jackson, R. Hide, *Geophys. J. Int.* **125**(3), 925–927 (1996)
- A. Jackson, J. Bloxham, D. Gubbins, in *Dynamics of Earth's Deep Interior and Earth Rotation*, Geophysical Monograph, vol. 72 (1993), pp. 97–107
- A. Jackson, A.R.T. Jonkers, M.R. Walker, *Philos. Trans. R. Soc. Lond. A* **358**, 957–990 (2000)
- A. Jackson, C.C. Constable, N. Gillet, *Geophys. J. Int.* **171**(3), 995–1004 (2007a). doi:[10.1111/j.1365-246X.2007.03530.x](https://doi.org/10.1111/j.1365-246X.2007.03530.x)
- A. Jackson, C.G. Constable, M.R. Walker, R.L. Parker, *Geophys. J. Int.* **171**(1), 133–144 (2007b). doi:[10.1111/j.1365-246X.2007.03526.x](https://doi.org/10.1111/j.1365-246X.2007.03526.x)
- J.A. Jacobs, *Nature* **172**, 297–300 (1953)
- J.A. Jacobs, in *Encyclopedia of Geomagnetism and Paleomagnetism*, ed. by D. Gubbins, E. Herrero-Bervera (Springer, Heidelberg, 2007)
- J. Jankowski, C. Sucksdorff, *IAGA Guide for Magnetic Measurements and Observatory Practice* (IAGA, Warszawa, 1996)
- D. Jault, *Phys. Earth Planet. Int.* **166**(1–2), 67–76 (2008)
- D. Jault, J.L. Le Mouél, J. Geomagn. Geoelectr. **43**(2), 111–129 (1991a)
- D. Jault, J.L. Le Mouél, *Phys. Earth Planet. Int.* **68**(1–2), 76–84 (1991b)
- D. Jault, C. Gire, J.L. Le Mouél, *Nature* **333**, 353–356 (1988)
- C.L. Johnson, C.G. Constable, *Geophys. J. Int.* **122**(2), 489–519 (1995)
- C.L. Johnson, C.G. Constable, *Philos. Trans. R. Soc. Lond. A* **354**(1704), 89–141 (1996)
- C.L. Johnson, C.G. Constable, *Geophys. J. Int.* **131**(3), 643 (1997)
- C.L. Johnson, C.G. Constable, *Geophys. Res. Lett.* **25**(7), 1011–1014 (1998)
- C.L. Johnson, P. McFadden, in *Treatise on Geophysics*, vol. 5, ed. by M. Kono (Elsevier, Amsterdam, 2007)
- C.L. Johnson, C.G. Constable, L. Tauxe, R. Barendregt, L.L. Brown, R.S. Coe, P. Layer, V. Mejia, N.D. Opdyke, B.S. Singer, H. Staudigel, D.B. Stone, *Geochem. Geophys. Geosyst.* **9**(4), Q04032 (2008). doi:[10.1029/2007GC001696](https://doi.org/10.1029/2007GC001696)
- G.M. Jones, *J. Geophys. Res.* **82**(11), 1703–1709 (1977)
- A.R.T. Jonkers, *Geophys. J. Int.* **171**(2), 581–593 (2007). doi:[10.1111/j.1365-246X.2007.03551.x](https://doi.org/10.1111/j.1365-246X.2007.03551.x)
- A.R.T. Jonkers, A. Jackson, A. Murray, *Rev. Geophys.* **41**(2), 1006 (2003). doi:[10.1029/2002RG000115](https://doi.org/10.1029/2002RG000115)

- M.T. Juarez, L. Tauxe, *Earth Planet. Sci. Lett.* **175**(3–4), 169–180 (2000)
- M.T. Juarez, L. Tauxe, J.S. Gee, T. Pick, *Nature* **394**(6696), 878–881 (1998)
- A. Kageyama, T. Miyagoshi, T. Sato, *Nature* **454**(7208), 1106–1109 (2008). doi:[10.1038/nature07227](https://doi.org/10.1038/nature07227)
- P. Kelly, D. Gubbins, *Geophys. J. Int.* **128**(2), 315–330 (1997)
- D.V. Kent, F.M. Gradstein, in *The Geology of North America*, vol. M, ed. by P.R. Vogt, B.E. Tucholke (Geological Society of America, Boulder, 1986), pp. 45–50
- D.V. Kent, M.A. Smethurst, *Earth Planet. Sci. Lett.* **160**(3–4), 391–402 (1998)
- A. Khokhlov, G. Hulot, J.L. Le Mouél, *Geophys. J. Int.* **130**, 701–703 (1997)
- A. Khokhlov, G. Hulot, J.L. Le Mouél, *Geophys. J. Int.* **137**, 816–820 (1999)
- A. Khokhlov, G. Hulot, J. Carlut, *Geophys. J. Int.* **145**(1), 157–171 (2001)
- A. Khokhlov, G. Hulot, C. Bouligand, *Geophys. J. Int.* **167**(2), 635–648 (2006). doi:[10.1111/j.1365-246X.2006.03133.x](https://doi.org/10.1111/j.1365-246X.2006.03133.x)
- K.P. Kodama, W.W. Sun, *Geophys. J. Int.* **111**(3), 465–469 (1992)
- M. Kono, H. Tanaka, J. Geomagn. Geoelectr. **47**(1), 115–130 (1995)
- M. Kono, A. Sakuraba, M. Ishida, *Philos. Trans. R. Soc. Lond. A* **358**(1768), 1123–1139 (2000a)
- M. Kono, H. Tanaka, H. Tsunakawa, *J. Geophys. Res.* **105**(B3), 5817–5833 (2000b)
- K. Korhonen, F. Donadini, P. Riisager, L. Pesonen, *Geochem. Geophys. Geosyst.* **9**(4), Q04029 (2008). doi:[10.1029/2007GC001893](https://doi.org/10.1029/2007GC001893)
- M. Korte, C. Constable, *Geochem. Geophys. Geosyst.* **6**(1), Q02H16 (2005). doi:[10.1029/2004GC000801](https://doi.org/10.1029/2004GC000801)
- M. Korte, A. Genevey, C.G. Constable, U. Frank, E. Schnepp, *Geochem. Geophys. Geosyst.* **6**(2), Q02H15 (2005). doi:[10.1029/2004GC000800](https://doi.org/10.1029/2004GC000800)
- M. Korte, F. Donadini, C. Constable, *Geochem. Geophys. Geosyst.* **10**(6), Q06008 (2009). doi:[10.1029/2008GC002297](https://doi.org/10.1029/2008GC002297)
- W. Kuang, A. Tangborn, W. Jiang, D. Liu, Z. Sun, J. Bloxham, Z. Wei, *Commun. Comput. Phys.* **3**(1), 85–108 (2008)
- C. Kutzner, U.R. Christensen, *Geophys. J. Int.* **157**(3), 1105–1118 (2004). doi:[10.1111/j.1365-246X.2004.02309.x](https://doi.org/10.1111/j.1365-246X.2004.02309.x)
- S. Labrosse, M. Macouin, C. R. Geosci. **335**(1), 37–50 (2003). doi:[10.1016/S1631-0713\(03\)00013-0](https://doi.org/10.1016/S1631-0713(03)00013-0)
- S. Labrosse, J.P. Poirier, J.L. Le Mouél, *Earth Planet. Sci. Lett.* **190**(3–4), 111–123 (2001)
- S. Labrosse, J.W. Hearn, N. Coltice, *Nature* **450**(7171), 866–869 (2007). doi:[10.1038/nature06355](https://doi.org/10.1038/nature06355)
- C. Laj, A. Mazaud, R. Weeks, M. Fuller, E. Herrero-Bervera, *Nature* **351**(6326), 447 (1991)
- C. Laj, C. Kissel, A. Mazaud, J.E.T. Channell, J. Beer, *Philos. Trans. R. Soc. Lond. A* **358**(1768), 1009–1025 (2000)
- C. Laj, C. Kissel, J. Beer, in *Timescales of the Paleomagnetic Field*, ed. by J.E.T. Channell, D.V. Kent, W. Lowrie, J.G. Meert, *Geophysical Monograph Series*, vol. 145 (2004), pp. 255–265. 0-87590-410-6. doi:[10.1029/145GM19](https://doi.org/10.1029/145GM19)
- P. Lancaster, K. Salkauskas, *Curve and Surface Fitting* (Academic Press, San Diego, 1986)
- R.A. Langel, in *Geomagnetism*, vol. 1, ed. by J.A. Jacobs (Academic Press, London, 1987), pp. 249–512
- R.A. Langel, R.H. Estes, *Geophys. Res. Lett.* **9**, 250–253 (1982)
- R.A. Langel, W.J. Hinze, *The Magnetic Field of the Earth's Lithosphere: The Satellite Perspective* (Cambridge University Press, Cambridge, 1998)
- C.G. Langereis, A.A.M. van Hoof, P. Rochette, *Nature* **358**(6383), 226–230 (1992)
- B. Langlais, V. Lesur, M.E. Purucker, J.E.P. Connerney, M. Manda, *Space Sci. Rev.* (2009). doi:[10.1007/s11214-009-9557-y](https://doi.org/10.1007/s11214-009-9557-y)
- R.L. Larson, P. Olson, *Earth Planet. Sci. Lett.* **107**(3–4), 437–447 (1991)
- K.P. Lawrence, C.G. Constable, J.L. Johnson, *Geochem. Geophys. Geosyst.* **7**(7), Q07007 (2006). doi:[10.1029/2005GC001181](https://doi.org/10.1029/2005GC001181)
- M. Le Huy, M. Alexandrescu, G. Hulot, J.L. Mouél, *Earth Planets Space* **50**(9), 723–732 (1998)
- S. Lee, PhD thesis, Austr. Nat. Univ., Canberra, 1983
- B. Lehnert, *Astrophys. J.* **119**, 647–654 (1954)
- J.L. Le Mouél, *Nature* **311**, 734–735 (1984)
- R. Leonhardt, K. Fabian, *Earth Planet. Sci. Lett.* **253**(1–2), 172–195 (2007). doi:[10.1016/j.epsl.2006.10.025](https://doi.org/10.1016/j.epsl.2006.10.025)
- R. Leonhardt, K. Fabian, M. Winklhofer, A. Ferk, C. Laj, C. Kissel, *Earth Planet. Sci. Lett.* **278**(1–2), 87–95 (2009). doi:[10.1016/j.epsl.2008.11.028](https://doi.org/10.1016/j.epsl.2008.11.028)
- V. Lesur, I. Wardinski, M. Rother, M. Manda, *Geophys. J. Int.* **173**, 382–294 (2008)
- S. Levi, S.K. Banerjee, *Earth Planet. Sci. Lett.* **29**(1), 219–226 (1976)
- D.E. Loper, K. McCartney, *Geophys. Res. Lett.* **13**(13), 1525–1528 (1986)
- J.J. Love, *J. Geophys. Res.* **103**(B6), 12435–12452 (1998)
- J.J. Love, C.G. Constable, *Geophys. J. Int.* **152**(3), 515–565 (2003)
- F.J. Lowes, *Geophys. J. R. Astron. Soc.* **36**, 717–730 (1974)
- F.J. Lowes, *Geophys. J. R. Astron. Soc.* **42**, 637–651 (1975)

- W. Lowrie, D.V. Kent, in *Timescales of the Paleomagnetic Field*, ed. by J.E.T. Channell, D.V. Kent, W. Lowrie, J.G. Meert, Geophysical Monograph Series, vol. 145 (2004), pp. 117–129. 0-87590-410-6. doi:[10.1029/145GM09](https://doi.org/10.1029/145GM09)
- S. Macmillan, S. Maus, *Earth Planets Space* **57**, 1135–1140 (2005)
- M. Macouin, J.P. Valet, J. Besse, *Phys. Earth Planet. Int.* **147**(2–3), 239–246 (2004). doi:[10.1016/j.pepi.2004.07.003](https://doi.org/10.1016/j.pepi.2004.07.003)
- S.R.C. Malin, E.C. Bullard, *Philos. Trans. R. Soc. Lond. A* **299**, 357–423 (1981)
- E.A. Mankinen, *Geochem. Geophys. Geosyst.* **9**(5), Q05017 (2008). doi:[10.1029/2008GC001957](https://doi.org/10.1029/2008GC001957)
- W. Marzocchi, *J. Geophys. Res.* **102**(B3), 5157–5171 (1997)
- G. Masters, S. Johnson, G. Laske, H. Bolton, *Philos. Trans. R. Soc. Lond. A* **354**(1711), 1385–1410 (1996)
- H. Matsui, B.A. Buffett, *Phys. Earth Planet. Int.* **153**(1–3, Sp. Iss.), 108–123 (2005). doi:[10.1016/i.pepi.2005.03.019](https://doi.org/10.1016/i.pepi.2005.03.019)
- H. Matsui, B.A. Buffett, *Geophys. Astrophys. Fluid Dyn.* **101**(5–6), 451–468 (2007). doi:[10.1080/03091920701562145](https://doi.org/10.1080/03091920701562145)
- M. Matsushima, *Geophys. Astrophys. Fluid Dyn.* **100**(4–5), 363–377 (2006). doi:[10.1080/03091920600768397](https://doi.org/10.1080/03091920600768397)
- S. Maus, M. Rother, C. Stolle, W. Mai, S. Choi, H. Lühr, D. Cooke, C. Roth, *Geochem. Geophys. Geosyst.* **7**(7), Q07008 (2006). doi:[10.1029/2006GC001269](https://doi.org/10.1029/2006GC001269)
- S. Maus, F. Yin, H. Lühr, C. Manoj, M. Rother, J. Rauberg, I. Michaelis, C. Stolle, R. Müller, *Geochem. Geophys. Geosyst.* **9**(7), Q07021 (2008). doi:[10.1029/2008GC001949](https://doi.org/10.1029/2008GC001949)
- A. Mazaud, in *Encyclopedia of Geomagnetism and Paleomagnetism*, ed. by D. Gubbins, E. Herrero-Bervera (Springer, Heidelberg, 2007)
- M.W. McElhinny, in *Encyclopedia of Geomagnetism and Paleomagnetism*, ed. by D. Gubbins, E. Herrero-Bervera (Springer, Heidelberg, 2007)
- M.W. McElhinny, P.L. McFadden, *Geophys. J. Int.* **131**(2), 240–252 (1997)
- M.W. McElhinny, P.L. McFadden, *Paleomagnetism: Continents and Oceans* (Academic Press, London, 2000)
- M.W. McElhinny, P.L. McFadden, R.T. Merrill, *Earth Planet. Sci. Lett.* **143**(1–4), 13–22 (1996a)
- M.W. McElhinny, P.L. McFadden, R.T. Merrill, *J. Geophys. Res.* **101**(B11), 25007–25027 (1996b)
- P.L. McFadden, *J. Geophys. Res.* **89**(NB5), 3363–3372 (1984)
- P.L. McFadden, R.T. Merrill, *J. Geophys. Res.* **89**(NB5), 3354–3362 (1984)
- P.L. McFadden, R.T. Merrill, *J. Geophys. Res.* **98**(B4), 6189–6199 (1993)
- P.L. McFadden, R.T. Merrill, *J. Geophys. Res.* **105**(B12), 28455–28460 (2000)
- P.L. McFadden, R.T. Merrill, M.W. McElhinny, *J. Geophys. Res.* **93**(B10), 11583–11588 (1988)
- P.L. McFadden, R.T. Merrill, M.W. McElhinny, S.H. Lee, *J. Geophys. Res.* **96**(B3), 3923–3933 (1991)
- P.L. McFadden, C.E. Barton, R.T. Merrill, *Nature* **361**(6410), 342–344 (1993)
- D.G. McMillan, C.G. Constable, R.L. Parker, G.A. Glatzmaier, *Geochem. Geophys. Geosyst.* **2**(11), 2000GC000130 (2001)
- R. Merrill, P. McFadden, M. McElhinny, *The Magnetic Field of the Earth: Paleomagnetism, the Core, and the Deep Mantle* (Academic Press, San Diego, 1996)
- R.T. Merrill, P.L. McFadden, *Rev. Geophys.* **37**(2), 201–226 (1999)
- L. Meynadier, J.P. Valet, F.C. Bassinot, N.J. Shackleton, Y. Guyodo, *Earth Planet. Sci. Lett.* **126**(1–3), 109–127 (1994)
- H.K. Moffatt, *Magnetic Field Generation in Electrically Conducting Fluids* (Cambridge University Press, Cambridge, 1978)
- R. Monchaux, M. Berhanu, M. Bourgoin, M. Moulin, P. Odier, J.F. Pinton, R. Volk, S. Fauve, N. Mordant, F. Petrelis, A. Chiffaudel, F. Daviaud, B. Dubrulle, C. Gasquet, L. Marie, F. Ravelet, *Phys. Rev. Lett.* **98**(4), 44502 (2007). doi:[10.1103/PhysRevLett.98.044502](https://doi.org/10.1103/PhysRevLett.98.044502)
- L.W. Morley, *A. Larochele, R. Soc. Can. Spec. Publ.* **8**, 39–50 (1964)
- J.E. Mound, B.A. Buffett, *J. Geophys. Res.* **110**(B8), 08103 (2005). doi:[10.1029/2004JB003555](https://doi.org/10.1029/2004JB003555)
- P.S. Naidu, *J. Geophys. Res.* **76**(11), 2649 (1971)
- H.C. Nataf, T. Alboussiere, D. Brito, P. Cardin, N. Gagniere, D. Jault, J.P. Masson, D. Schmitt, *Geophys. Astrophys. Fluid Dyn.* **100**(4–5), 281–298 (2006). doi:[10.1080/03091920600718426](https://doi.org/10.1080/03091920600718426)
- H.C. Nataf, T. Alboussiere, D. Brito, P. Cardin, N. Gagniere, D. Jault, D. Schmitt, *Phys. Earth Planet. Int.* **170**(1–2), 60–72 (2008). doi:[10.1016/j.pepi.2008.07.034](https://doi.org/10.1016/j.pepi.2008.07.034)
- T. Neubert, M. Manda, G. Hulot, R. von Frese, F. Primdahl, J.L. Joergensen, E. Friis-Christensen, P. Stauning, N. Olsen, T. Risbo, *EOS Trans. AGU* **82**(7), 81–88 (2001)
- F. Nimmo, in *Treatise on Geophysics*, vol. 8 (Elsevier, Amsterdam, 2007), pp. 31–65
- M.S. O'Brien, C.G. Constable, R.L. Parker, *Geophys. J. Int.* **128**(2), 434–450 (1997)
- N. Olsen, M. Manda, *Nat. Geosci.* **1**(6), 390 (2008)

- N. Olsen, R. Haagmans, T.J. Sabaka, A.V. Kuvshinov, S. Maus, M.E. Purucker, V. Lesur, M. Rother, M. Manda, *Earth Planets Space* **58**, 359–370 (2006)
- N. Olsen, M. Manda, T.J. Sabaka, L. Tøffner-Clausen, *Geophys. J. Int.* **179**(3), 1477–1487 (2009a). doi:[10.1111/j.1365-246X.2009.04386.x](https://doi.org/10.1111/j.1365-246X.2009.04386.x)
- N. Olsen, K. Glassmeier, X. Jia, *Space Sci. Rev.* (2009b). doi:[10.1007/s11214-009-9563-0](https://doi.org/10.1007/s11214-009-9563-0)
- P. Olson, H. Amit, *Naturwissenschaften* **93**(11), 519–542 (2006). doi:[10.1007/s00114-006-0138-6](https://doi.org/10.1007/s00114-006-0138-6)
- P. Olson, J. Aurnou, *Nature* **402**(6758), 170–173 (1999)
- P. Olson, U.R. Christensen, *Geophys. J. Int.* **151**(3), 809–823 (2002)
- P. Olson, U. Christensen, G.A. Glatzmaier, *J. Geophys. Res.* **104**(B5), 10383–10404 (1999)
- P. Olson, P. Driscoll, H. Amit, *Phys. Earth Planet. Int.* **173**(1–2), 121–140 (2009). doi:[10.1016/j.pepi.2008.11.010](https://doi.org/10.1016/j.pepi.2008.11.010)
- N. Opdyke, J. Channell, *Magnetic Stratigraphy* (Academic Press, London, 1996)
- A. Pais, G. Hulot, *Phys. Earth Planet. Int.* **118**, 291–316 (2000)
- A. Pais, D. Jault, *Geophys. J. Int.* **173**, 421–443 (2008)
- R. Parker, *Geophysical Inverse Theory* (Princeton University Press, Princeton, 1994)
- V. Pavlov, Y. Gallet, *Earth Planet. Sci. Lett.* **185**(1–2), 173–183 (2001)
- V. Pavlov, Y. Gallet, *Episodes* **28**(2), 78–84 (2005)
- V. Pavlov, Y. Gallet, *Geochem. Geophys. Geosyst.* **11**(1), Q01Z10 (2010). doi:[10.1029/2009GC002583](https://doi.org/10.1029/2009GC002583)
- M. Perrin, E. Schnepf, *Phys. Earth Planet. Int.* **147**(2–3), 255–267 (2004). doi:[10.1016/j.pepi.2004.06.005](https://doi.org/10.1016/j.pepi.2004.06.005)
- M. Perrin, V. Shcherbakov, *J. Geomagn. Geoelectr.* **49**(4), 601–614 (1997)
- F. Petrelis, S. Fauve, E. Dormy, J.P. Valet, *Phys. Rev. Lett.* **102**(14), 144503 (2009). doi:[10.1103/PhysRevLett.102.144503](https://doi.org/10.1103/PhysRevLett.102.144503)
- T. Pick, L. Tauxe, *Nature* **366**(6452), 238–242 (1993)
- K. Pinheiro, A. Jackson, *Geophys. J. Int.* **173**(3), 781–792 (2008). doi:[10.1111/j.1365-246X.2008.03762.x](https://doi.org/10.1111/j.1365-246X.2008.03762.x)
- G. Pouliquen, Y. Gallet, J. Dyment, P. Patriat, C. Tamura, *J. Geophys. Res.* **106**(B12), 30549 (2001)
- M. Prévot, P. Camps, *Nature* **366**(6450), 53–57 (1993)
- M. Prévot, M.E. Derder, M. McWilliams, J. Thompson, *Earth Planet. Sci. Lett.* **97**(1–2), 129–139 (1990)
- M.E. Purucker, *Icarus* **197**(1), 19–23 (2008)
- X. Quidelleur, V. Courtillot, *Phys. Earth Planet. Int.* **95**(1–2), 55–77 (1996)
- X. Quidelleur, J.P. Valet, V. Courtillot, G. Hulot, *Geophys. Res. Lett.* **21**(15), 1639–1642 (1994)
- C. Reigber, H. Lühr, P. Schwintzer, *Adv. Space Res.* **30**, 129–134 (2002)
- A.P. Roberts, M. Winklhofer, W.T. Liang, C.S. Hong, *Earth Planet. Sci. Lett.* **216**(1–2), 187–192 (2003). doi:[10.1016/S0012-821X\(03\)00480-1](https://doi.org/10.1016/S0012-821X(03)00480-1)
- P.H. Roberts, G.A. Glatzmaier, *Geophys. Astrophys. Fluid Dyn.* **94**(1–2), 47–84 (2001)
- P.H. Roberts, S. Scott, *J. Geomagn. Geoelectr.* **17**(2), 137–151 (1965)
- D.A. Ryan, G.R. Sarson, *Geophys. Res. Lett.* **34**(2), L02307 (2007). doi:[10.1029/2006GL028291](https://doi.org/10.1029/2006GL028291)
- D.A. Ryan, G.R. Sarson, *Europhys. Lett.* **83**(4), 49001 (2008). doi:[10.1209/0295-5075/83/49001](https://doi.org/10.1209/0295-5075/83/49001)
- T.J. Sabaka, N. Olsen, M.E. Purucker, *Geophys. J. Int.* **159**, 521–547 (2004). doi:[10.1111/j.1365-246X.2004.02421.x](https://doi.org/10.1111/j.1365-246X.2004.02421.x)
- T.J. Sabaka, N. Olsen, *Earth Planets Space* **58**, 371–395 (2006)
- A. Sakuraba, M. Kono, *Phys. Earth Planet. Int.* **111**(1–2), 105–121 (1999)
- A. Sakuraba, P.H. Roberts, *Nat. Geosci.* **2**(11), 802–805 (2009). doi:[10.1038/ngeo643](https://doi.org/10.1038/ngeo643)
- J. Saur, V. Neubauer, K.H. Glassmeier, *Space Sci. Rev.* (2009). doi:[10.1007/s11214-009-9581-y](https://doi.org/10.1007/s11214-009-9581-y)
- D. Schmitt, T. Alboussiere, D. Brito, P. Cardin, N. Gagniere, D. Jault, H.C. Nataf, *J. Fluid Mech.* **604**, 175–197 (2008). doi:[10.1017/S0022112008001298](https://doi.org/10.1017/S0022112008001298)
- D.A. Schneider, D.V. Kent, *J. Geophys. Res.* **93**(B10), 11621–11630 (1988)
- D.A. Schneider, D.V. Kent, *Rev. Geophys.* **28**(1), 71–96 (1990)
- W.E. Schröder, *Geomagnetism Research; Past and Present* (2000)
- G. Schubert, D.L. Turcotte, P. Olson, *Mantle Convection in the Earth and Planets* (Cambridge University Press, Cambridge, 2001)
- P.A. Selkin, L. Tauxe, *Philos. Trans. R. Soc. Lond. A* **358**(1768), 1065–1088 (2000)
- J.W. Si, R. Van der Voo, *Terra Nova* **13**(6), 471–478 (2001)
- R.D. Simitev, F.H. Busse, *Europhys. Lett.* **85**(1), 19001 (2009). doi:[10.1209/0295-5075/85/19001](https://doi.org/10.1209/0295-5075/85/19001)
- A.V. Smirnov, J.A. Tarduno, *Geophys. Res. Lett.* **31**(16), L16607 (2004). doi:[10.1029/2004GL020333](https://doi.org/10.1029/2004GL020333)
- D.P. Stern, *Rev. Geophys.* **40** (2002). doi:[10.1029/2000RG000097](https://doi.org/10.1029/2000RG000097)
- R. Stieglitz, U. Müller, *Phys. Fluids* **13**(3), 561–564 (2001)
- G. Strik, T.S. Blake, T.E. Zegers, S.H. White, C.G. Langereis, *J. Geophys. Res.* **108**(B12), 2551 (2003). doi:[10.1029/2003JB002475](https://doi.org/10.1029/2003JB002475)
- H. Tanaka, M. Kono, H. Uchimura, *Geophys. J. Int.* **120**(1), 97–102 (1995)
- S. Tanaka, H. Hamaguchi, *J. Geophys. Res.* **102**(B2), 2925–2938 (1997)

- A. Tarantola, *Inverse Problem Theory and Methods for Model Parameter Estimation* (SIAM, Philadelphia, 2005)
- J.A. Tarduno, *Elements* **5**(4), 217–222 (2009). doi:[10.2113/gselements.5.4.217](https://doi.org/10.2113/gselements.5.4.217)
- J.A. Tarduno, R.D. Cottrell, A.V. Smirnov, *Proc. Natl. Acad. Sci.* **99**(22), 14020–14025 (2002). doi:[10.1073/pnas.222373499](https://doi.org/10.1073/pnas.222373499)
- J.A. Tarduno, R.D. Cottrell, A.V. Smirnov, *Rev. Geophys.* **44**(1), RG1002 (2006). doi:[10.1029/2005RG000189](https://doi.org/10.1029/2005RG000189)
- J.A. Tarduno, R.D. Cottrell, M.K. Watkeys, D. Bauch, *Nature* **446**(7136), 657–660 (2007). doi:[10.1038/nature05667](https://doi.org/10.1038/nature05667)
- L. Tauxe, *Earth Planet. Sci. Lett.* **233**(3–4), 247–261 (2005). doi:[10.1016/j.epsl.2005.01.027](https://doi.org/10.1016/j.epsl.2005.01.027)
- L. Tauxe, *Phys. Earth Planet. Int.* **156**(3–4), 223–241 (2006). doi:[10.1016/j.pepi.2005.03.022](https://doi.org/10.1016/j.pepi.2005.03.022)
- L. Tauxe, P. Hartl, *Geophys. J. Int.* **128**(1), 217–229 (1997)
- L. Tauxe, D.V. Kent, in *Timescales of the Paleomagnetic Field*, ed. by J.E.T. Channell, D.V. Kent, W. Lowrie, J.G. Meert, *Geophysical Monograph Series*, vol. 145 (2004), pp. 101–115. 0-87590-410-6. doi:[10.1029/145GM08](https://doi.org/10.1029/145GM08)
- L. Tauxe, H. Staudigel, *Geochem. Geophys. Geosyst.* **5**(2), Q02H06 (2004). doi:[10.1029/2003GC000635](https://doi.org/10.1029/2003GC000635)
- L. Tauxe, T. Yamazaki, in *Treatise on Geophysics*, vol. 5, ed. by M. Kono (Elsevier, Amsterdam, 2007)
- L. Tauxe, K.P. Kodama, D.V. Kent, *Phys. Earth Planet. Int.* **169**(1–4, Sp. Iss.), 152–165 (2008). doi:[10.1016/j.pepi.2008.05.006](https://doi.org/10.1016/j.pepi.2008.05.006)
- J. Taylor, *Proc. R. Soc. Lond. A* **9**, 274–283 (1963)
- E. Thébault, K. Hemant, G. Hulot, N. Olsen, *Geophys. Res. Lett.* **36**, L01307 (2009). doi:[10.1029/2008GL036416](https://doi.org/10.1029/2008GL036416)
- J.C. Thomas, H. Perroud, P.R. Cobbold, M.L. Bazhenov, V.S. Burtman, A. Chauvin, E. Sadybakasov, *J. Geophys. Res.* **98**(B6), 9571–9589 (1993)
- A.W.P. Thomson, *V. Lesur, Geophys. J. Int.* **169**(3), 951–963 (2007)
- N. Thouveny, D.L. Bourles, G. Saracco, J.T. Carcaillet, F. Bassinot, *Earth Planet. Sci. Lett.* **275**(3–4), 269–284 (2008). doi:[10.1016/j.epsl.2008.08.020](https://doi.org/10.1016/j.epsl.2008.08.020)
- A. Tilgner, in *Treatise on Geophysics*, vol. 8, ed. by P. Olson (Elsevier, Amsterdam, 2007)
- M.A. Tivey, in *Encyclopedia of Geomagnetism and Paleomagnetism*, ed. by D. Gubbins, E. Herrero-Bervera (Springer, Heidelberg, 2007a)
- M.A. Tivey, in *Encyclopedia of Geomagnetism and Paleomagnetism*, ed. by D. Gubbins, E. Herrero-Bervera (Springer, Heidelberg, 2007b)
- M.A. Tivey, W.W. Sager, S.M. Lee, M. Tominaga, *Geology* **34**(9), 789–792 (2006). doi:[10.1130/G22894.1](https://doi.org/10.1130/G22894.1)
- M. Tominaga, W.W. Sager, M.A. Tivey, S.M. Lee, *J. Geophys. Res.* **113**(B7), B07110 (2008). doi:[10.1029/2007JB005527](https://doi.org/10.1029/2007JB005527)
- T.H. Torsvik, R. Van der Voo, *Geophys. J. Int.* **151**(3), 771–794 (2002)
- G.M. Turner, J.L. Rasson, C.V. Reeves, in *Treatise on Geophysics*, vol. 5, ed. by M. Kono (Elsevier, Amsterdam, 2007)
- P. Ultré-Guérard, M. Hamoudi, G. Hulot, *Geophys. Res. Lett.* **22**(16), 3201–3204 (1998)
- J.P. Valet, *Rev. Geophys.* **41**(1), 1004 (2003). doi:[10.1029/2001RG000104](https://doi.org/10.1029/2001RG000104)
- J.P. Valet, L. Meynadier, *Nature* **366**(6452), 234–238 (1993)
- J.P. Valet, G. Plenier, *Phys. Earth Planet. Int.* **169**(1–4, Sp. Iss.), 178–193 (2008). doi:[10.1016/j.pepi.2008.07.031](https://doi.org/10.1016/j.pepi.2008.07.031)
- J.P. Valet, P. Tucholka, V. Courtillot, L. Meynadier, *Nature* **356**(6368), 400–407 (1992)
- J.P. Valet, L. Meynadier, Y. Guyodo, *Nature* **435**(7043), 802–805 (2005). doi:[10.1038/nature03674](https://doi.org/10.1038/nature03674)
- J.P. Valet, E. Herrero-Bervera, J.L. Le Mouél, G. Plenier, *Geochem. Geophys. Geosyst.* **9**(1), Q01008 (2008). doi:[10.1029/2007GC001728](https://doi.org/10.1029/2007GC001728)
- R. Van der Voo, T.H. Torsvik, *Earth Planet. Sci. Lett.* **187**(1–2), 71–81 (2001)
- S.A. Van Loo, J.L. Rasson, in *XIII IAGA Workshop on Geomagnetic Observatory Instruments, Data Acquisition and Processing*, Abstract volume 21, 2006
- D. Vandamme, *Phys. Earth Planet. Int.* **85**(1–2), 131–142 (1994)
- J.M. Vaquero, R.M. Trigo, *Phys. Earth Planet. Int.* **157**, 8–15 (2006)
- P. Varga, C. Denis, T. Varga, *J. Geophys.* **25**(1–2), 61–84 (1998)
- G. Verhille, N. Plihon, M. Bourgoïn, P. Odier, J.F. Pinton, *Space Sci. Rev.* (2009). doi:[10.1007/s11214-009-9546-1](https://doi.org/10.1007/s11214-009-9546-1)
- F.J. Vine, D.H. Matthews, *Nature* **199**(489), 947–949 (1963)
- C.V. Voorhies, T.J. Sabaka, M. Purucker, *J. Geophys. Res.* **107**(E6), 5034 (2002). doi:[10.1029/2001JE001534](https://doi.org/10.1029/2001JE001534)
- M.R. Walker, A. Jackson, *Geophys. J. Int.* **143**, 799–808 (2000)
- I. Wardinski, M. Korte, *J. Geophys. Res.* **113**(B5), B05101 (2008). doi:[10.1029/2007JB005024](https://doi.org/10.1029/2007JB005024)
- J. Wicht, *Phys. Earth Planet. Int.* **132**(4), 281–302 (2002)

- J. Wicht, *Geophys. J. Int.* **162**(2), 371–380 (2005). doi:[10.1111/j.1365-246X.2005.02665.x](https://doi.org/10.1111/j.1365-246X.2005.02665.x)
- J. Wicht, P. Olson, *Geochem. Geophys. Geosyst.* **5**(3), Q03H10 (2004). doi:[10.1029/2003GC000602](https://doi.org/10.1029/2003GC000602)
- A.P. Willis, B. Sreenivasan, D. Gubbins, *Phys. Earth Planet. Int.* **165**(1–2), 83–92 (2007). doi:[10.1016/j.pepi.2007.08.002](https://doi.org/10.1016/j.pepi.2007.08.002)
- C. Xuan, J.E.T. Channell, *Phys. Earth Planet. Int.* **169**(1–4, Sp. Iss.), 140–151 (2008). doi:[10.1016/j.pepi.2008.07.017](https://doi.org/10.1016/j.pepi.2008.07.017)
- S. Zatman, J. Bloxham, *Nature* **388**, 760–763 (1997)
- S. Zatman, J. Bloxham, *Geophys. J. Int.* **138**(3), 679–686 (1999)